INSTITUTO POLITÉCNICO DE BRAGANÇA
Escola Superior de Tecnologia e Gestão

Development of Tailored Materials for the Valorization of Olive Leaf and Olive Oil Subproducts through Sorption Processes

Rita Martins Gaspar

Thesis presented to

Escola Superior de Tecnologia e Gestão

Instituto Politécnico de Bragança

To obtain a master's degree in

Chemical Engineering

Under the guidance and supervision of the

Professor Doutor Rolando Carlos Pereira Simões Dias

Bragança, 9 of June, 2025

Development of Tailored Materials for the Valorization of Olive Leaf and Olive Oil Subproducts through Sorption Processes

Rita Martins Gaspar

Thesis presented to **Escola Superior de Tecnologia e Gestão - Instituto Politécnico de Bragança** to obtain a master's degree in **Chemical Engineering,** under the guidance and supervision of the **Professor Doutor Rolando Carlos Pereira Simões Dias.**

Bragança, 9 of June, 2025

Agradecimentos

Ao olhar para trás, vejo mais do que dados, gráficos e páginas escritas. Vejo pessoas, gestos e palavras que deram sentido a cada etapa deste percurso.

A todas essas pessoas, deixo agora o meu mais sincero agradecimento.

Agradeço, antes de mais, ao meu orientador, Rolando Dias, pela confiança, pela exigência que me fez crescer e pela orientação atenta e constante. A sua disponibilidade, rigor e paixão pela ciência foram uma inspiração ao longo de todo este trabalho.

The support through the OLEAF4VALUE project is acknowledged. This project had received funding from the Bio-Based Industries Joint Undertaking under the European Union's Horizon 2020 research and innovation programme under grant agreement no. 101023256. This work was also supported by Foundation for Science and Technology (FCT, Portugal) through national funds FCT/ MCTES (PIDDAC) to CIMO (UIDB/00690/2020 and UIDP/00690/2020) and SusTEC (LA/P/0007/2020).

Agradeço também a todos os colegas do laboratório pelo ambiente de partilha, entreajuda e boa disposição. Um agradecimento especial à Cláudia e à Catarina, pela amizade genuína, pelas risadas, e por tudo o que aprendi convosco, dentro e fora do laboratório. E um agradecimento ainda mais profundo à Ayssata, por ter sido muito mais do que uma colega: pela orientação paciente, pela ajuda constante, pela amizade sincera e pelo exemplo de dedicação e generosidade. A tua presença fez toda a diferença, e muito do que aqui deixo feito também te pertence.

À minha família, o meu mais profundo agradecimento. Em especial, aos meus pais e ao meu irmão: obrigada pelo amor incondicional, pela paciência, pelas palavras certas e por nunca deixarem que me faltasse apoio, mesmo quando o caminho parecia mais difícil. A vossa presença foi, e é, a minha base.

Aos meus avós, pela ternura e sabedoria, pelos gestos simples mas cheios de significado, e por tudo o que me ensinaram sem nunca precisarem de o dizer. Cada conquista minha tem um bocadinho vosso.

Um agradecimento muito especial ao Afonso, pelo apoio constante, pela presença nos momentos de maior cansaço, por acreditar sempre em mim e por ter vivido cada conquista minha com o mesmo orgulho e alegria com que viveria as suas. Obrigado.

Agradeço às minhas colegas de casa, as duas Maria João, pela amizade de todos os dias, pelas conversas e gargalhadas, e por me fazerem sentir verdadeiramente em casa. Foi um privilégio viver esta etapa com ambas.

Por fim, agradeço a todos os que de perto ou de longe, fizeram parte deste percurso. Cada palavra, gesto ou apoio discreto ajudou a construir este caminho e ficará sempre na memória do que vivi.

Abstract

The increasing demand for sustainable strategies to recover high-value compounds from agro-industrial subproduct has highlighted the potential of olive leaf as a rich yet underexploited resource. This thesis presents the development of cellulose-based molecularly imprinted polymers (MIPs) functionalized with pyridyl groups, designed for the selective extraction of bioactive compounds from olive leaf extracts. Through surface-initiated atom transfer radical polymerization, a total of ten MIPs were synthesized using quercetin and oleanolic acid as templates, along with their corresponding non-imprinted polymers (NIPs), prepared under identical conditions but in the absence of template molecules. Functional monomers were selected based on their compatibility with the target compounds. Characterization of the synthesized sorbents through FTIR, SEM and BET confirmed successful functionalization and surface grafting. The materials were tested in both solid phase extraction and recirculating column systems. Results showed that quercetin-imprinted MIPs exhibited high retention capacity and selectivity for flavonoids, especially in low-polarity solvents like acetonitrile, with statistically significant imprinting factors. In polar media (ethanol/water), retention remained structure-dependent but was largely driven by non-specific interactions. Application with industrial extracts (NATAC OPA 20 and VR2 SS1) demonstrated the capacity of the MIPs to enrich flavonoid glycosides, such as luteolin-7-O-glucoside, with enrichment factors up to 5 in gradient desorption steps. MIP3 was further scaled up and validated under continuous flow, confirming stability, efficiency, and reusability. A second imprinting strategy targeting triterpenoids using oleanolic acid as template was also explored. Although no molecular recognition was observed under tested conditions, the functionalized polymers still improved retention compared to unmodified cellulose, indicating potential for optimization under pH-adjusted systems. Overall, this work proposes a modular and sustainable approach to sorbent design for the valorization of olive leaves. It contributes to the advancement of selective extraction technologies and provides a framework for future applications in circular bioeconomy contexts.

Keywords: Molecularly imprinted polymers; Olive leaf; Selective sorption; Bioactive compounds; Circular Bioeconomy.

Resumo

A crescente procura por estratégias sustentáveis para a recuperação de compostos de elevado valor a partir de resíduos agroindustriais tem destacado o potencial da folha de oliveira como um recurso rico, mas subaproveitado. Esta tese apresenta o desenvolvimento de polímeros molecularmente impressos (MIPs) à base de celulose, funcionalizados com grupos piridilo, concebidos para a extração seletiva de compostos bioativos a partir de extratos de folha de oliveira. Através de polimerização radicalar por transferência de átomo iniciada na superfície, foram sintetizados dez MIPs utilizando quercetina e ácido oleanólico como moldes, juntamente com os respetivos polímeros não impressos (NIPs), preparados nas mesmas condições, mas na ausência das moléculas molde. Os monómeros funcionais foram selecionados com base na sua compatibilidade com os compostos-alvo. A caracterização por FTIR, SEM e BET confirmou a funcionalização e enxertia superficial bem-sucedidas. Os materiais foram testados em sistemas de extração em fase sólida e em colunas com recirculação. Os resultados demonstraram que os MIPs impressos com quercetina apresentaram elevada capacidade de retenção e seletividade para flavonoides, especialmente em acetonitrilo, com fatores de impressão estatisticamente significativos. Em etanol/água, a retenção manteve-se dependente da estrutura molecular, mas foi maioritariamente influenciada por interações não específicas. A aplicação a extratos industriais (NATAC OPA 20 e VR2 SS1) demonstrou a capacidade dos MIPs para enriquecer glicosídeos de flavonoides, como a luteolina-7-O-glicosídeo, com fatores de enriquecimento até 5. O MIP3 foi escalado e validado sob fluxo contínuo, confirmando estabilidade, eficiência e reutilização. Uma segunda estratégia de impressão, com ácido oleanólico como molde, também foi explorada. Embora não se tenha verificado reconhecimento molecular nas condições testadas, os polímeros funcionalizados mostraram melhor retenção face à celulose nativa, com potencial para otimização em sistemas com pH ajustado. Este trabalho propõe uma abordagem modular e sustentável para o design de solventes aplicados à valorização da folha de oliveira. Contribui para o avanço das tecnologias de extração seletiva e estabelece bases para futuras aplicações no contexto da bioeconomia circular.

Palavras-chave: Polímeros molecularmente impressos; Folha de oliveira; Adsorção seletiva; Compostos bioativos; Bioeconomia circular.

Index

Index of Figures

Index of Tables

Appendix List

Abbreviations List

4VP - 4-vinylpyridine

ACN - Acetonitrile

AGET - Activators Generated by Electron Transfer ATRP

AGU - Anhydrous Glucose Units

ATRP - Atom Transfer Radical Polymerization

BET - Brunauer-Emmett-Teller

BIBB - α-Bromoisobutyryl Bromide

CF - Cellulose Fibers

CF-Br - Cellulose Fibers modified with BIBB

DMAEMA - Poly(2-(dimethylamino)ethyl methacrylate)

DMAP - 4-Dimethylaminopyridine

DMF - Dimethylformamide

EGDMA - Ethylene Glycol Dimethacrylate

EtOH - Ethanol

FTIR-ATR - Fourier Transform Infrared Spectroscopy with Attenuated Total Reflectance

FTIR - Fourier Transform Infrared Spectroscopy

HPLC-DAD - High-Performance Liquid Chromatography with Diode Array Detector

IF - Imprinting Factors

MCC - Microcrystalline Cellulose

MCC-Br - Microcrystalline Cellulose modified with BIBB

MIP - Molecularly Imprinted Polymer

NIP - Non-Imprinted Polymer

NMP - Nitroxide-Mediated Polymerization

PMDETA - N,N,N′,N″,N‴-Pentamethyldiethylenetriamine

RAFT - Reversible Addition-Fragmentation Chain Transfer

SPE - Solid Phase Extraction

SBET - Specific Surface Area (BET Method)

SI-ATRP - Surface-Initiated Atom Transfer Radical Polymerization

STY - Styrene

UV-Vis - Ultraviolet-Visible Spectroscopy

1. Introduction

Olea europea L. (**Figure 1**), mostly known as the olive tree, is native to the Mediterranean basin and is characterized by a rich heritage of clonally propagated traditional varieties [1], [2]. Adapted to diverse climates, the olive tree has spread globally, producing approximately 2.564 million tons of olive oil in the 2023/2024 crop year. However, projections for 2024/2025 estimate a significant increase to 3.375 million tons, marking a 32% growth in global production [3].

Figure 1: Olea europea L.

Portugal exemplifies this global trend, ranking fourth in Europe in olive oil production during the 2023/2024 crop year, with an estimated 160,900 tons, reflecting a 28% increase compared to the previous year [3]. This achievement was possible because of the 361.177 thousand hectares of olive groves, 97.6% of which were dedicated to olive oil production, with the potential to become even bigger in the next decade. However, the increase of production also leads to greater subproduct generation during olive harvesting and olive oil production. This includes large quantities of leaves (**Figure 2**), olive pulp, pits and water. The disposal of these subproducts poses environmental risks, making sustainable subproduct management essential [1], [4].

Among these subproducts, olive leaves are often discarded by being burned or used as animal feed, but these leaves are a valuable source of cellulose, lignin, and bioactive compounds, such as secoiridoids (e.g., oleuropein, oleuroside), flavonoids (e.g., luteolin, quercetin) and many other phenolic molecules among lipids and volatiles. Thanks to the antioxidant and anti-inflammatory properties of these compounds, olive leaves hold great potential in diverse industries, including cosmetics, food, chemical, nutraceutical and pharmaceuticals [1], [4], [5], [6].

Figure 2: Sequential representation of the traditional olive harvesting process and the accumulation of leaves in the field. a) Preparation of the harvesting area with nets placed under the olive trees. b) Harvesting process, where olives and leaves fall onto the nets. c) Post-harvest stage, large accumulation of olive leaves left on the soil.

Olive leaf valorization depends on the development of stable, sustainable and economically feasible processes for the extraction of key compounds. In this regard, sorption and desorption processes are often considered, implementing commercial resins such as Reillex 402, Reillex 425 or XAD4 [5], [7]. However, there are challenges in processing diluted streams that contain various other compounds. To address this issue, the development of tailored sorbents specifically designed to extract specific compounds from olive leaf extracts using sorption and desorption techniques is being explored [5], [8].

Cellulose, derived from raw biomass, is an excellent choice for producing these types of sorbents, as it is abundant, renewable and biodegradable. More importantly, cellulose offers ease of interaction and modification due to its repeating anhydrous glucose units (AGU) covalently linked by acetal bonds, which contain numerous hydroxyl groups (OH). These OH groups along the macromolecule chains are easily modified through interactions with functional groups, resulting in a wide range of cellulose derivatives [9], [10].

The grafting of synthetic polymers onto cellulose backbones, especially via Atom Transfer Radical Polymerization (ATRP), enables the formation of hybrid materials that combine the biodegradability of cellulose with the enhanced functionality of the synthetic polymer. This modification improves the sorption capabilities of cellulose, making it highly effective in targeting specific compounds, including ions, dyes, and bioactive compounds. For instance, cellulose modified with polymers like poly(4-vinylpyridine) has proven particularly efficiency in adsorbing heavy metals and polyphenols [9], [11], [12], [13].

While modified cellulose-based sorbents show enhanced sorption capabilities, challenges in selectivity remain when targeting specific molecules, especially when in the presence of complex mixtures encountered in vegetable matrices. In this context, Molecularly Imprinted Polymers (MIPs) emerge as a promising solution. MIPs are polymer networks designed with tailor-made cavities that

exhibit high specificity and strong binding affinity for a particular target molecule. Once the polymer network is formed, the resulting binding sites maintain their structural stability, allowing repeated cycles of target molecule uptake and release [5], [6], [14], [15], [16].

In this context, the development of molecularly imprinted particles with a base of modified cellulose via ATRP, can be considered an efficient way of exploitation of target molecules [14]. The present study will explore this approach to develop tailored materials for the valorization of olive leaf and olive oil subproducts through sorption/desorption processes.

2. Olive oil production subproducts and their valorization potential

The global demand for agricultural products is increasing, driven by population growth and changing diets. However, this growth presents sustainability challenges, including resource limitations and the impacts of climate change. The bioeconomy framework, which focuses on turning renewable resources and agricultural subproducts into valuable products like food, feed, and bio-based materials, provides a promising solution [17].

In Europe, the olive oil industry generates 9.6 million tons/year of subproducts, including olive leaves, olive pomace and stone, pits and wastewater [17]. These subproducts are generated at different stages of the olive oil production process, as illustrated in **Figure 3**. Improper disposal of these subproducts poses significant environmental risks due to their phytotoxic properties, particularly olive mill wastewater, which can harm the ecosystems if directly released [1], [2], [17], [18]

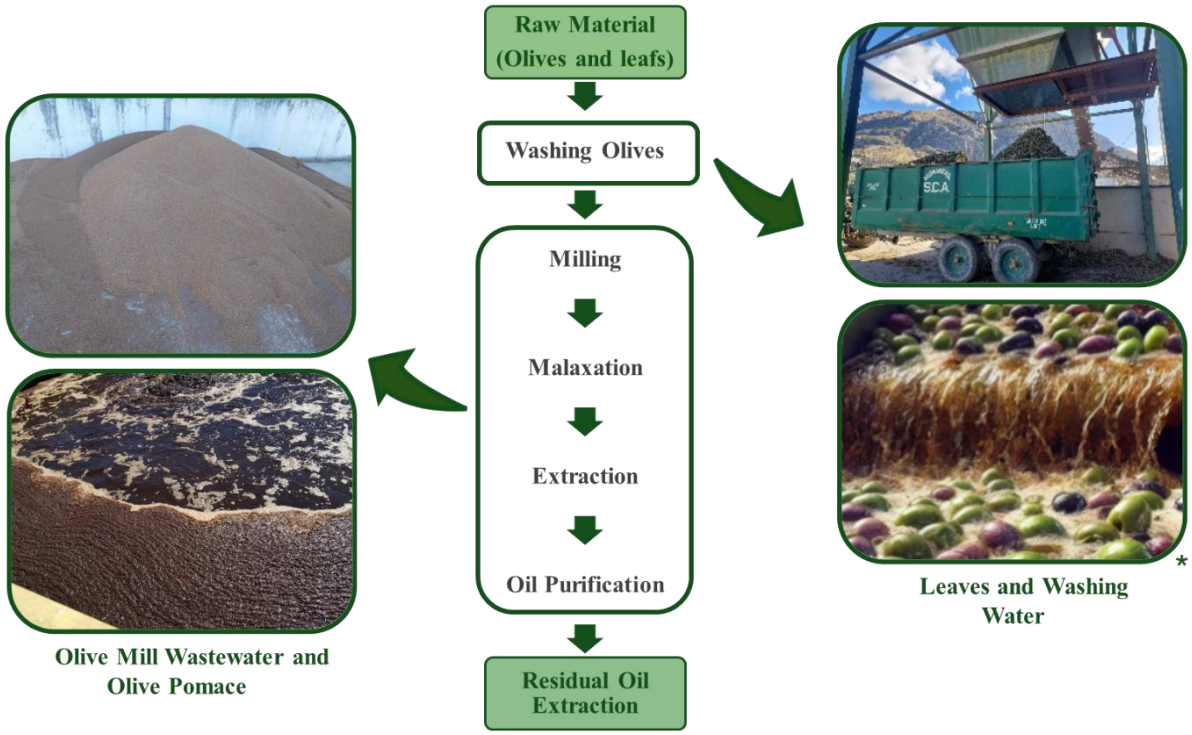

Figure 3: Layout of the main stages of olive oil production and the subproducts generated during the process. *Source: generated by AI.

Each year, the global olive industry generates approximately 4.5 million tons of olive leaves, produced abundantly during tree pruning, representing about 10% of the total weight of harvested olives [19], [20].

Current practices typically channel olive leaves towards energy generation, composting, or direct field application [17], [18]. Economic and sustainability incentives increasingly favour the valorization of these subproducts, primarily due to their richness in bioactives. These can be classified

into several families based on their chemical structure and biological activity. **Table 1** provides an overview of the compound groups found in olive leaves, along with representative compounds and their properties [18], [19], [21].

Table 1: Classification of bioactive compounds found in olive leaves, categorized into groups and subgroups and some examples of key compounds along with their biological properties.

Group	Subgroups	Compounds	Properties	References
Phenolic compounds	Simple phenols and phenolic alcohols	Hydroxytyrosol, tyrosol and, hydroxytyrosol-glucoside	Antioxidant properties	[18], [19], [21], [22]
	Secoiridoids	Oleuropein, demethyloleuropein, oleuropein aglycone and ligstroside	Anti-inflammatory, antihypertensive, and hypoglycemic properties	[18], [21], [22]
	Flavonoids	Quercetin, luteolin, rutin, apigenin, and their glycosides	Antioxidant and anti-inflammatory properties	[18], [21], [22]
	Lignans	Pinoresinol, acetoxypinoresinol and syringaresinol	Antioxidant properties and potential applications in cancer prevention	[18], [21]
	Phenolic acids	Caffeic acid, p-coumaric acid, ferulic acid, vanillic and homovanillic	Overall bioactivity of the subproducts	[18], [19], [21]
Triterpenic acids	-	Maslinic and oleanolic acid	Anti-inflammatory and antitumor properties, antioxidant and hepatoprotective effects	[18]
Tocopherols (vitamin E compounds)	-	α-Tocopherol, β-tocopherol, α-tocotrienol γ-tocopherol and α-tocopherol	Prevent oxidative stress in biological systems.	[18]

Polyphenols are of particular interest due to their abundance and are classified into several groups, such as simple phenols and phenolic alcohols, secoiridoids, flavonoids, lignans and phenolic acids. Some key compounds within these groups include oleuropein, hydroxytyrosol, tyrosol, luteolin and quercetin. These compounds are widely recognized for their strong antioxidant, anti-inflammatory, antimicrobial, and cardio-protective properties. Beyond health applications, they are also integrated in

cosmetics, offering anti-aging and antimicrobial benefits [18], [19], [21], [23]. **Figure 4** shows the chemical structures of selected compounds, helping to visualize their molecular diversity.

To fully harness the potential of these compounds, significant challenges must be addressed, particularly in their selective extraction from complex subproducts matrices. Advanced and efficient extraction methods are essential to recover these high-value compounds and integrate them effectively into a sustainable bioeconomy framework [18].

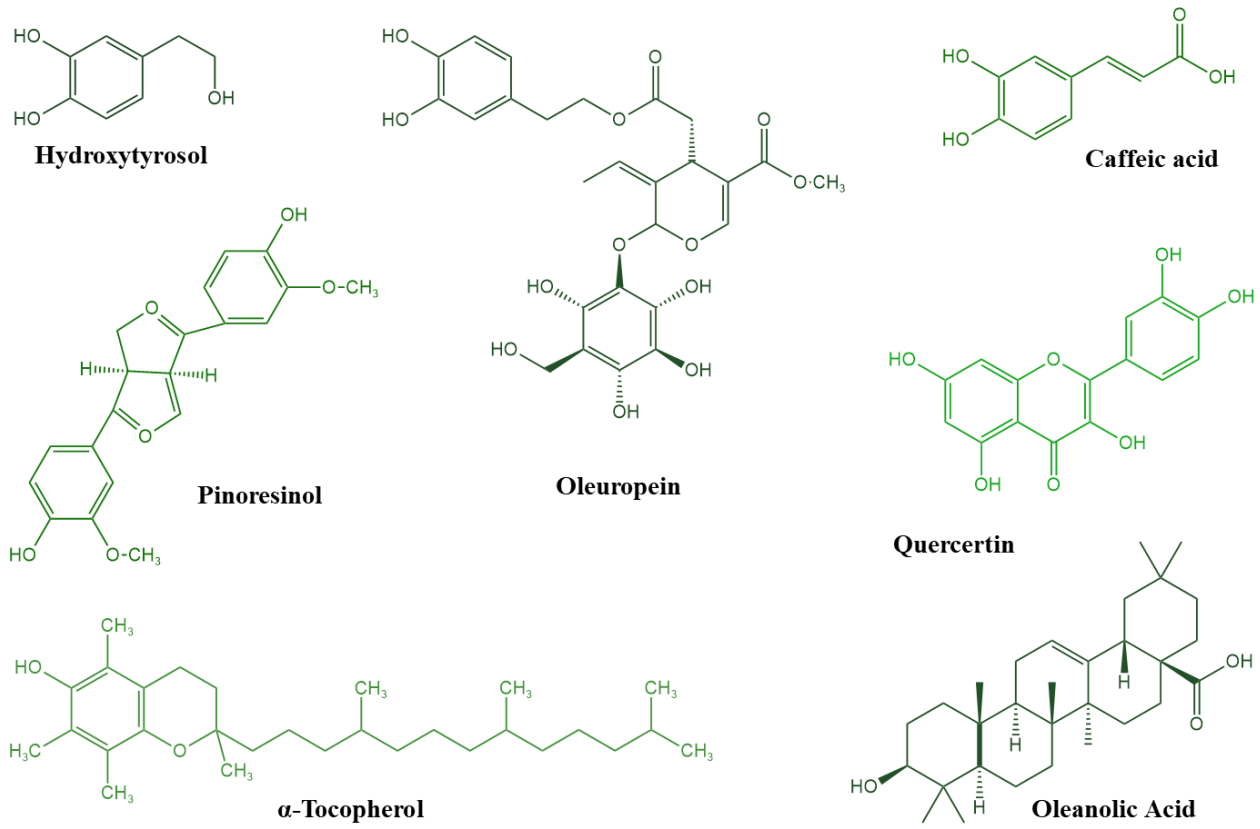

Figure 4: Chemical structure of some bioactive compounds present in olive leaves.

Sorption plays a crucial role in overcoming these challenges by allowing the separation and concentration of valuable compounds from complex mixtures. This technique enables the enrichment and purification of target compounds while maintaining their bioactive properties, making it indispensable for integrating polyphenols into various applications [8], [23].

In addition to sorption, various conventional and non-conventional extraction techniques, including solvent extraction, distillation, ultrasonication, microwave-assisted extraction, and sub- or supercritical fluid extractions, have been employed to recover high-added-value compounds from olive oil subproducts. These methods can be efficient and reduce extraction time but often require specialized equipment, precise control to prevent damage to sensitive compounds and come with high costs and complex operational requirements [23], [24], [25].

In contrast, sorption provides a simpler, more cost-effective alternative that is both scalable and energy efficient [7], [8], [15]. Unlike olive mill wastewater, which is a liquid waste stream that can be processed directly through sorption-based recovery methods, olive leaves require an initial extraction step to obtain solutions rich in bioactives before sorption can be applied. Despite this additional step, sorption remains advantageous as it minimizes the use of solvents, preserves the integrity of bioactive compounds, and integrates easily into industrial processes. These advantages make it a better choice for the sustainable extraction and concentration of valuable compounds from natural sources, particularly in the valorization of solid subproducts like olive leaves [5], [8].

The olive oil industry exemplifies the potential of a bioeconomy framework to transform agricultural subproducts into high-value resources. By leveraging simple fractionation techniques, such as sorption and advanced technology like surface imprinting, it is possible to recover bioactive compounds with significant applications in food, pharmaceuticals, and cosmetics, paving the way for a more sustainable and circular agricultural economy.

3. Molecularly imprinted polymers (MIP's) for selective sorption

3.1. Principles of molecular imprinting and MIP design

MIPs are synthetic materials designed to have high specificity for a target molecule (template), achieved through the formation of binding sites complementary in size, shape, and functional groups to the template molecule. This specificity is achieved through a process called molecular imprinting, where a template molecule interacts with functional monomers during polymerization. Once the polymer is formed, the template is removed, leaving behind cavities that can selectively bind to the target molecule [6], [15], [26]. This process is illustrated in **Figure 5**, using quercetin as a model template. This ability to create highly specific binding sites has made MIPs highly valuable in applications such as separation and purification [6], [15], [26].

The role of the template molecule is crucial to the molecular imprinting process. By guiding the arrangement of functional monomers, the template ensures that the resulting polymer network has high affinity for the target compound. The interactions between the template and monomers can be covalent, non-covalent, or semi-covalent, each offering different advantages. Non-covalent interactions, such as hydrogen bonding and π-π stacking, are commonly employed because they facilitate mild conditions and rapid rebinding during use [8], [15].

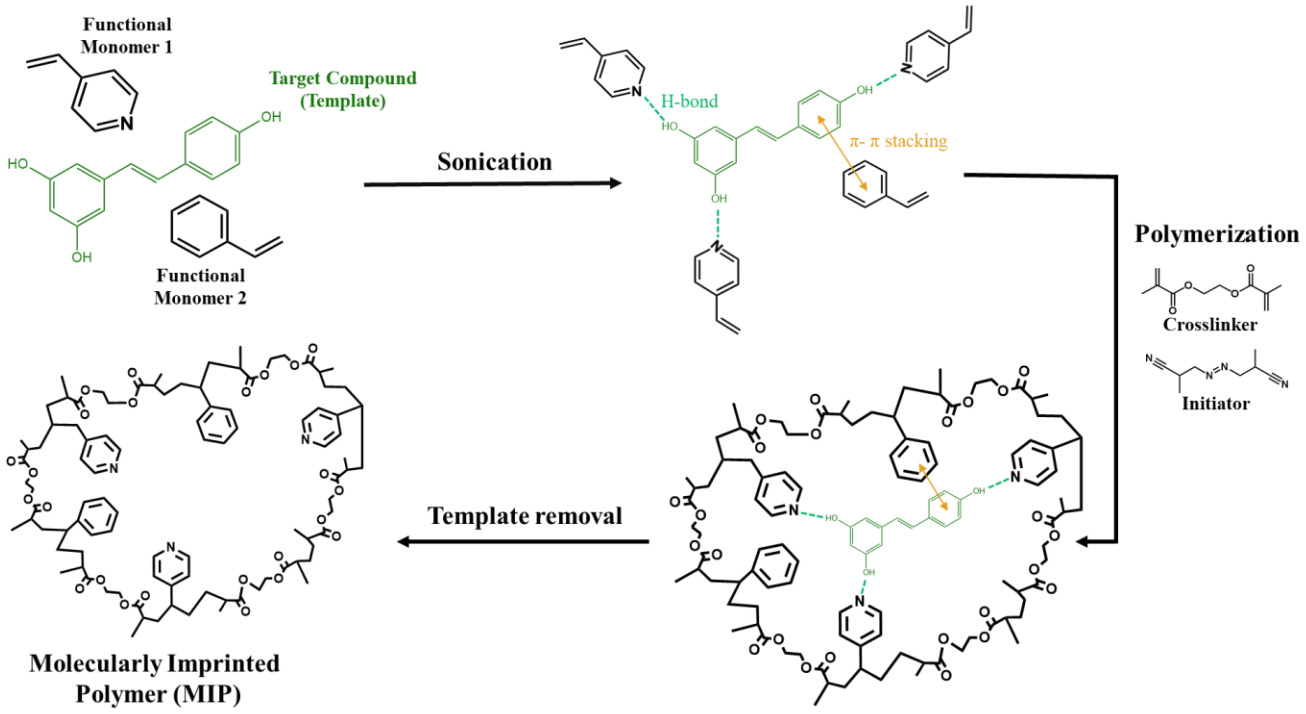

Figure 5: Schematic representation of the polymerization of a quercetin MIP.

The performance and specificity of MIPs relies on several critical design factors, including the choice of functional monomers, crosslinking agents, polymerization techniques, and template-monomer interactions. Each of these components plays a distinct role in determining the efficiency and selectivity of the final material [15].

At the core of MIP formation, functional monomers interact with the template molecule during polymerization, creating complementary binding sites. The selection of these monomers is guided by their ability to establish strong and specific interactions with the target, whether through hydrogen bonding, ionic forces, or other mechanisms. Careful selection ensures that the imprinted sites achieve the necessary precision and effectiveness, ultimately enhancing the polymer's affinity for the target molecule, by forming a rigid network around the template molecule during polymerization [5], [8], [9]. The selection of the crosslinking agent is also important in defining the polymer's physical properties, with key factors such as rigidity, porosity, and durability playing a vital role in maintaining the selectivity and effectiveness of MIPs [8], [15].

The polymerization technique chosen is essential in MIP design, as it affects particle size, porosity, and overall binding efficiency. Bulk polymerization, though commonly used for large-scale production, can result in heterogeneous particle sizes and reduced binding performance. Precipitation polymerization, in contrast, produces more uniform particles but requires precise control of reaction conditions to achieve optimal results. Among these methods, inverse suspension polymerization stands out for generating larger, porous particles with enhanced surface area and improved accessibility to binding sites, making it a preferred choice for applications requiring high sorption capacity [8], [15].

The interactions between the template and monomer determine the specificity and functionality of the resulting binding sites. Covalent imprinting offers precise and stable binding site formation but requires rigorous conditions for template removal, which can limit its practicality. Non-covalent imprinting, while more flexible and widely used, relies on weaker interactions such as hydrogen bonding and ionic forces, which can occasionally result in non-specific binding. A balance between these methods can be achieved through semi-covalent imprinting, which combines covalent bonds during polymerization with non-covalent interactions during rebinding, offering improved specificity and easier template removal. Optimizing these interactions involves not only selecting suitable monomers but also controlling external factors such as solvent and polymerization conditions to ensure robust and selective binding site formation [8], [15].

3.2. Application of MIPs in olive subproduct valorization

Olive subproducts, such as leaves and pomace, are rich in bioactive compounds like polyphenols, flavonoids, and secoiridoids. These compounds are highly valued for their antioxidant, anti-inflammatory, and antimicrobial properties. However, their extraction and purification are challenging due to the complexity of the mixtures in which they are found. Studies have demonstrated that MIPs offer a solution to these challenges, by enabling the selective sorption of target compounds from these complex matrices. For example, MIPs have demonstrated high efficiency in isolating phenolic compounds, such as flavonoids (e.g., quercetin) and secoiridoids (e.g., oleuropein), from olive leaf extracts, even in complex mixtures with competing compounds [8], [16], [27].

Targeted extraction using advanced materials like MIPs combines precision and efficiency, maintaining binding capacity and selectivity across multiple sorption-desorption cycles. This capability enables the recovery of specific bioactives with high enrichment factors, making it possible to produce high-purity fractions from agricultural subproduct [8], [16], [27].

In olive subproduct valorization, these polymers offer significant benefits. Their remarkable specificity reduces the need for extensive downstream purification, simplifying the process and boosting overall efficiency. Additionally, their energy-efficient sorption-desorption mechanisms outperform traditional methods, cutting energy costs and environmental impact. By enabling the recovery of valuable compounds from agricultural subproducts, these technologies also advance sustainability goals, aligning with the principles of the circular bioeconomy [8], [16], [27].

3.3. Innovations in MIP technology

The field of MIPs has undergone significant advancements, driven by innovations in material design and polymerization techniques. These developments aim to improve their selectivity, efficiency, and scalability for diverse applications, particularly in the recovery of valuable bioactive compounds from complex matrices [5], [9].

One notable innovation is surface imprinting, which addresses challenges related to the accessibility of binding sites in traditional bulk-imprinted MIPs. By forming a thin imprinted layer on the surface of materials, surface imprinting enhances the availability of binding sites, reducing mass transfer limitations and improving the overall binding efficiency. This approach ensures faster interactions between the target molecules and the imprinted sites, making surface-imprinted MIPs especially suitable for applications requiring high specificity and rapid sorption-desorption cycles [5], [9].

Another transformative advancement is the integration of ATRP into imprinting technology. It is a controlled radical polymerization technique that uses a transition metal catalyst and a halogen-based initiator to regulate the activation and deactivation of growing polymer chains. This precise control allows for the synthesis of polymers with uniform chain lengths and well-defined architecture.

By integrating ATRP with molecular imprinting, materials with enhanced specificity, stability, and controlled porosity can be developed. This approach demonstrates the versatility of ATRP in functionalizing cellulose-based materials for selective sorption, enabling the efficient isolation of high-value bioactive compounds from complex mixtures [5], [9]

The development of continuous sorption systems incorporating MIPs represents another major step forward. By enabling cyclic sorption and desorption, continuous systems reduce downtime and operational costs while maintaining high recovery rates of target compounds. This approach has proven particularly effective in processing complex mixtures, such as agricultural subproduct, where precise fractionation of valuable compounds is required. Continuous sorption systems also align with sustainable processing goals by minimizing waste and energy consumption, further demonstrating the potential of MIPs in industrial scale applications [5], [9].

These innovations have significantly expanded the capabilities of MIPs, enabling their application in more complex and demanding processes. By focusing on enhancing selectivity, structural control, and scalability, these advancements lay the groundwork for broader adoption of MIP technology across various sectors.

4. Cellulose as a backbone in molecularly imprinted polymers

4.1. Advantages of using cellulose in MIP-based sorbents

Cellulose is the most abundant biopolymer on Earth, sourced from diverse plant and raw biomass materials. Its biocompatibility, derived from its natural origin, non-toxic properties and, its renewability makes it ideal for applications in food, pharmaceuticals, and environmental remediation [9], [10].

The structural properties of cellulose are composed by repeating anhydrous glucose units (AGU) that are covalently connected by acetal bonds containing high density hydroxyl groups (OH), as illustrated in **Figure 6**. The OH groups are easily modified by interacting with functional groups, providing reactive sites for chemical modification, enabling the creation of tailored active sites for specific binding [10].

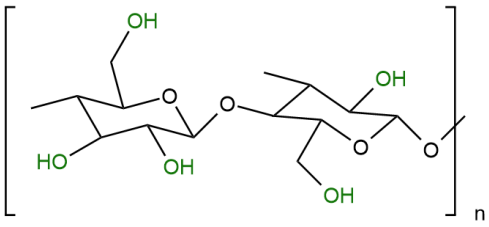

Figure 6: Chemical structure of cellulose.

These qualities make cellulose a sustainable choice to use as the backbone of MIPs. Moreover, the inherent rigidity and crystallinity of cellulose contribute to the stability of MIPs, ensuring that the polymer matrix maintains its structural integrity during repeated sorption-desorption cycles [9], [10].

Compared to synthetic polymer-based MIPs, cellulose-based MIPs present a reduced environmental impact. Synthetic polymers often involve non-renewable raw materials and energy-intensive production processes, where cellulose-based systems utilize biodegradable and renewable resources. Furthermore, the disposal of cellulose-based MIPs is more environmentally friendly due to their natural degradation pathways, which significantly lowers the risk of microplastic pollution [9], [10].

4.2. Modification of cellulose for enhanced sorption in MIPs

The modification of cellulose backbone is a critical step to enhance the performance of MIPs. Various strategies can be employed to create active sites on cellulose and improve its compatibility with the functional monomers and crosslinkers used during imprinting [9], [10].

Two primary strategies are used to modify cellulose: chemical modified and physical modification. Chemical modification involves processes such as surface modification that works by attaching reactive groups like hydroxyl, carboxyl, or sulfonate to the cellulose backbone. The material's binding specificity is enhanced, by improving its interactions with template molecules and making it more effective in sorption processes. It also includes grafting techniques, such as Atom Transfer Radical Polymerization (ATRP) and Reversible Addition-fragmentation Chain Transfer (RAFT) that enable the attachment of synthetic polymers to cellulose [13]. These hybrid materials provide tailored binding sites while preserving cellulose's natural advantages [9], [10], [13].

Physical modifications enhance the structural properties of cellulose by altering its morphology and stability, making it more suitable for various applications. One key approach is crosslinking, which reinforces the cellulose network, creating a mechanically robust and chemically stable structure. This structural reinforcement improves durability, allowing the material to withstand multiple sorption and desorption cycles without significant degradation. Another crucial technique is nanostructuring, where cellulose is converted into nanocrystals or nanofibers. This transformation dramatically increases the surface area, leading to a higher density of active sites available for molecular interactions. As a result, nanostructured cellulose exhibits superior performance in molecular imprinting and sorption processes, as well as improved compatibility with functional monomers and crosslinkers used in polymerization. These modifications, though distinct from chemical modification, play a vital role in optimizing cellulose-based materials for advanced applications [9], [10]

Chemical modifications are pivotal in boosting cellulose's affinity for target molecules. Carboxylation, for instance, introduces carboxylic acid groups (-COOH), which enhance the material's ability to form hydrogen bonds and ionic interactions with target molecules. Similarly, sulfonation adds sulfonic acid groups (-SO3H), increasing cellulose's affinity for polar and positively charged compounds. By combining these chemical modifications with polymer grafting, hybrid materials with superior sorption properties can be developed [9], [10].

Modifications of cellulose significantly enhance its mechanical strength and recyclability, making it crucial for its use in MIPs. Crosslinking improves structural stability, enabling the material to endure repeated sorption cycles and high-pressure conditions. Additionally, functional groups introduced through chemical modifications, such as carboxylation and sulfonation, ensure consistent performance over multiple uses. These enhancements make cellulose-based MIPs both durable and sustainable, offering long-term efficiency in various applications while maintaining environmental benefits [9], [10].

5. Atom transfer radical polymerization (ATRP) in sorbent development

5.1. Introduction to ATRP and its advantages in sorbent design

ATRP is a controlled radical polymerization technique that has revolutionized polymer science by allowing precise control over molecular architecture. The process is governed by a dynamic equilibrium between propagating radicals and dormant species, primarily in the form of alkyl halides (P_nX). Dormant species periodically react with the rate constant of activation (k_{eact}) with transition with a transition metal complexes in its lower oxidation state (Mt^m/L) to form active radicals (P_{n^*}), which propagate the polymer chain. Simultaneously, a higher oxidation state metal complex ($X - Mt^{m+1}/L$) deactivates these radicals, regenerating the dormant species. This reversible activation and deactivation (k_{deact}) cycle minimizes termination reactions and ensures controlled polymer growth. Copper-based catalysts are commonly used in ATRP due to their efficiency, with ligands stabilizing the metal complexes and influencing reaction kinetics. This equilibrium is crucial for achieving polymers with narrow molecular weight distributions and well-defined architectures [12], [28]. This mechanism is schematically illustrated in **Figure 7**.

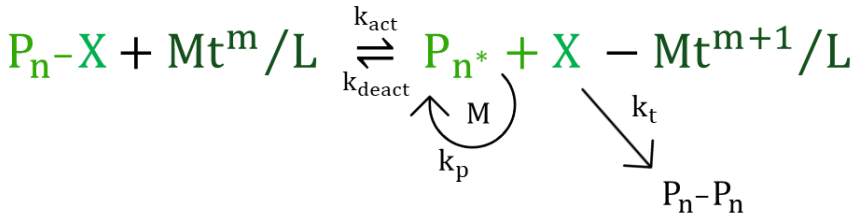

Figure 7: ATRP equilibrium, showing the activation and deactivation of the polymer chain, the role of the metal catalyst, and the propagation and termination steps. Adapted from: Matyjaszewski, 2012.

The advantages of ATRP in sorbent design are profound. By enabling the creation of well-defined polymer architectures, this technique facilitates the introduction of specific functional groups with a high degree of precision. This is particularly valuable for designing sorbents with tailored binding affinities and selective sorption capabilities. Its versatility in polymerization extends to a wide range of monomers, allowing for the synthesis of block copolymers, star-shaped polymers, and graft copolymers. These structures are ideal for applications that require precise interaction with target molecules [11], [12].

When compared to other polymerization methods, such as RAFT or NMP (Nitroxide-Mediated Polymerization), ATRP offers superior flexibility in designing complex polymer architectures. Additionally, advancements like AGET (Activators Generated by Electron Transfer) ATRP and ARGET (Activator Regeneration by Electron Transfer) ATRP have reduced the environmental impact of this technique by lowering the required concentrations of transition metal catalysts to ppm levels.

These "green" ATRP approaches address concerns about catalyst removal and environmental sustainability while maintaining excellent control over polymerization [11], [12].

ATRP stands out for its ability to produce high-performance sorbents with minimal environmental impact and exceptional structural precision. This makes it an indispensable tool in modern sorbent design, providing solutions that are both effective and sustainable.

5.2. ATRP in the functionalization of cellulose-based sorbents for olive subproducts valorization

ATRP plays a transformative role in the functionalization of cellulose-based sorbents, particularly in the valorization of olive oil industry subproducts. Through this technique, functional groups such as carboxyl, sulfonate, and hydroxyl are grafted onto cellulose surfaces, influencing the precise control of polymer chain growth, allowing the creation of tailored sorbents with high specificity, binding efficiency and enhanced sorption capacity [11], [13]. This process is illustrated in **Figure 8**, which shows the ATRP reaction on cellulose, including surface modification and subsequent polymer growth.

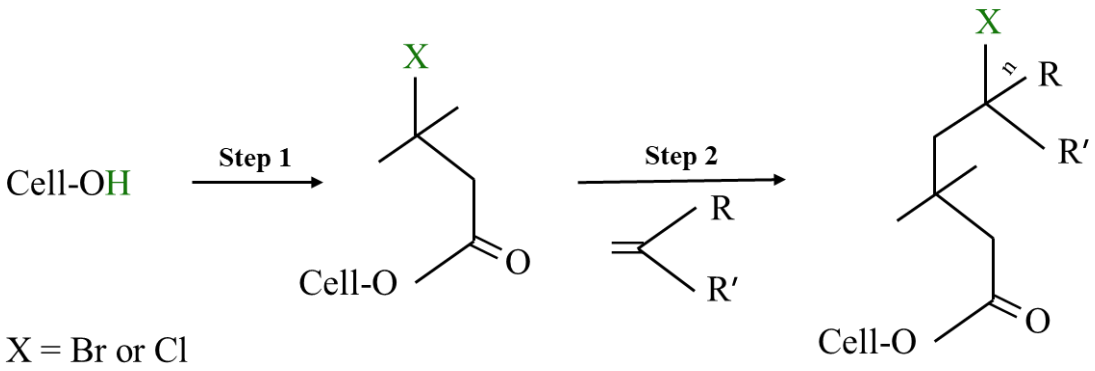

Figure 8: Schematic representation of the ATRP reaction on cellulose. In Step 1, the hydroxyl group of cellulose is modified with a halogenated initiator (X = Br or Cl). In Step 2, polymerization occurs, leading to the growth of polymer chains from the cellulose backbone. Adapted from: Mondal Editor, n.d.

Studies have shown that this technique has been effectively used to modify cellulose for the selective sorption and enrichment of bioactive compounds from olive oil industry subproducts, particularly flavonoids and polyphenols. Hybrid materials synthesized via ATRP have demonstrated remarkable performance in sorption/desorption processes. These materials are designed by grafting synthetic polymer chains onto cellulose using ATRP, resulting in highly functionalized surfaces with enhanced specificity and binding efficiency for target compounds, from complex mixtures [5], [9], [13].

In addition to selectivity and sorption capacity, ATRP offers numerous benefits in developing robust cellulose-based sorbents. The method's precise control over polymerization parameters allows the synthesis of highly functionalized materials with uniform properties making them well suited for industrial applications, including large-scale valorization of olive subproducts [5], [9], [13].

5.3. Integration of ATRP and molecular imprinting for tailored cellulose-based sorbents

The combination of cellulose modification via ATRP and MIPs offers a powerful strategy for developing advanced sorbents with high selectivity and efficiency. By merging the natural abundance, biodegradability, and versatility of cellulose with the precision of ATRP and the specificity of molecular imprinting, hybrid materials can be tailored to selectively target and enrich valuable bioactive compounds [5], [9].

The preparation of these hybrid particles typically follows a two-step procedure. First, cellulose, which can be microcrystalline cellulose (MCC) or another form such as nanocellulose (NC) or cellulose fibers (CF), is modified to introduce initiating sites for controlled polymerization. This modification step often involves the reaction of the hydroxyl groups on the cellulose surface with a reagent, such as α-bromoisobutyryl bromide (BIBB), to create ATRP macroinitiator particles. This modification allows the cellulose to serve as a reactive platform for polymer growth, enabling the subsequent grafting of synthetic polymers. Analytical techniques like Fourier transform infrared spectroscopy (FTIR) are commonly used to confirm successful modification through the detection of chemical changes, such as the formation of ester bonds [5], [9].

The second step involves grafting a synthetic polymer layer onto the modified cellulose via ATRP. Functional monomers, such as 4-vinylpyridine (4VP) or methacrylates, are polymerized in the presence of a crosslinker, like ethylene glycol dimethacrylate (EGDMA), to form a thin, crosslinked shell around the cellulose core. During this process a template molecule is incorporated into the reaction mixture to create molecularly imprinted cavities. After polymerization, the template is removed, leaving behind cavities that are complementary in size and functionality to the target molecule. These cavities enable the hybrid particles to selectively bind and enrich compounds such as flavonoids, phenolic acids, or other phenolic compounds [5], [9]. This two-step process is illustrated in **Figure 9**.

The molecular imprinting process enhances the material's ability to concentrate bioactive compounds, achieving enrichment factors of up to four times their original concentration. Quercetin is a great candidate to be used as a template due to its structural similarity to many flavonoids, this approach is adaptable to other target molecules depending on the application [5], [9].

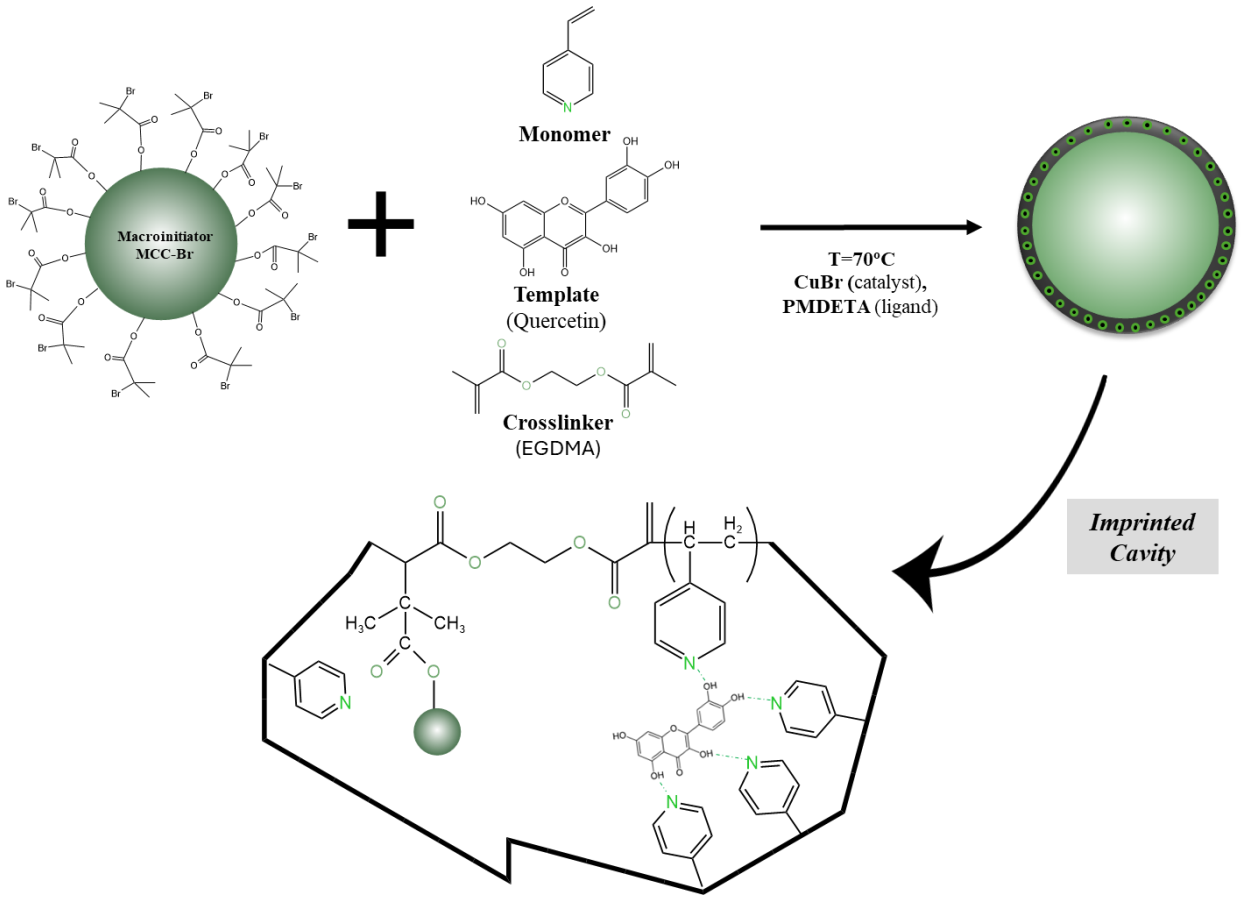

Figure 9: Schematic representation of the synthesis of cellulose-based MIPs. The process involves the grafting of a crosslinked polymer shell onto the macromolecular initiator (MCC-Br) using ATRP. The imprinting process occurs in the presence of a template molecule (quercetin), a functional monomer, and a crosslinker (EGDMA), leading to the formation of selective recognition cavities on the particle surface.

This process highlights the versatility of ATRP in creating functionalized cellulose-based materials with high specificity and binding efficiency, by leveraging the molecular imprinting technique, these hybrid materials are tailored for selective sorption, enabling the isolation of high-value bioactive compounds from complex mixtures. Their application in olive leaf valorization showcases their potential in circular bioeconomy efforts [5], [9]. The general nature of this approach ensures it can be extended to other plant sub-products and target compounds, offering a sustainable and scalable solution for bioactive compound enrichment.

6. Sorption-desorption processes for subproduct valorization

6.1. Mechanisms of sorption-desorption in MIPs

MIPs are designed to mimic biological recognition systems, making them highly effective for selective sorption-desorption processes. These mechanisms are governed by key molecular interactions, the structural features of the imprinted cavities, and the material's ability to maintain functionality over multiple cycles. Among the various interactions that influence MIP performance, hydrogen bonding, π-π stacking, hydrophobic interactions, and electrostatic forces all contribute to the material's specificity and sorption efficiency. However, hydrogen bonding and π-π stacking are the dominant forces, playing a pivotal role in ensuring high selectivity and strong binding affinity [5], [8], [15], [27].

Hydrogen bonding is the most frequently employed interaction in non-covalent molecular imprinting, ensuring high specificity during sorption. Functional monomers such as methacrylic acid and 4-vinylpyridine form strong hydrogen bonds with template molecules like flavonoids, stabilizing the imprinted sites and allowing for effective molecular recognition [5], [9], [15]. π-π stacking also plays a key role in the binding mechanisms of MIPs, particularly for aromatic bioactive compounds such as quercetin [14], [15]. These molecules interact strongly with aromatic functional monomers like styrene (STY) and 4-vinylpyridine (4VP), which are commonly incorporated into MIP synthesis to enhance specificity and sorption efficiency [26]. By leveraging these interactions, cellulose-based MIPs exhibit high selectivity for their target molecules, ensuring strong and efficient sorption. During desorption, these interactions are strategically disrupted using solvents, temperature manipulation, or pH adjustments, weakening the hydrogen bonds or destabilizing π-π interactions to release the target compound [5], [9]. Studies on cellulose-based MIPs demonstrate that these imprinted particles maintain high sorption capacity and retain their structural integrity even after repeated cycles, making them highly effective for extracting and recovering bioactive compounds from complex matrices [5], [9].

6.2. Comparing cellulose-based MIPs and conventional sorbents for bioactive compound valorization from subproduct

The comparison of cellulose-based MIPs and conventional sorbents, such as activated carbon, Reillex 402, Reillex 425, XAD4, XAD7HP, DAX8 and silica, reveals the unique advantages of these hybrid materials in terms of selectivity, reusability, and industrial applicability [5], [7], [9], [15], [26].

Traditional sorbents have shown effectiveness in sorbing a broad range of compounds due to their generalized interaction mechanisms, such as hydrophobic and van der Waals forces. However, its lack of specificity often leads to inefficiencies in separating valuable bioactive compounds from complex matrices [7], [9], [15]. In contrast, cellulose-based MIPs leverage molecular imprinting techniques to target and purify specific molecules (template) [5], [7], [9], [15].

Some studies have directly compared traditional resins and MIPs in their ability to retain phenolic compounds, such as quercetin. Resins with a high percentage of 4VP, such as Reillex 402 and Reillex 425, have demonstrated higher retention rates. Additionally, DAX8 and XAD7HP, which contain carbonyl functionalities, exhibited superior performance compared to XAD4 and silica. However, despite these variations in efficiency, none of these conventional resins matched the retention rate and selectivity achieved by MIPs [9], [26].

One of the major advantages of cellulose-based MIPs is their ability to maintain performance across multiple sorption-desorption cycles. Conventional sorbents like activated carbon often experience significant capacity loss after repeated use due to fouling or pore clogging [7], [15].

Conversely, the crosslinked polymer matrix of MIPs ensures that the imprinted cavities remain intact, preserving both selectivity and sorption capacity. For instance, cellulose-based MIPs designed for flavonoid recovery have been shown to retain their binding efficiency and selectivity over multiple cycles, while conventional sorbents show diminished efficiency in similar applications [5], [7], [9], [15]. In terms of operational costs, the selectivity of cellulose-based MIPs reduces the need for extensive downstream purification, since they can specifically isolate only the target compounds [5], [9], [15].

6.3. Desorption techniques and sorbent regeneration

Desorption is a critical step in sorbent-based processes, as it facilitates the recovery of target compounds while allowing the sorbent material to be regenerated for subsequent cycles. Effective desorption techniques ensure the release of target molecules without compromising the structural integrity or functionality of the sorbent. In MIPs, the choice of desorption method is influenced by the nature of the molecular interactions between the sorbent and the target molecule, as well as the operational requirements of the process [5].

Several techniques are commonly employed for desorption. Solvent-based desorption is one of the most widely used methods, leveraging solvents that disrupt the interactions between the target molecule and the imprinted cavities. For instance, hydroalcoholic mixtures or organic solvents like

ethanol and methanol are effective in releasing hydrophobic or polar compounds, such as flavonoids and polyphenols, from cellulose-based MIPs [5], [9]. Studies have shown that selective desorption processes are often triggered by using a sequence of solvents with different elution strengths and/or temperature modifications mechanisms [5], [9].

pH-adjusted desorption is another technique, where the pH of the desorption solution is altered to weaken hydrogen bonds or disrupt ionic interactions. This method is particularly effective for traditional sorbents targeting bioactive with pH sensitive functional groups, allowing efficient release under mild conditions that preserve the sorbent's functionality [7]. Thermal desorption, although less commonly used for bioactive, involves heating the sorbent to break physical or chemical interactions, such as van der Waals forces or weak hydrophobic interactions, and is often applied in gas-phase adsorption processes in traditional sorbents [7].

Despite the effectiveness of these techniques, there are significant challenges in maintaining the integrity and functionality of sorbents during repeated sorption-desorption cycles. For MIPs, the crosslinked polymer structure provides robustness, ensuring that imprinted cavities retain their specificity and binding capacity across multiple cycles. However, excessive use of aggressive solvents or extreme pH conditions can lead to chemical degradation or loss of active functional groups on the sorbent surface, reducing its efficiency over time. Additionally, thermal desorption, if not carefully controlled, may cause structural damage to the polymer matrix or degrade temperature-sensitive target molecules [5].

Maintaining sorbent integrity requires optimizing the desorption protocol to balance effective compound recovery with minimal impact on the sorbent material. Advancements in molecular imprinting and polymer synthesis, such as ATRP-functionalized cellulose-based MIPs, have improved the resilience of sorbents [5], [7].

The choice of desorption technique and optimization of conditions are vital for preserving the functionality and longevity of sorbents, particularly in MIPs. By addressing challenges associated with repeated cycles, MIPs continue to emerge as robust and sustainable materials for applications in bioactive compound recovery.

7. Prospects and innovations in sorbent-based subproduct valorization

The field of subproducts valorization using sorbents is evolving rapidly, with significant innovations in material design, process automation, and targeted applications. These advancements aim to enhance the efficiency, scalability, and sustainability of sorbent technologies for recovering high-value compounds.

The development of hybrid materials, which combine the properties of natural polymers like cellulose with synthetic polymers, is gaining prominence. By leveraging techniques such as ATRP and molecular imprinting, hybrid sorbents achieve enhanced selectivity, sorption capacity, and mechanical stability. Integration of nano-MIPs also represents another key advancement, offering significantly increased surface area to volume ratios, leading to enhanced mass transfer kinetics and binding efficiency. These materials are designed at the nanoscale using precision polymerization techniques, ensuring uniformity and highly accessible imprinted cavities [5], [7], [15].

Alongside these material innovations, automation and optimization of sorption processes are transforming the industrial application of sorbents. Automated systems incorporating advanced sensors, data analytics, and process control algorithms are improving the efficiency and consistency of sorption-desorption cycles. These systems allow real-time monitoring of key parameters, such as flow rates, sorbent saturation levels, and desorption efficiency, enabling precise adjustments to maximize recovery rates while minimizing energy and solvent use. Additionally, computational modelling and machine learning are being employed to optimize sorbent design and predict performance under various operating conditions [7], [15].

Research is increasingly focusing on leveraging sorbent technologies for the valorization of agricultural subproducts, such as those from olive oil production. An important area is the development of multifunctional sorbents that not only isolate target compounds, such as flavonoids, but also facilitate downstream processing, such as fractionation or chemical conversion. The use of bioinspired materials and green chemistry principles in sorbent synthesis is another emerging focus, aligning with sustainability goals and circular bioeconomy principles [5], [7], [15].

Further research is also needed to scale up cellulose-based MIPs production, reduce costs, and develop eco-friendly methods for sorbent regeneration. These efforts aim to maximize the recovery of high-value compounds, such as polyphenols, while minimizing waste and environmental impact [5], [7], [15].

The future of sorbent-based subproducts valorization lies in the continued innovation of materials, processes, and interdisciplinary approaches. Hybrid materials, nano-MIPs, and automation are leading the way in advancing the field, while research into sustainable and multifunctional sorbents promises to unlock the full potential of agricultural subproducts. These advancements will play a critical role in creating sustainable, high-value solutions for industries ranging from nutraceuticals to pharmaceuticals.

8. Materials and methods

8.1. Materials and equipment

This section presents the materials, reagents, and equipment used in the experimental work, including those required for cellulose modification, MIP synthesis, and polyphenol analysis.

8.1.1. Reagents used throughout the experimental work

Various chemical reagents were used throughout the experimental work. **Table 2**, lists the compounds used. For each reagent, information on chemical structure, molecular weight, density (when applicable), and supplier is provided to ensure traceability and reproducibility. All reagents were used as received, without further purification.

Table 2: Reagents used throughout the experimental work. For each compound, the chemical structure, molecular weight, density (when applicable), and supplier are provided.

Compounds	Chemical structure	Molecular weight (g/mol)	Density (g/mL)	Supplier
4-Dimethylaminopyridine (DMAP)	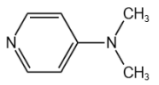	122.17	-	Sigma-Aldrich
4-Vinylpyridine (4VP)	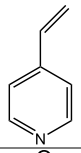	105.14	0.9890	Thermo scientific
Acetic acid glacial	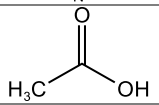	60.05	-	Fisher Scientific
Acetonitrile (ACN)	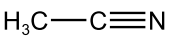	41.05	-	Fisher Scientific
Cellulose (MMC/CF)	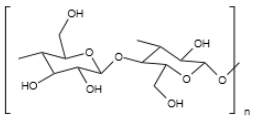	-	-	Sigma-Aldrich
Copper (I) bromide (CuBr)		-	4.710	Sigma-Aldrich
Dimethylformamide (DMF)	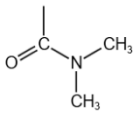	73.09	-	Fisher Scientific
Ethanol (EtOH)	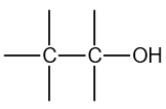	46.07	-	Fisher Scientific

Table 2: Continuation.

Compounds	Chemical structure	Molecular weight (g/mol)	Density (g/mL)	Supplier
Ethylene glycol dimethylacrylate (EGDMA)	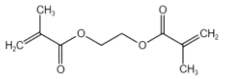	-	1.051	Sigma-Aldrich
Maslinic Acid	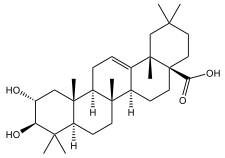	-	-	Cayman Chemical Company
Methanol	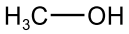	32.04	-	Fisher Scientific
N,N,N',N'',N'''-Pentamethyldiethylenetriamine (PMDETA)	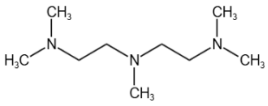	-	0.829	Sigma-Aldrich
Oleuropein	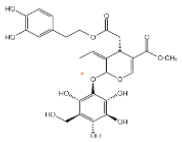	-	-	Cayman Chemical Company
Oleanolic Acid	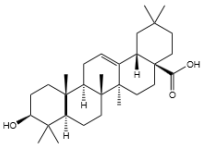	-	-	Acros Organics
Phosphoric acid	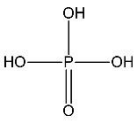	98.00	1.721	Labkem
Poly(2-(dimethylamino) ethyl methacrylate (DMAEMA)	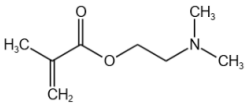	-	0.932	Sigma-Aldrich
Quercetin	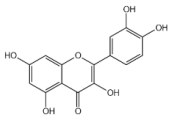	-	-	Sigma-Aldrich
Rutin	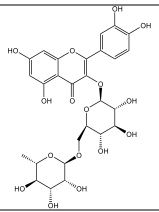	-	-	Acros Organics

Table 2: Continuation.

Compounds	Chemical structure	Molecular weight (g/mol)	Density (g/mL)	Supplier
Triethylamine	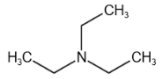	101.19	0.7280	Acros Organics
Vanillic Acid	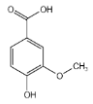	-	-	Sigma-Aldrich
α-Bromoisobutyryl bromide (BIBB)	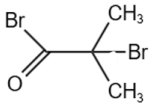	229.90	1.86	Sigma-Aldrich

8.1.2. Equipment

This section lists the main equipment used during experimental work, including instruments for synthesis, characterization, and analytical procedures. **Table 3** provides details of the additional equipment employed, specifying the model, brand, and software associated with each device.

Table 3*:* Additional equipment used, including model, brand, and software.

Equipment	Model	Brand	Software
Analytical balance	AS 220/C/2	RADWAG®	-
Centrifuge	CompactStar CS 4	VWR	-
	Centrifuge 5810 R	Eppendorf	-
FTIR	Spectrum Two™	Perkin Elmer	Spectrum IR
Heating/ stirring plate	VMS-C7	VWR Advanced	-
pH meter	Level 1	InoLab	-
Pump	P4.1S	KNAUER	-
SPE	Visiprep	Supelco	-
Ultrasound bath	Ultrassons-H	P SELECTA	-
	SW1	Sono Swiss	-
Vacuum hoven	VUS-B2V-M/VU 55	VACUCELL	-
Vacuum pump	R2O series	Ibx instruments	-

8.2. Experimental procedure

Several experimental procedures were carried out to synthesize and evaluate the performance of pyridyl-functionalized cellulose-based sorbents. These procedures encompassed the surface modification of cellulose via ATRP, the synthesis of molecularly imprinted and non-imprinted polymers (MIPs/NIPs), and sorption-desorption testing.

The aim was to assess not only the sorption efficiency for individual polyphenolic compounds, but also the broader applicability of these materials to structurally diverse analytes found in olive leaf, including flavonoids, triterpenoids, and secoiridoids. All sorption experiments were conducted under flow conditions, using SPE cartridges or packed columns, to replicate realistic operating environments

and to evaluate sorbent selectivity, cross-reactivity, and reusability in systems of increasing complexity.

8.2.1. Modification of cellulose

The modification of microcrystalline cellulose (MCC) and cellulose fibers (CF) was carried out via an esterification reaction, following procedures previously reported in the literature [5], [9], [14]. The aim was to introduce bromine-containing initiating groups compatible with ATRP.

Initially, the cellulose substrates (2 g) were dispersed in dimethylformamide (DMF) (200 mL), during to 30 minutes, using ultrasonication to promote better accessibility of the hydroxyl groups. Under continuous stirring, triethylamine (TEA) (16 mL) and 4-(dimethylamino)pyridine (DMAP) (8 g) were added to the dispersion, serving respectively as base and catalyst. After stabilization of the reaction medium, α-bromoisobutyryl bromide (BIBB) (16 mL) was slowly added dropwise at 0 °C to avoid uncontrolled side reactions.

The esterification reaction was allowed to proceed under continuous stirring at room temperature for 24 hours, promoting the covalent attachment of the bromoisobutyryl groups to the hydroxyl groups of the cellulose. At the end of the reaction, ethanol was added to stop the esterification process.

After immobilization, the modified cellulose, MCC-Br and CF-Br were initially purified by repeated centrifugation cycles to remove residual reagents and by-products from the reaction medium. Following this, the materials were subjected to dialysis or column washing, against deionized water to eliminate low impurities. The purified materials were then dried in a vacuum hoven at 70ºC. This procedure is illustrated in **Figure 10**.

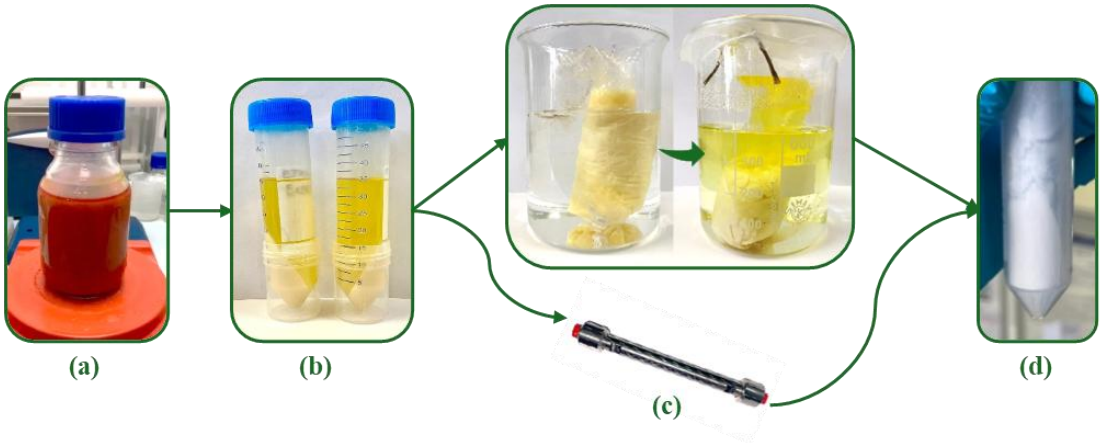

Figure 10:Visual sequence of cellulose modification and purification steps. **a)** Esterification of cellulose; **b)** Initial purification by centrifugation; **c)** Removal of unreacted species via dialysis or column washing; **(d)** Final dried product after purification.

8.2.2. Synthesis of MIPs on the cellulose surface via ATRP

MIPs were synthesized on the surface of modified cellulose substrates (CF-Br and MCC-Br) via surface-initiated ATRP (SI-ATRP), following previously reported methodologies adapted for imprinting on solid core [5], [9], [14]. For template-specific recognition, two sets of MIPs were synthesized: using quercetin (flavonoid template) and oleanolic acid (triterpenoid template).

In a typical procedure, the modified cellulose is dispersed in the chosen solvent, either ethanol or DMF, along with the functional monomer (4-vinylpyridine (4-VP) or Poly(2-(dimethylamino) ethyl methacrylate (DMAEMA)) and the template molecule (quercetin or oleanolic acid). This mixture was stirred at low temperature for 30 minutes to allow the formation of pre-polymerization complexes between the monomer and the template on the cellulose surface. Afterwards, the remaining components, ethylene glycol dimethacrylate (EGDMA) as crosslinker, copper(I) bromide (CuBr) as catalyst and PMDETA as ligand, were added to the mixture. The reaction mixture was then subjected to ultrasonication for 10 minutes to promote homogeneity and ensure solubilization of CuBr.

To remove oxygen and initiate the ATRP process, the solution was purged with argon and kept under an inert atmosphere. The polymerization was carried out at 70 °C for 5 days.

A summary of all MIPs synthesized, including variations in macroinitiator, monomer, solvent, and template used, is presented in **Table 4**.

Table 4: Summary of MIPs synthesized on modified cellulose substrates. The table includes the type of macroinitiator, functional monomer, crosslinker, catalyst, ligand, solvent, and template used in each formulation.

Name	Macro-initiator	Monomer	Crosslinker	Catalyst	Ligand	Solvent	Template
MIP1	CF Br	4VP	EGDMA	CuBr	PMDETA	EtOH	Quercetin
MIP2	MCC-Br	4VP	EGDMA	CuBr	PMDETA	EtOH	Quercetin
MIP3	CF-Br	4VP	EGDMA	CuBr	PMDETA	EtOH	Quercetin
MIP4	MCC-Br	4VP	EGDMA	CuBr	PMDETA	EtOH	Quercetin
MIP5	CF-Br	4VP	EGDMA	CuBr	PMDETA	EtOH	Quercetin
MIP6	MCC-Br	4VP	EGDMA	CuBr	PMDETA	EtOH	Quercetin
MIP7	CF-Br	4VP	EGDMA	CuBr	PMDETA	DMF	Quercetin
MIP8	MCC-Br	4VP	EGDMA	CuBr	PMDETA	DMF	Quercetin
MIP9	CF-Br	DMAEMA	EGDMA	CuBr	PMDETA	EtOH	Oleanolic Acid
MIP10	CF-Br	DMAEMA	EGDMA	CuBr	PMDETA	DMF	Oleanolic Acid

As a control for each MIP, a blank sample was synthesized without the addition of a template. This sample is named non-imprinted polymer (NIP).

Table 5: Experimental conditions for synthesis of the MIPs and NIPs, including reagent quantities of modified cellulose, solvents, template, monomer, catalyst, crosslinker, ligand, and key synthesis parameters (Y_M, Y_{CL}, $Y_{FM/T}$).

Material	CF-Br (mg)	MCC-Br (mg)	EtOH (mL)	DMF (mL)	Quercetin (mg)	Oleanolic Acid (mg)	4VP (mL)	DMAEMA (mL)	CuBr (mg)	EGDMA (µL)	PMDETA (µL)	Y_M (% mass)	Y_{CL} (% mass)	$Y_{FM/T}$ (% mass)
MIP1	100	-	19	-	38	-	0.21	-	5.74	75	8	1.90	27.38	5.53
NIP1	100				-	-		-						
MIP2	-	100	19	-	38	-	0.21	-	5.74	75	8	1.90	27.38	5.53
NIP2		100			-	-		-						
MIP3	100	-	18	-	36	-	1.06	-	28.69	377	42	9.25	27.38	29.21
NIP3	100				-	-		-						
MIP4	-	100	18	-	36	-	1.06	-	28.69	377	42	9.25	27.38	29.21
NIP4		100			-	-		-						
MIP5	100	-	17	-	34	-	2.13	-	57.38	754	84	17.76	27.38	61.85
NIP5	100				-	-		-						
MIP6	-	100	17	-	34	-	2.13	-	57.38	754	84	17.76	27.38	61.85
NIP6		100			-	-		-						
MIP7	100	-	-	18	36	-	1.06	-	28.69	377	42	7.85	27.38	29.21
NIP7	100				-	-		-						
MIP8	-	100	-	18	36	-	1.06	-	28.69	377	42	7.85	27.38	29.21
NIP8		100			-	-		-						
MIP9	200	-	36	-	-	180	-	3.22	60	761	84	11.80	21.05	16.67
NIP9	200				-	-	-							
MIP10	200	-	-	36	-	1080	-	3.22	60	761	84	10.06	21.05	2.78
NIP10	200				-	-	-							

The exact quantities of reagents used in each synthesis are listed in **Table 5**, together with key polymerization parameters calculated to characterize each formulation. These parameters include: $\boldsymbol{Y_M}$, the mass fraction of functional monomer and crosslinker in the total polymerization solution (%); $\boldsymbol{Y_{CL}}$, the molar fraction of crosslinker within the monomer and crosslinker mixture (%) and $\boldsymbol{Y_{FM/T}}$, the molar ratio between functional monomer and template molecule. These values reflect both the density of the polymer network and the availability of functional groups for imprinting, which are crucial for the formation of effective recognition sites [6], [26], [29].

Upon completion, the synthesized hybrid MIP materials were purified using a sequence of solvents, starting with the mixture of methanol and acetic acid (90:10, v/v), followed by DMF. The purification process was conducted using centrifugation, dialysis or SPE. After, the materials were dried in an oven at 70 °C.

8.2.3. MIP characterization

To confirm the successful synthesis of the cellulose-based materials and to evaluate their physicochemical properties, a series of analytical techniques was employed. These included Fourier-transform infrared spectroscopy (FTIR), scanning electron microscopy (SEM), and nitrogen sorption-desorption isotherms (BET method).

8.2.3.1. FTIR analysis

FTIR spectroscopy was used to assess the chemical structure of the functionalized materials. Spectra were acquired using a Perkin Elmer Spectrum Two™ spectrometer, with Spectrum IR software. Using the attenuated total reflectance (FTIR-ATR) mode or, when necessary, KBr pellet preparation.

8.2.3.2. SEM analysis

The morphology of the cellulose-based hybrid particles was evaluated by SEM. Analyses were performed using an FEI Quanta 650 FEG microscope operating at 10 kV with a spot size of 3 and a working distance of 1-10 mm. Prior to imaging, the samples were sputter-coated with gold for 30 seconds at 30 mA. Images were collected at magnifications ranging from 25,000× to 100,000×.

8.2.3.3. Surface area, pore volume, and textural analysis

Nitrogen sorption-desorption isotherms were obtained to determine the specific surface area and pore characteristics of selected hybrid particles. The analyses were performed at the International Iberian Nanotechnology Laboratory (INL) using a Quantachrome NOVA 4200e instrument. Samples were degassed at 60 °C prior to measurement. The surface area was calculated by the Brunauer-

Emmett-Teller (BET) method, and the pore size distribution and volume were determined by the Barrett-Joyner-Halenda (BJH) method.

8.2.4. High-performance liquid chromatography with diode array detection (HPLC-DAD)

HPLC-DAD was employed for the identification and quantification of analytes across different experimental stages, including sorption/desorption solutions and crude plant extracts.

Analyses were performed using a Knauer system composed of a gradient pump (P6.1 L), a column thermostat (CT2.1), an autosampler (6.1 L), and a diode array detector (DAD 6.1 L). The system was controlled using ClarityChrom software. Separation of analytes was achieved on a reverse-phase C18 column (Ascentis®, Supelco; 25 cm × 4.6 mm, 5 μm particle size).

Two chromatographic methods were employed depending on the compound class. For the analysis of polyphenols, a linear gradient elution was applied using two mobile phases: solvent A (water/acetonitrile 90:10, v/v) and solvent B (water/acetonitrile 10:90, v/v), both acidified to pH 3 with acetic acid. The gradient transitioned from 100% A to 100% B over 45 minutes at a flow rate of 1 mL/min and a temperature of 45 ºC. For the quantification of triterpenoids, an isocratic method was used with acetonitrile/water (85:15, v/v) containing 0.05% formic acid, over a 25-minute run at 25 °C.

Detection wavelengths were selected according to the maximum absorbance of each analyte: typically, 280 nm for most polyphenols and 210 nm for triterpenoids. All samples were filtered through 0.45 μm nylon syringe filters prior to injection.

8.2.5. UV-vis ultraviolet visible

Ultraviolet-visible (UV-Vis) spectroscopy was employed for the quantification of analytes during the sorption and desorption steps carried out in flow-based systems, including SPE cartridges and packed columns. All measurements were performed using a VWR P9 Double Beam spectrophotometer with 1 cm path length quartz cuvettes. Absorbance was recorded in the 200-600 nm range, and quantification was based on the maximum absorbance wavelength specific to each compound. Prior to analysis, all samples were filtered through 0.45 μm nylon syringe filters to remove any particulates. UV-Vis measurements were used primarily for rapid monitoring of the concentration of compounds in the loading, washing, and elution fractions collected throughout the experiments.

8.2.6. Sorption and desorption tests

To evaluate the retention capacity, selectivity, and elution behavior of the synthesized MIPs, a series of sorption and desorption experiments were designed and conducted under controlled

conditions using two experimental setups: SPE and a closed-cycle packed column system. In both approaches, different solvents and analytes were used to systematically assess the performance of the materials, considering their affinity for the respective template molecules, cross-selectivity towards structurally related compounds, and the efficiency of analyte recovery through desorption. The following sections describe the methodologies and experimental conditions applied.

8.2.6.1. Tests using SPE

SPE was employed to assess the retention capacity and selectivity of the synthesized MIPs under predefined experimental conditions. For all experiments, 50 mg of the dried polymeric material was packed into SPE packing cartridges (Agilent Bond Elut reservoir, 1 mL capacity) to serve as the stationary phase, as shown in **Figure 11**.

Each test followed a consistent procedure involving the cleaning of the sorbent using methanol/acetic acid (9:1, v/v), solvent conditioning for the sorption step, and subsequent loading of the analyte solution. This was followed by a washing step with the same solvent as the solution from loading and final elution with methanol/acetic acid (9:1, v/v). In all steps, the solution passed through the sorbent at a constant flow rate of approximately 1 mL/min. The collected fractions were analyzed by UV-Vis spectroscopy or HPLC-DAD, depending on the analyte. This methodology allowed for a systematic comparison of analyte retention and desorption profiles under various solvent systems and analyte compositions.

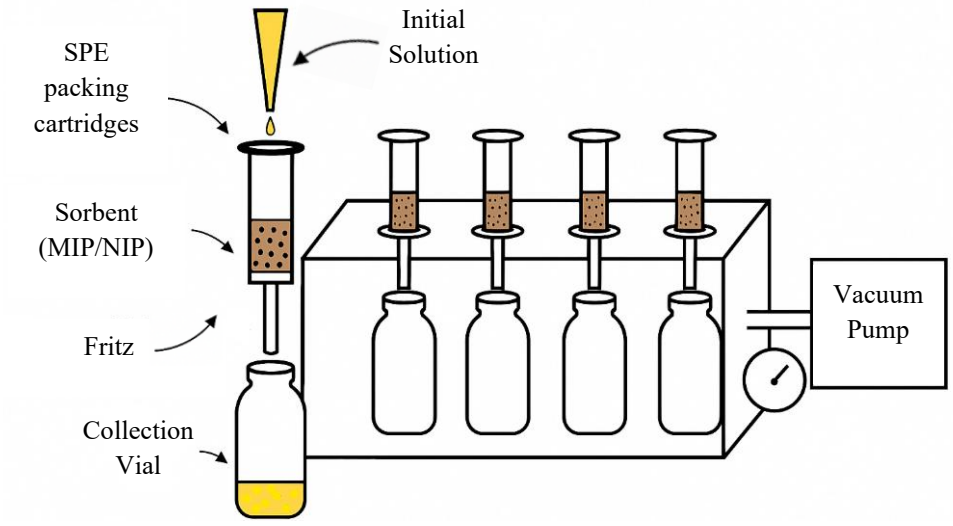

Figure 11: Schematic representation of the SPE setup used for sorption and desorption experiments. SPE packing cartridges, packed with 50 mg of sorbent material (MIP and NIP), are placed on a vacuum manifold connected to a vacuum pump. Solutions were sequentially passed through the stationary phase, and the resulting fractions (loading, washing, and elution) were collected in separate vials for subsequent analysis.

8.2.6.1.1. Comparison of retention efficiency in ACN

To compare the retention performance of MIPs, a series of sorption-desorption experiments was conducted using ACN as solvent. This solvent was selected due to its aprotic and low-polarity nature, which minimizes non-specific interactions such as hydrogen bonding, thereby enhancing the observation of selective binding effects.

The materials MIP/NIP1 to MIP/NIP8 were tested using a 0.05 mg/mL solution of quercetin in ACN, under strictly identical conditions. All experiments followed the previously described SPE protocol: loading, washing, and elution using 5 mL of solution/solvent. In each step, the analyte was detected by UV-Vis spectroscopy at approximately 370 nm, corresponding to quercetin's maximum absorbance in this solvent system.

These results provide a reference point for evaluating the impact of solvent polarity in subsequent tests.

8.2.6.1.2. Retention efficiency under competitive conditions in ethanol/water (80:20 v/v)

To evaluate the selectivity and potential cross-selectivity of the synthesized MIPs, sorption-desorption experiments were conducted using a polar solvent system composed of ethanol and water (80:20, v/v). This solvent mixture was selected to simulate more hydrophilic environments and to promote hydrogen bonding and polar interactions during the retention process.

A range of sorbent materials was tested under identical conditions, including quercetin-imprinted polymers (MIP1 to MIP8), their corresponding non-imprinted controls (NIPs), and two cellulose reference materials (CF and MCC). All sorbents were tested with an equimolar mixture of quercetin, oleuropein, rutin, and vanillic acid, each at a concentration of 0.4 mM. For each analyte, 2.5 mL of solution was loaded using the standardized SPE procedure, including sequential loading, washing, and elution steps. The collected fractions were analyzed by HPLC-DAD.

This setup enabled a direct comparison of retention performance across all sorbents, highlighting the effects of imprinting and formulation. The use of a fixed analyte mixture also allowed for the detection of non-specific or cross-reactive binding under polar conditions.

8.2.6.1.3. Enrichment tests with complex extracts

To evaluate the performance of the synthesized MIPs with real samples, sorption-desorption experiments were performed using two industrial olive leaf extracts provided by the NATAC (Alcorcón, Madrid, Spain) (**Figure 12**). These extracts differ significantly in composition and were selected to test the materials under varied chemical complexity. NATAC OPA 20 contains

approximately 20% oleuropein and a variety of other compounds, namely verbascoside and luteolin-7-O-glucoside. NATAC VR2 SS1 is a side-stream extract with a more complex matrix, combining triterpenes such as oleanolic and maslinic acid and a broad range of flavonoids, including luteolin-7-O-glucoside and luteolin. These extracts were used to assess the MIP's capacity to selectively retain a specific class of compounds.

Figure 12: Industrial olive leaf extracts used in the SPE experiments. NATAC VR2 SS1 and NATAC OPA 20 were provided in liquid and solid forms, respectively. The liquid extract (VR2 SS1) was lyophilized prior to use. Both extracts were subsequently dissolved in a hydroethanolic medium to prepare the working solutions used in the saturation and SPE protocol steps.

The experience consisted of the same loading, washing, and elution steps. For each extract, the loading phase was performed using increasing volumes of solution (from 10 mL to 40 mL) applied in 10 mL increments to the SPE cartridges. The NATAC OPA 20 extract solution was used at a concentration of 5 mg/mL in ethanol/water 80:20 (v/v), while VR2 SS1 was prepared at 3.5 mg/mL in ethanol/water 65:35 (v/v).

Unlike previous desorption protocols, the experiments using NATAC OPA 20 and VR2 SS1 involved a sequential elution strategy with increasing solvent polarity. This method allowed for the gradual recovery of compounds based on their binding strength and elution profile, providing a deeper insight into the interaction mechanisms between the MIP surfaces and target analytes. The desorption steps are summarized in **Table 6**.

Table 6: Solvent compositions used in the sequential desorption steps for the NATAC OPA 20 and NATAC VR2 SS1 extracts. The solvents were applied in 2 mL increments per step, following a gradient of increasing polarity and elution strength, to enable the differential recovery of compounds adsorbed onto the surfaces of MIPs and NIPs.

Extract	Elution step	Solvent composition	Volume (mL)
NATAC OPA 20	1	Water	2
	2	Water pH3	2
	3	Ethanol/water 25:75 (v/v)	2
	4	Ethanol/water 50:50 (v/v)	2
	5	Ethanol/water 75:25 (v/v)	2
	6	Ethanol	2
	7	Methanol	2

Table 6: Continuation.

Extract	Elution step	Solvent composition	Volume (mL)
NATAC VR2 SS1	1	Ethanol/water 65:35 (v/v)	2
	2	Ethanol/water 75:25 (v/v)	2
	3	Ethanol/water 80:20 (v/v)	2
	4	Ethanol/water 85:15 (v/v)	2
	5	Ethanol/water 90:10 (v/v)	2
	6	Ethanol/water 95:5 (v/v)	2
	7	Ethanol	2
	8	Methanol	2

8.2.6.2. Tests using a packed column

To complement the SPE-based experiments, dynamic sorption studies were conducted using a packed HPLC column system in closed-loop mode (**Figure 13**). The column (125 mm × 8 mm) was packed with 7 g of MIP3 via the slurry method and operated at a constant flow rate of 1 mL/min using an external pump. Six analyte solutions with increasing concentrations (0.05, 0.1, 0.2, 0.3, 0.5 and 0.8 mM) were circulated sequentially, each for 4 hours, allowing equilibrium to be reached at each step. The analyte was continuously recirculated between the reservoir and the packed column. This setup enabled the assessment of sorption kinetics and binding capacity under flow conditions.

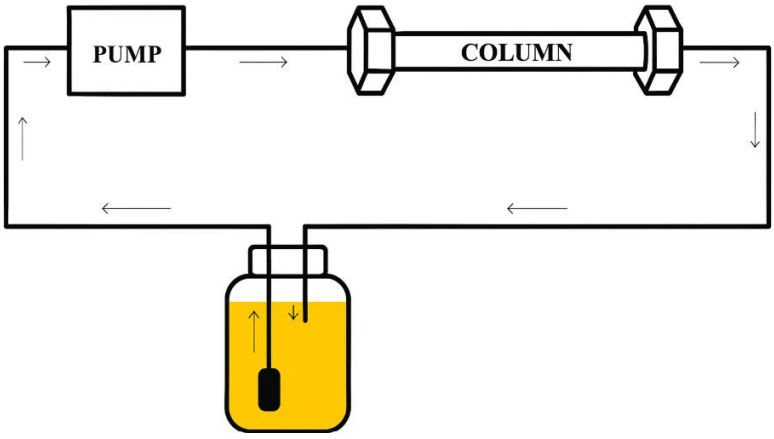

Figure 13: Schematic representation of the recirculating packed-column system used in dynamic sorption experiments. Analyte solutions were pumped through the column packed with MIP3 and returned to the reservoir, maintaining continuous contact for 4 hours per concentration step.

8.2.6.2.1. Effect of solvent composition on quercetin sorption isotherms

To assess the effect of solvent polarity on adsorption performance, two hydroethanolic mixtures were used as mobile phases: ethanol/water (80:20, v/v) and ethanol/water (50:50, v/v). Six quercetin solutions of 0.05 to 0.8 mM were prepared and tested under identical recirculating conditions in each solvent system. The analyte was detected by UV-Vis spectroscopy for all solvent systems.

This experiment aimed to evaluate how the balance between hydrophobic and polar interactions influences analyte retention. The system rich in ethanol was expected to enhance π-π stacking and hydrophobic interactions, while the higher water content in the 50:50 mixture could favor hydrogen bonding and modulate the accessibility of quercetin to the imprinted binding sites.

8.2.6.2.2. Sorption isotherms under competitive multi-analyte conditions

To simulate competitive binding scenarios and evaluate selectivity under more realistic conditions, an equimolar (2.4 mM) mixture containing quercetin, vanillic acid, and oleuropein was prepared in ethanol/water (50:50, v/v). This solution was subsequently diluted to obtain concentrations ranging from 0.05 to 0.8 mM, as described earlier.and recirculated through the MIP3 packed column under the same conditions described previously. The final analytes were analyzed by HPLC-DAD.

This experiment was designed to assess the preferential retention of the template molecule in the presence of structurally distinct competitors, providing insight into the selectivity of the material under dynamic, multi-analyte conditions relevant to real extract applications.

8.2.6.3. Evaluation of sorbent selectivity toward structurally diverse olive leaf compounds

While previous experiments demonstrated strong performance of MIP materials imprinted with quercetin, the chemical complexity of olive leaf extracts that are rich in triterpenoids, phenolic acids, and secoiridoids, requires a broader evaluation of material selectivity. To address this, additional tests were performed using sorbents synthesized with oleanolic acid as the template molecule. These experiments aimed to assess the ability of the materials to selectively retain this class of compounds.

8.2.6.3.1. Sorption of maslinic acid and oleanolic acid

In this experiment, the materials MIP/NIP9, MIP/NIP10, CF, and MIP3 were tested for their ability to retain two triterpenoids: maslinic acid and oleanolic acid. The analytes were prepared at a concentration of 0.15 mM in ethanol/water (80:20, v/v), and sorption tests were performed using the standard SPE format consisted of loading, washing, and elution steps, using 5 mL of solution/solvent per step. The analytes were analyzed by HPLC, and all the experiments were performed in duplicate (n=2). The retention of the analytes was calculated based on the difference in absorbance between the initial loaded solution and the recovered fractions. The results are expressed as mean values and standard deviations.

8.2.6.3.2. Sorption of quercetin in ethanol/water (80:20, v/v)

To assess the cross-selectivity of the sorbents, a complementary experiment was performed using quercetin, a flavonoid structurally distinct from triterpenoids. The same materials (MIP/NIP9,

MIP/NIP10, CF, and MIP3) were assessed using a quercetin solution at 0.05 mg/mL in ethanol/water (80:20, v/v). The sorption procedure followed the same three-step SPE protocol with 5 mL per step. Quantification was performed by UV-Vis spectroscopy at approximately 375 nm.

This experiment enabled the evaluation of cross-recognition behavior in the oleanolic acid-based MIPs and served as a comparative assessment against MIP3, which was specifically imprinted with quercetin. The results provide insight into the influence of template-analyte compatibility on sorption behavior.

9. Results and discussion

This chapter presents and discusses the results obtained during the development of this work. The analysis begins with the synthesis of MIPs, followed by the evaluation of their performance in sorption and desorption experiments carried out using both SPE and recirculating column systems. The effectiveness of each material was assessed using standard solutions and, in selected cases, industrial olive leaf extracts. This approach allowed for a comprehensive comparison of template-specific retention, cross-selectivity, and analyte recovery efficiency. The results are interpreted in consideration of the chemical structure of the analytes, the formulation of each polymer, and the experimental conditions used in each assay.

9.1. Synthesis of MIPs

A total of ten MIPs and their corresponding NIPs were successfully synthesized via surface-initiated ATRP on modified cellulose substrates. The formulations varied in three main parameters: the template molecule (quercetin or oleanolic acid), the functional monomer (4-vinylpyridine or DMAEMA), and the solvent system (ethanol or DMF). All syntheses employed EGDMA as the crosslinker and CuBr/PMDETA as the catalyst system.

MIPs 1 to 8 were imprinted with quercetin, designed to target flavonoids and synthesized using 4-vinylpyridine (4VP) as monomer, an aromatic nitrogen-containing monomer capable of establishing π-π interactions and hydrogen bonds with phenolic structures [5], [6], [8], [29], [30]. In contrast, MIP9 and MIP10 were imprinted with oleanolic acid, to target triterpenoids, employing DMAEMA as monomer, an aliphatic tertiary amine monomer that promotes acid-base interactions and hydrogen bonding with carboxylic acid groups present in triterpenoids [6], [29].

This strategic choice reflects the importance of matching monomer chemistry to the functional groups of the target analyte, optimizing non-covalent interactions during the imprinting process. The aromatic 4VP favors interaction with the phenolic rings of quercetin [5], [6], [8], [29], [30], while DMAEMA's aliphatic, proton-acceptor nature is more suitable for interacting with the acidic moiety of oleanolic acid [6], [29].

The imprinting process relied on non-covalent pre-polymerization interactions between the template and the functional monomer. The selection of quercetin and oleanolic acid as templates was based on their analytical relevance and their structural similarity to broader families of olive leaf bioactives, aiming to achieve both selectivity and industrial applicability.

Ethanol was predominantly used as the polymerization solvent due to its compatibility with the reaction medium and its classification as a greener alternative, aligned with sustainable chemistry principles. In contrast, DMF was selected for MIPs 7, 8, and 10, as it offers better compatibility with the cellulose substrate and promotes improved dispersion and solubilization of the polymerization components. These solvent choices are known to influence the morphology and structural properties of the resulting materials [5], [29].

Each MIP had a corresponding NIP synthesized under identical conditions but in the absence of the template, allowing for direct comparison of sorption behavior and the evaluation of imprinting efficiency. Differences in polymer recovery were noted between 4VP and DMAEMA formulations, indicating that monomer structure and solvent polarity significantly influence polymer growth and morphology.

Although all MIPs were synthesized using a unified surface-initiated ATRP strategy, variations in formulation parameters such as solvent polarity, monomer structure and template identity led to significant differences in the final properties of the materials. For instance, higher Y_M and $Y_{FM/T}$ ratios tend to produce bulkier polymer structures, while lower ratios are associated with more dispersed or finer particles. Moreover, the presence or absence of the template also plays a critical role in particle formation and morphology, as previously reported for similar systems [6], [26], [29].

For example, MIP1 had a very low Y_M value (1.90%) and a $Y_{FM/T}$ ratio of 5.53, indicating a less dense formulation with fewer monomer units and functional groups available for interaction with the template. In contrast, MIP5, also prepared with CF-Br and quercetin, showed much higher values (Y_M = 17.76%, $Y_{FM/T}$ = 61.85), suggesting a thicker and more compact polymer layer.

A similar comparison can be made between MIP3 and MIP7, which share the same basic formulation but were synthesized using different solvents (ethanol for MIP3 and DMF for MIP7). Although their $Y_{FM/T}$ values are identical (29.21), the use of DMF in MIP7 led to a more homogeneous and compact structure, reflecting the better compatibility of DMF with the cellulose substrate.

In the case of DMAEMA-based materials (MIP9 and MIP10), the differences in $Y_{FM/T}$ values were mainly due to the amount of oleanolic acid used as the template. These variations influenced the formation of recognition sites, as later confirmed in the sorption experiments.

To better understand how these synthesis conditions affected the structure and surface characteristics of the resulting materials, all MIPs were subjected to a set of complementary characterization techniques.

9.2. MIP characterization

The synthesized MIPs were characterized using a combination of analytical techniques to evaluate their chemical structure, surface morphology, and textural properties. These techniques include FTIR-ATR spectroscopy, SEM, and BET surface area analysis. Together, they provide a comprehensive understanding of the material's structural features and the influence of synthesis conditions on their physical characteristics.

9.2.1. FTIR analysis

The modification of the cellulose substrates and the resulting hybrid materials was evaluated by FTIR-ATR spectroscopy. The spectra are shown in **Figure 14**, which includes representative examples of the different cellulose-based systems analyzed: (a) displays the spectra of CF and CF-Br, along with MIP/NIP1 and MIP/NIP3; part (b) presents the corresponding spectra for MCC and MCC-Br, together with MIP/NIP2 and MIP/NIP4; and part (c) shows CF-Br-based materials prepared with DMAEMA, including MIP/NIP9 and MIP/NIP10. The remaining spectra for additional MIP/NIP pairs are provided in **Appendix 1**.

In both CF-Br and MCC-Br spectra, a new absorption band appears at 1740 cm^{-1}, corresponding to the C=O stretching vibration of ester groups, confirming the successful immobilization of α-bromoisobutyryl bromide onto the cellulose surface [30]. This observation is in agreement with previous studies on ATRP initiator grafting on cellulose [5], [8], [9], [14].

Following polymerization with 4VP and EGDMA, the FTIR-ATR spectra of the hybrid MIP materials MIP/NIP1 to MIP/NIP8 revealed characteristic signals of the grafted polymer. These include the pyridyl C=N stretching at approximately 1418 cm^{-1}, and additional pyridyl-associated groups C=H at 820 and 755 cm^{-1}, as well as a strong band at 1600 cm^{-1}, attributed to both C=C aromatic stretching and residual vinyl groups from EGDMA. Differences in the intensity of the pyridyl-related bands, particularly at 1418 cm^{-1}, were observed between MIPs synthesized with varying monomer concentrations, indicating differences in the degree of surface functionalization [30].

In DMAEMA-based systems (**Figure 14 (c)**, MIP/NIP9 and MIP/NIP10), additional peaks were observed at ~2820 and 2920 cm^{-1}, corresponding to C-H stretching, and a strong C=O signal associated with the ester group. In all cases, the FTIR-ATR spectra of the hybrid materials also shows signals characteristic of the CF-Br macroinitiator, indicating the preservation of the cellulose backbone. The results suggest that the synthesis approach via ATRP successfully produced chemically stable and well-defined hybrid materials. While the high intensity of the EGDMA related bands tends to dominate the spectra, especially in formulations with elevated crosslinker content, the presence of

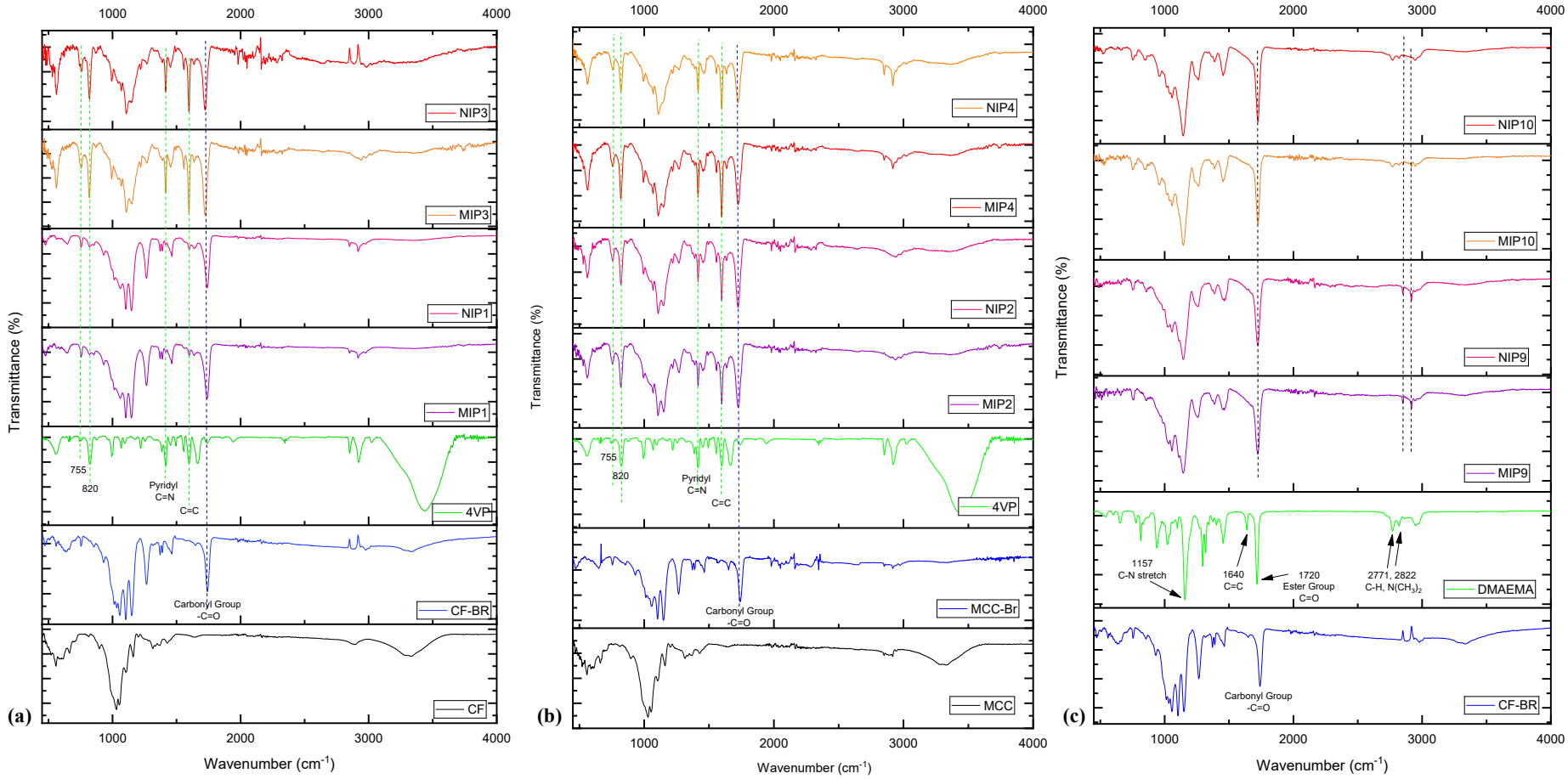

Figure 14: Comparative FTIR-ATR spectra of native and modified cellulose materials, functional monomers, and the resulting MIPs and NIPs. **(a)** Spectra of CF, CF-Br, 4VP, and MIP/NIP1 and MIP/NIP3; **(b)** Spectra of MCC, MCC-Br, 4VP, and MIP/NIP2 and MIP/NIP4; **(c)** Spectra of CF, CF-Br, DMAEMA, and MIP/NIP9 and MIP/NIP10. In all cases, the appearance of new absorption bands confirms the successful immobilization of the ATRP initiator and subsequent polymer grafting with pyridyl or DMAEMA functional groups [30].

functional monomer signals confirm their incorporation. These findings align with prior reports in the literature, where strong contributions from crosslinker bands were observed to mask finer details of monomer-specific features [29].

The FTIR-ATR results collectively confirm the successful modification of the cellulose substrates and the formation of MIPs with the expected chemical features. These findings support further investigation of the material's structural and morphological properties by SEM and BET analysis.

9.2.2. SEM analysis

SEM analysis was performed to evaluate the surface morphology and particle structure of the synthesized MIPs and their corresponding NIPs. This technique provided visual confirmation of the surface modification achieved through ATRP, allowing comparisons between cellulose fibers, microcrystalline cellulose, and the resulting hybrid MIP/NIP particles.

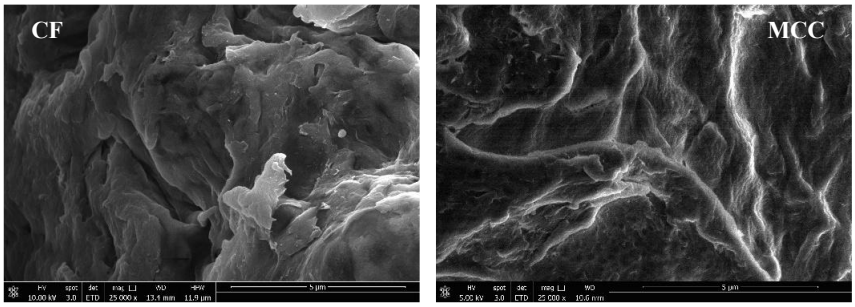

Figure 15: SEM images of cellulose substrates used as natural cores for the synthesis of the hybrid materials. The images correspond to CF and MCC, on a scale of 5 µm at a magnification of 25,000× [30].

As shown in **Figure 15** the surface of CF and MCC appeared smooth and well-defined. In contrast, in **Figures 16 and 17** all hybrid materials displayed noticeable roughness on the surface, confirming the successful growth of a functional monomer-based synthetic shell [30]. The difference in surface texture between the unmodified substrates and the grafted particles is consistent with previous reports on ATRP modification of cellulose [9], [14].

The extent of surface modification varied according to the synthesis conditions. In materials synthesized with lower monomer and crosslinker content (MIP/NIP1 to MIP/NIP4), the grafted polymer layer appeared thinner and more uniform. In contrast, higher monomer loadings (e.g., in MIP/NIP5 to MIP/NIP8) resulted in thicker and more heterogeneous polymer structures, indicating increased bulk and less controlled growth. This observation reflects the direct impact of monomer and crosslinker concentration on the final polymer morphology.

Interestingly, MIP materials synthesized under milder conditions (e.g., MIP1 to MIP4) showed slightly more defined structures than their non-imprinted counterparts, indicating that the presence of the template may influence the organization of the grafted polymer.

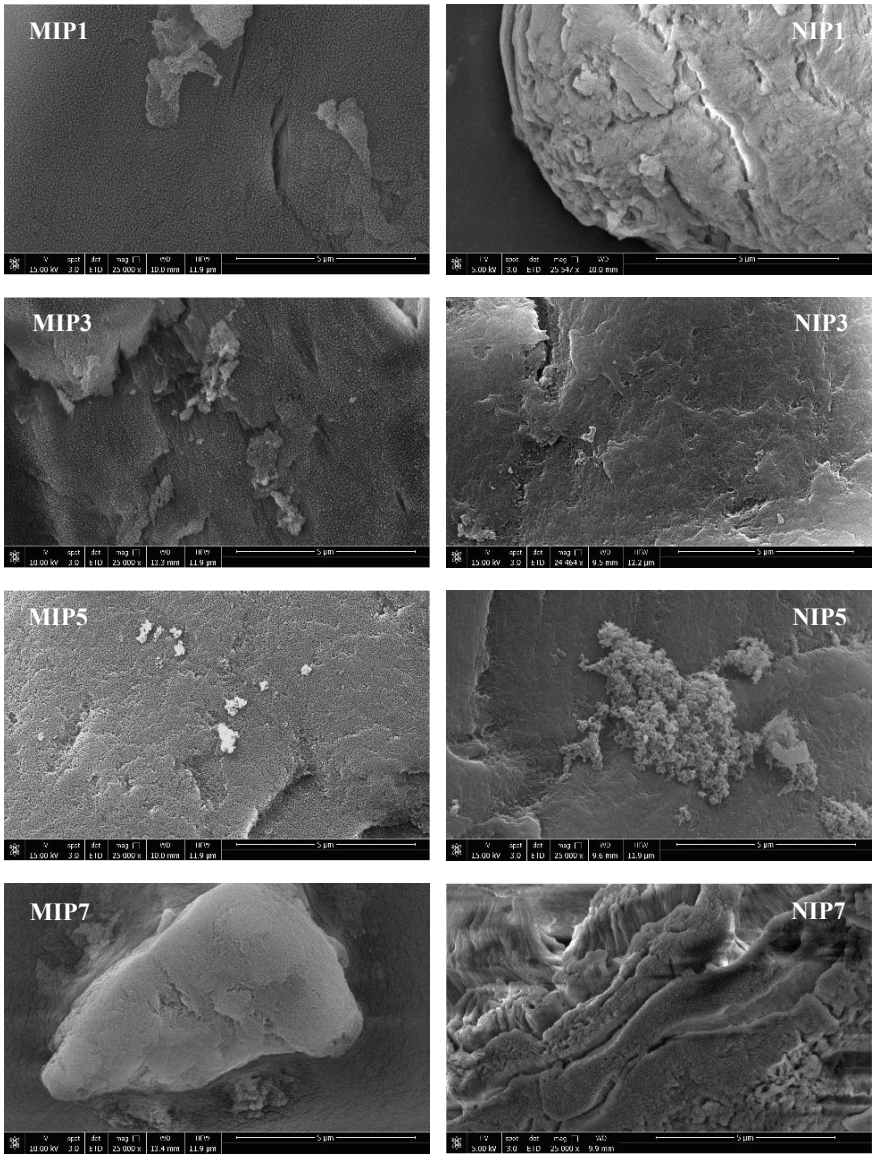

Figure 16: SEM images of hybrid pyridyl-functionalized cellulose fiber-based particles. All images were acquired at a scale bar of 5 µm at a magnification of 25,000× [30].

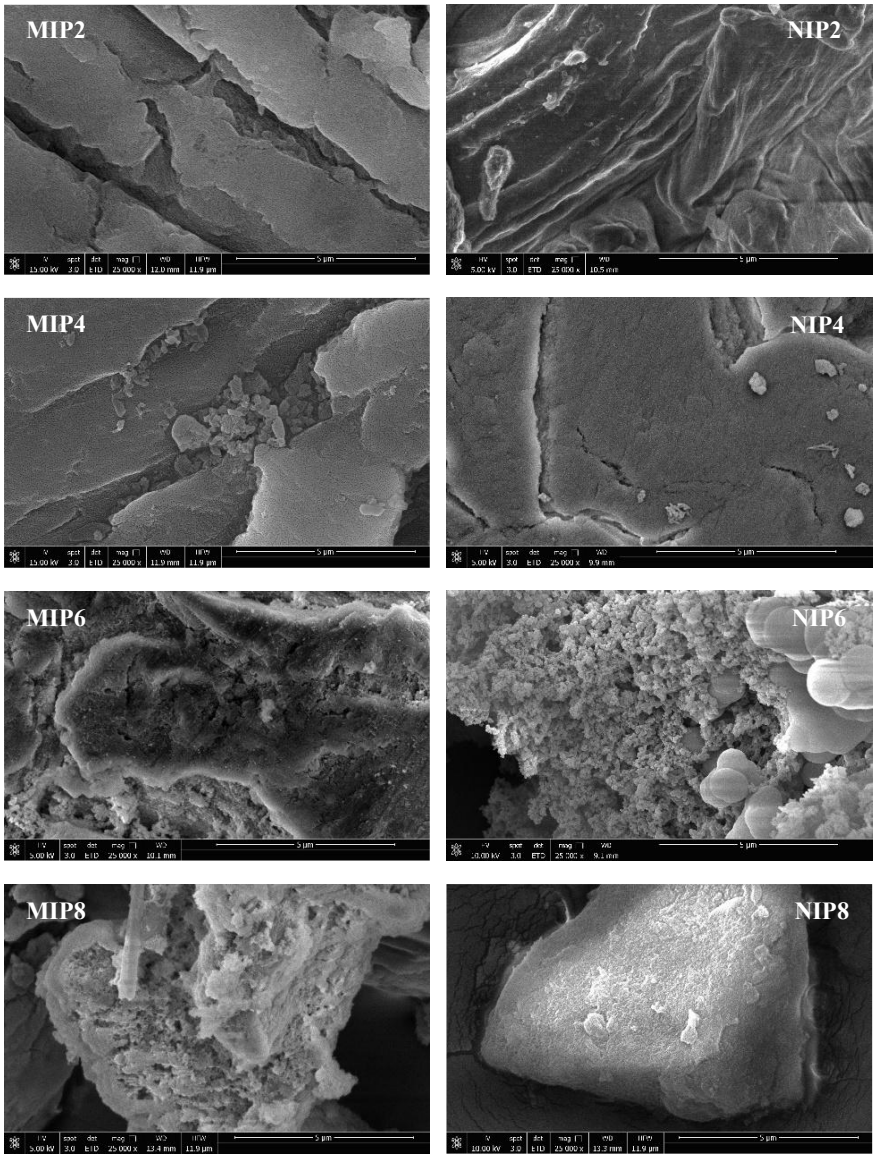

Figure 17: SEM images of hybrid pyridyl-functionalized microcrystalline cellulose-based particles. All images were acquired at a scale bar of 5 µm at a magnification of 25,000× [30].

Overall, these SEM observations confirm the success of the surface functionalization strategy and highlight the role of both template and monomer formulation in determining the morphology of the hybrid sorbent particles.

9.2.3. Surface area, pore volume and textural analysis

To further investigate the influence of synthesis conditions on the structural characteristics of the hybrid materials, nitrogen sorption-desorption isotherms at −196 °C were obtained for selected MIPs and NIPs. The specific surface area (S_{BET}) was calculated using the BET method, while pore volume and average pore diameter were determined using the Barrett-Joyner-Halenda (BJH) model. Prior to analysis, all materials were degassed at 60 °C to ensure complete removal of moisture and volatile subproducts [30].

The results, summarized in **Table 7**, show significant variations in surface area and porosity among the tested materials. NIP1 exhibited the highest surface area (155 m^2/g), while its imprinted analogue, MIP1, displayed a substantially lower value (24 m^2/g), suggesting that the presence of the quercetin template may have led to a denser or more collapsed polymer network. Similar effects have been previously associated with template-induced steric hindrance during polymerization [6], [9].

Table 7: BET surface area, pore volume, and average pore diameter of selected MIPs and NIPs.

Sample	S_{BET} [$m^2\ g^{-1}$]	$V_{pores;P/P0:0.95}$ [$cm^3\ g^{-1}$]	d_{pores} [nm]
MIP1	24	0.019	2.12
NIP1	155	0.12	0.93
MIP3	41	0.042	1.91
MIP8	53	0.14	0.93
NIP8	23	0.03	1.75

In contrast, the MIP8/NIP8 pair exhibited comparable surface areas (53 and 23 m^2/g, respectively), indicating that the imprinting effect on porosity is not uniform and likely depends on the overall formulation. MIP8 showed the highest pore volume (0.042 cm^3/g) the smallest average pore diameter (0.93 nm) among the imprinted materials, which may reflect a tighter network structure.

Importantly, the use of DMF as the solvent in the synthesis of MIP8 appears to have favored a more homogeneous dispersion of the cellulose substrate and led to the formation of a more compact and uniform polymer structure. This agrees with elemental analysis results showing higher incorporation of 4VP in DMF-based systems [30]. However, the use of DMF has been associated with the formation of smaller and more compact particles, which can compromise their applicability in continuous sorption systems by increasing column backpressure and reducing flow stability [5], [8], [9].

These textural characteristics play an important role in practical applications, such as continuous sorption/desorption processes, where surface area and pore accessibility impact both binding kinetics and column performance.

Overall, the BET analysis confirms that the imprinting process and synthesis parameters influence not only the chemical recognition capacity but also the physical structure of the hybrid materials. However, the obtained values are significantly smaller than the values typically reported for other sorbents. For instance, activated carbons often exhibit pore volumes ranging from 0.3 to 2.4 cm^3/g, depending on the activation method and precursor materials [31]. Similarly, commercial

resins like Reillex HPQ have been reported to have pore volumes around 0.5 cm^3/g [32]. These findings reinforce the mechanisms of hydrogen bonding, π-π stacking, and electrostatic interactions as the predominant interactions in sorption/desorption processes with molecularly imprinted materials [6], [8], [14], [29].

9.3. Sorption/desorption in SPE

9.3.1 Comparison of retention efficiency in ACN

To evaluate the effect of molecular imprinting on quercetin retention, MIP/NIP pairs from MIP1 to MIP8 were tested using quercetin as the model analyte in ACN. Due to its low polarity and aprotic nature, ACN minimizes non-specific interactions such as hydrogen bonding, thus allowing a more accurate assessment of specific binding within the imprinted cavities. The experiments were conducted under identical conditions using the standard SPE procedure, and analyte detection was performed by UV-Vis spectroscopy at 370 nm, corresponding to the characteristic absorption maximum of quercetin in this solvent system.

The retention efficiency for each material is presented in **Figure 18**, and differences between MIPs and their respective NIPs are interpreted as a direct reflection of the imprinting effect.

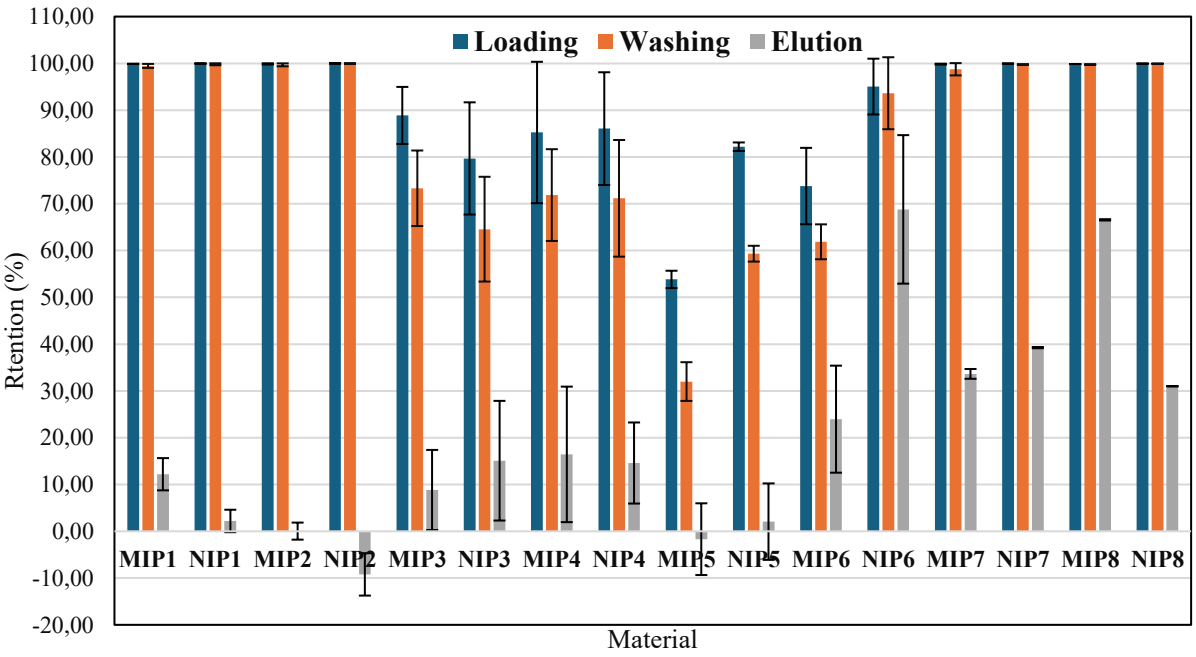

Figure 18: Retention percentage of quercetin in each SPE step (loading, washing, elution) for MIP1-MIP8 and corresponding NIPs. Values were calculated from UV-Vis absorbance at 370 nm, averaged over three replicates. Results are shown as mean ± standard deviation (n = 3) [30].

The results revealed that most materials showed high quercetin retention during the loading and washing phases, with differences between MIPs and NIPs becoming more evident in the elution step. During the elution phase, materials such as MIP2, MIP5, and MIP7 exhibited release profiles

comparable to those of their respective NIPs. This suggests that the retention observed in these materials is largely driven by non-specific interactions, rather than true molecular recognition.

A more dynamic profile was observed in MIP3, MIP4 and MIP6, where retention during loading and washing was lower than in other MIPs (e.g., MIP3: 88.9% and 73.3%, respectively), and notably higher elution values were recorded (MIP6: 24.0%). These results suggest a more accessible and stronger binding environment.

Notably, some NIPs, such as NIP6 (68.8%) and NIP8 (31.0%), retained significant amounts of analyte even after the elution step. This does not contradict the imprinting effect; rather, it reflects the high degree of crosslinking and functionalization, which can promote non-specific retention in both MIPs and NIPs.

From a statistical perspective (**Appendix 2**), the use of acetonitrile as loading solvent minimized solvent-mediated interference, allowing a more accurate assessment of the imprinting effect. ANOVA results confirmed statistically significant differences between MIPs and their corresponding NIPs in several cases, most notably for MIP1 (estimated imprinting factor (IF) = 5.5) and MIP8 (IF = 2.1). A moderate, yet detectable, imprinting effect was observed for MIP3 (IF = 1.3). In contrast, MIP/NIP5 and MIP/NIP6 showed no significant differences, indicating that retention in these materials is likely governed by non-specific interactions or poorly accessible binding sites [30].

These findings support the successful formation of selective recognition cavities in specific MIP formulations and demonstrate that imprinting is best revealed under low-polarity solvent conditions, where non-specific interactions are minimized.

9.3.2. Retention efficiency under competitive conditions in ethanol/water (80:20 v/v)

To assess the imprinting effect under more realistic conditions, SPE experiments were performed using an equimolar mixture of quercetin, vanillic acid, rutin, and oleuropein in ethanol/water (80:20, v/v), a solvent system representative of typical extraction media and conducive to hydrogen-bonding interactions.

The performance of imprinted (MIP1-MIP8) and non-imprinted (NIP1-NIP8) materials was compared to CF and MCC. As shown in **Figure 19**, both unmodified celluloses exhibited minimal retention across all analytes, confirming their low affinity for polyphenolic compounds. In contrast, all hybrid materials demonstrated substantially higher retention, attributed to the pyridyl-functionalized shell, which enhances binding through π-π interactions and hydrogen bonding.

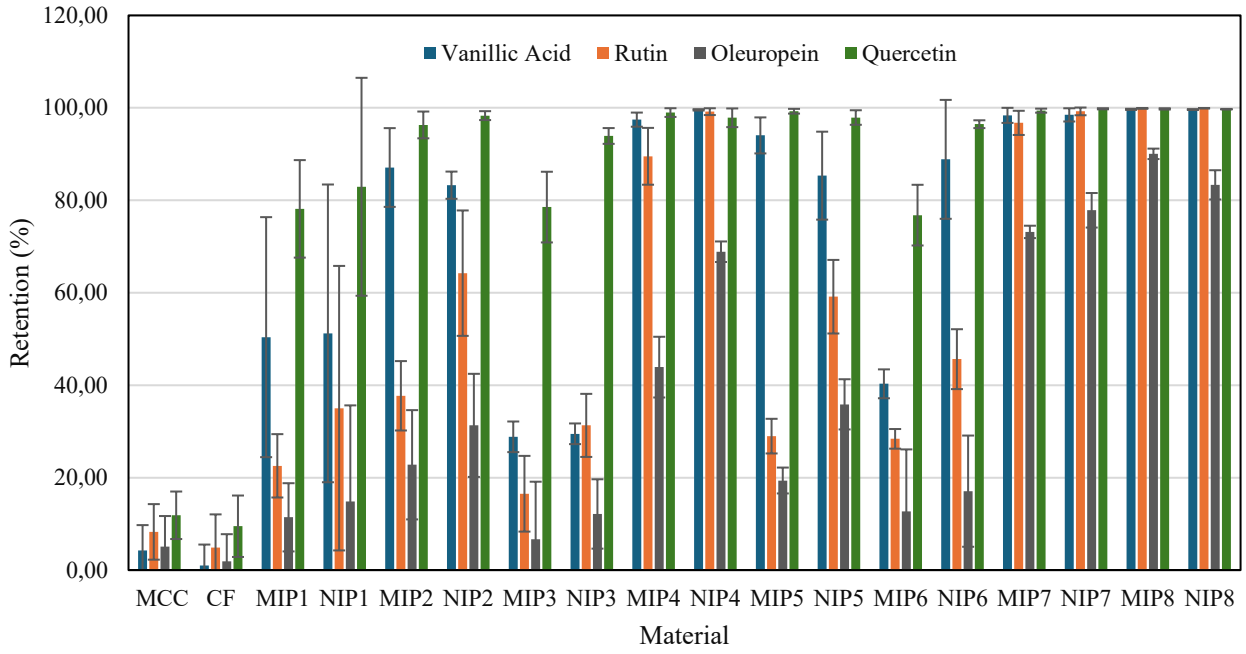

Figure 19: Average retention (%) of vanillic acid, rutin, oleuropein, and quercetin in the loading step of the SPE experiments for all tested materials. Results are shown as mean ± standard deviation (n = 3) [30].

Among the analytes, quercetin was consistently the most retained compound, followed by vanillic acid, rutin, and oleuropein. This order reflects differences in molecular structure, hydrogen bonding potential, and aromatic character. The higher affinity for quercetin is in line with its aromatic structure and multiple hydroxyl groups, which favor strong interactions with the pyridyl moieties [30].

Regarding the MIP/NIP comparison, clear imprinting effects were only observed in some materials. In MIP1, MIP3, and MIP8, quercetin retention was notably higher than in their respective NIPs, suggesting successful imprinting and the formation of selective binding sites. For other pairs such as MIP/NIP2, MIP/NIP5, and MIP/NIP7, no significant differences were observed, indicating a predominance of non-specific retention mechanisms. This can be confirmed by **Figure 37** (**Appendix 3**) of the elution.

Interestingly, materials like MIP7, MIP8, and their NIPs exhibited globally high retention for all analytes, but without clear selectivity. This behavior is likely related to their higher 4VP content and synthesis in DMF, which may result in more accessible surfaces and smaller particle sizes, enhancing overall retention but potentially diminishing selectivity due to increased non-specific sorption [30].

These observations are consistent with the structural and chemical characteristics of the pyridyl group, which can act as a weak base and hydrogen bond acceptor due to the non-conjugated lone pair on the nitrogen [8], [9], [14], [30]. The affinity for polyphenols is thus modulated by both the acidity

of the analyte and the solvent environment. In ethanol/water, hydrogen bonding competition may mask subtle imprinting effects, which are better observed under aprotic conditions, such as in acetonitrile.

ANOVA analysis (**Appendix 4**) of the experimental data confirmed statistically significant higher retention of all compounds in MIP/NIP1MIP/NIP8 compared to the unmodified cellulose materials. Moreover, the analysis revealed that quercetin retention was significantly greater than that of the other compounds across nearly all materials, reinforcing its stronger interaction with the pyridyl-functionalized matrix. However, no statistically significant difference was found between MIPs and NIPs in most MIP/NIP pairs, confirming that under hydrophilic solvent conditions, specific recognition effects are partially suppressed, and non-specific interactions dominate the sorption behavior [30].

9.3.3. Enrichment tests with complex extracts

Given the complexity and variability of industrial plant extracts, detailed chromatographic characterization was performed to assess the compound diversity in NATAC OPA 20 and VR2 SS1. These profiles are key to contextualizing the subsequent sorption and elution studies.

The 3D HPLC-DAD chromatograms presented in **Figures 20** and **21** confirm the compositional features previously described. In the case of NATAC OPA 20, oleuropein appears as the dominant compound, and flavonoid glycosides such as luteolin-7-O-glucoside and verbascoside can also be found as minor components, supporting its classification as a moderately complex extract. In contrast, the chromatographic profiles of NATAC VR2 SS1 reveal a richer and more diverse matrix: the method used to analyze polyphenols confirms the abundance of polyphenolic compounds, including luteolin and luteolin-7-O-glucoside. While the method used to analyze triterpenoids, evidences a significant presence of triterpenic acids predominantly maslinic and oleanolic acids. These chromatographic fingerprints validate the selection of both extracts for testing the sorbents under chemically distinct and realistic sample conditions [30].

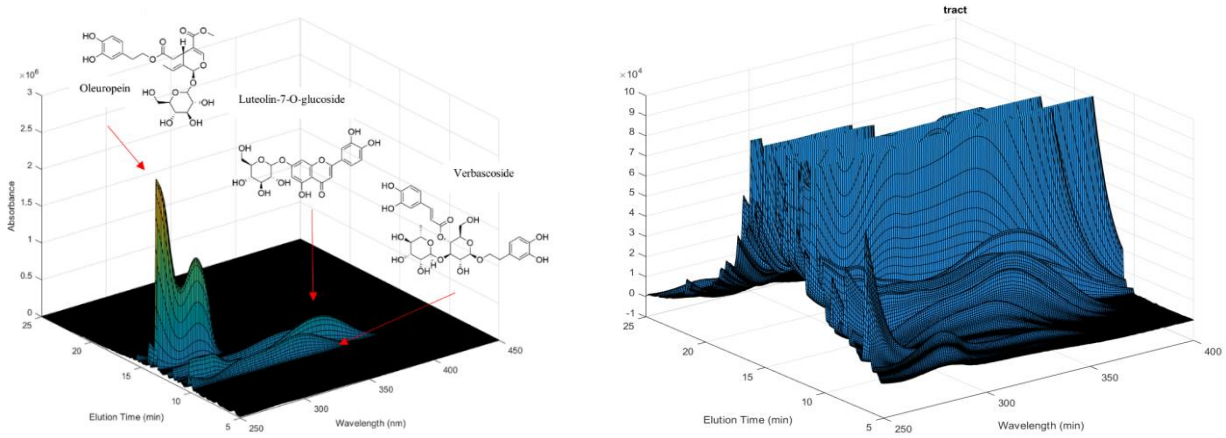

***Figure 20*:** 3D HPLC-DAD chromatogram of the industrial olive leaf extract NATAC OPA 20, which includes oleuropein as the major component. Left: complete chromatogram. Right: zoomed-in region highlighting minor constituents and the complexity of the extract (right) [30].

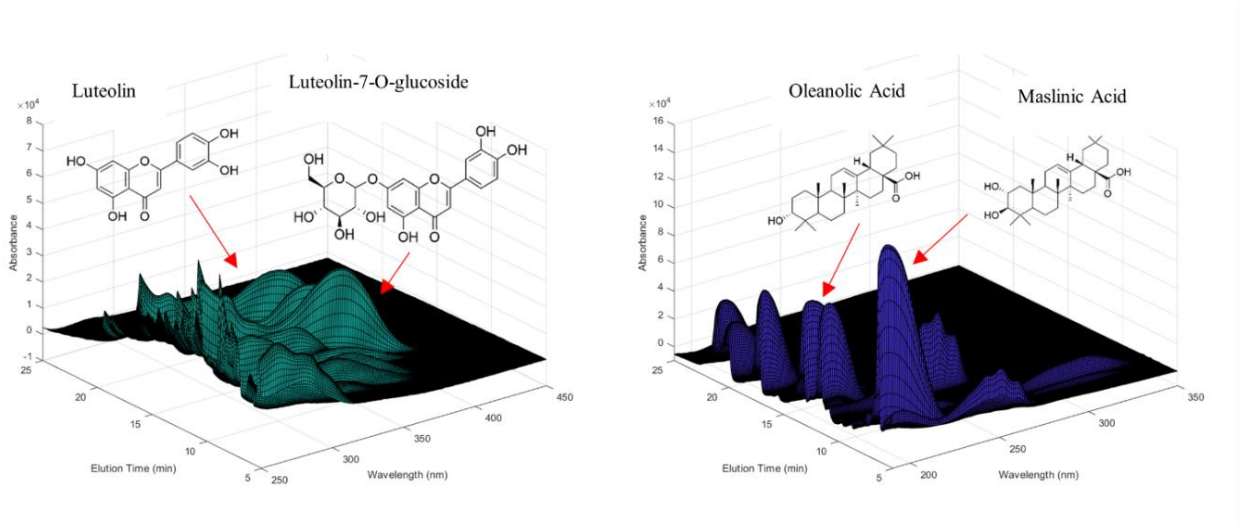

Figure 21: 3D HPLC-DAD chromatographic profile of the industrial olive leaf extract NATAC VR2 SS1, illustrating polyphenols (left) and triterpenoids (right) [30].

The performance of the hybrid materials was tested via SPE using NATAC OPA 20, aiming to assess the ability of pyridyl-functionalized materials to retain and enrich flavonoids under realistic matrix conditions.

MIP/NIP1 and MIP/NIP8 were selected for comparison due to their contrasting degrees of polymer grafting and pyridyl group density. Saturation experiments were conducted by incrementally loading increasing volumes of extract (from 10 mL up to 40 mL) onto the packed materials. After each loading volume, the amount of material retained on the sorbent was analyzed by HPLC-DAD.

MIP1 and NIP1 (**Figure 22**) exhibited progressive retention with increasing loading volume, with MIP1 showing slightly higher absorbance values. However, these differences alone are not

sufficient to confirm selective binding, and only the elution results can clarify whether specific interactions are involved.

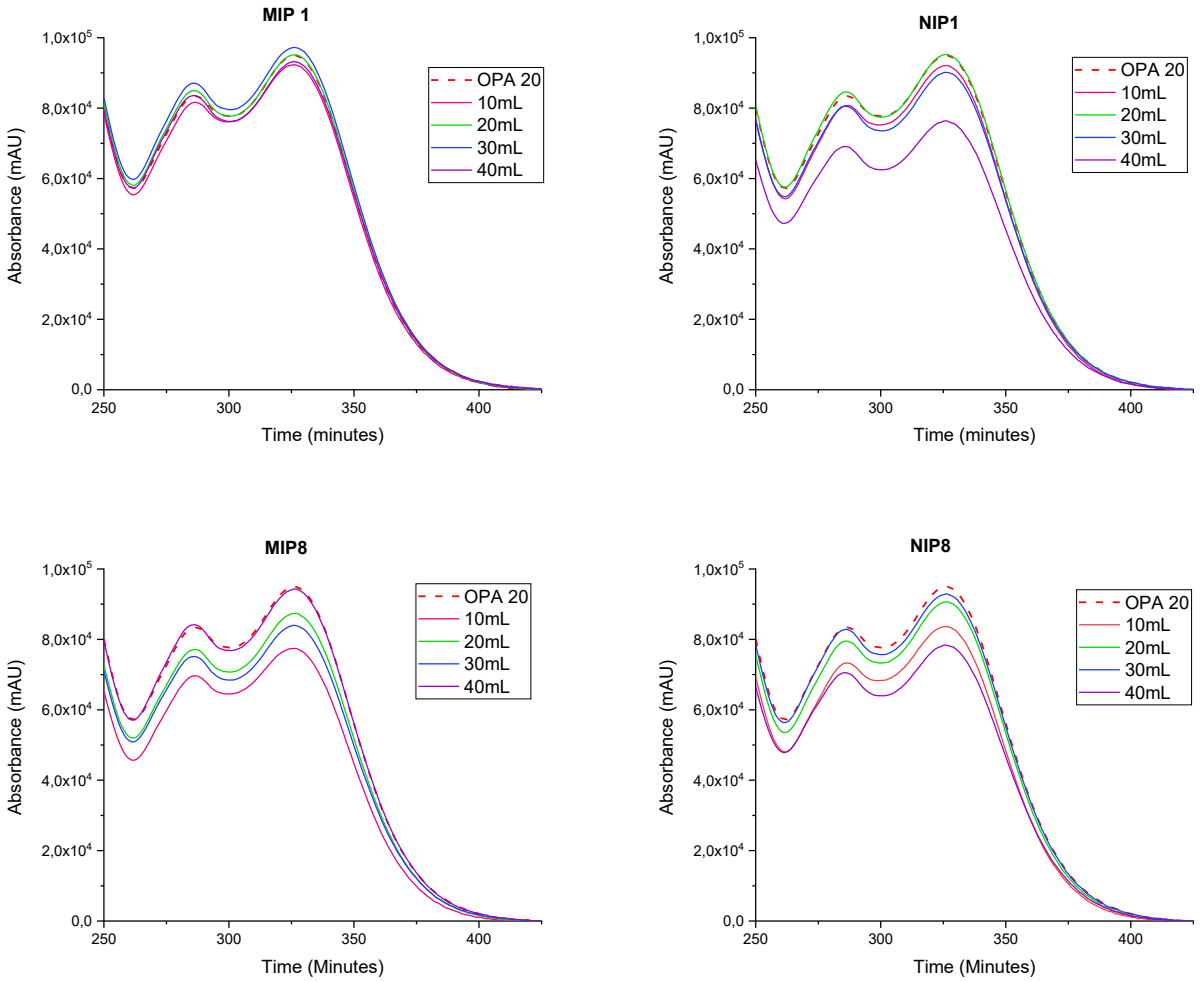

Figure 22: HPLC-DAD chromatograms using the polyphenols method after loading 10-40 mL of the OPA 20 extract. The profiles correspond to the saturation behavior of MIP/NIP 1 and 8, showing the evolution of retained compounds with increasing extract volume.

MIP8 and NIP8 (**Figure 22**) demonstrated different behavior. While both showed high retention even at lower volumes, the similarity between MIP8 and its non-imprinted analogue NIP8 during loading suggests that the high pyridyl density and polymer thickness led to strong but less selective binding. This behavior is consistent with no specific interactions dominating at higher functionalization levels.

Figure 23 highlights important differences in the saturation behavior of the tested materials. MIP8 and NIP8 showed a more progressive and homogeneous increase in signal with increasing loading volume, indicating gradual site occupation and higher overall retention capacity. In contrast, MIP1 and NIP1 retained a large portion of the extract within the first 10 mL, with only slight variations with the next volumes, indicating early saturation. Given the high concentration of the extract (5

mg/mL), these results should be interpreted with caution. Nonetheless, the irregular progression observed, particularly in NIP8, points to the presence of strong non-specific interactions that may dominate the retention process under these conditions.

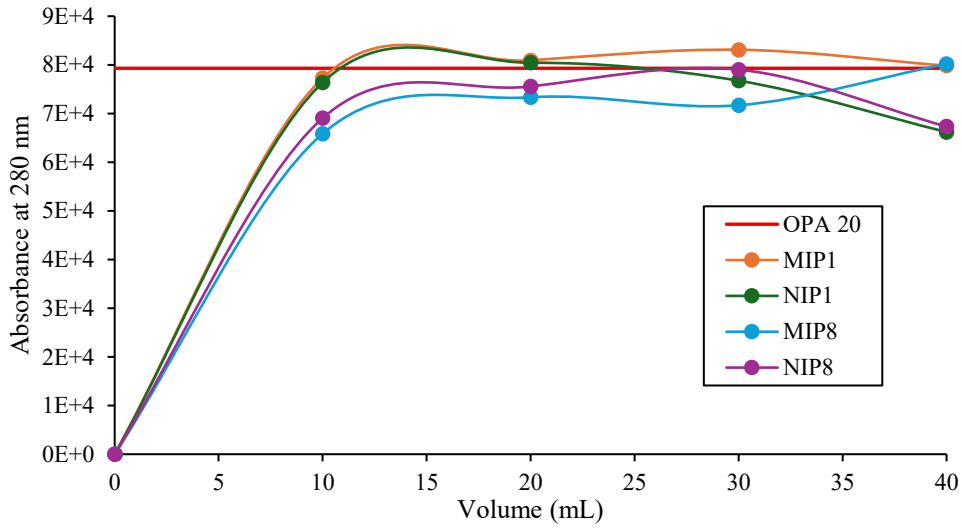

Figure 23: HPLC-DAD analysis of eluates collected after increasing loading volumes (10-40 mL) of the OPA 20 extract for polyphenols (λ = 280 nm).

To assess the separation performance of the materials, HPLC-DAD chromatograms at 280 nm were recorded for all the elution fractions of MIP1, NIP1, MIP8 and NIP8, along with the crude extract. These profiles enabled a comparative assessment of the eluted polyphenol compositions. **Figure 24** shows chromatograms for elution fraction 4 (ethanol/water 50:50, v/v), while the remaining fractions are presented in **Appendix 5**.

In this representative elution step, MIP1 released sharper and more defined peaks for flavonoid glycosides, indicating effective desorption under these conditions. NIP1 also eluted polyphenols, though with lower resolution, suggesting less selective release.

In the case of MIP8 and NIP8, the elution profiles were largely similar, indicating a high degree of non-specific interactions. Notably, NIP8 eluted higher amounts of luteolin-7-O-glucoside compared to MIP8, which may be related to the high density of pyridyl groups on its surface facilitating non-selective retention and release. Conversely, MIP8 showed slightly higher elution of apigenin-7-O-glucoside and oleuropein, suggesting that imprinting may still have a minor effect on the selective desorption of certain less abundant or structurally distinct compounds.

Overall, these findings reinforce that selectivity is more effective in thinner-shell materials like MIP1**,** where well-defined binding cavities are more accessible. In contrast, in highly functionalized systems such as MIP8, the high density of pyridyl groups can mask specific recognition sites, leading

to a binding profile dominated by non-specific interactions. These results underscore the importance of carefully tuning polymer formulation parameters, particularly monomer ratios, template presence, and shell thickness to optimize both retention capacity and molecular selectivity in complex matrices.

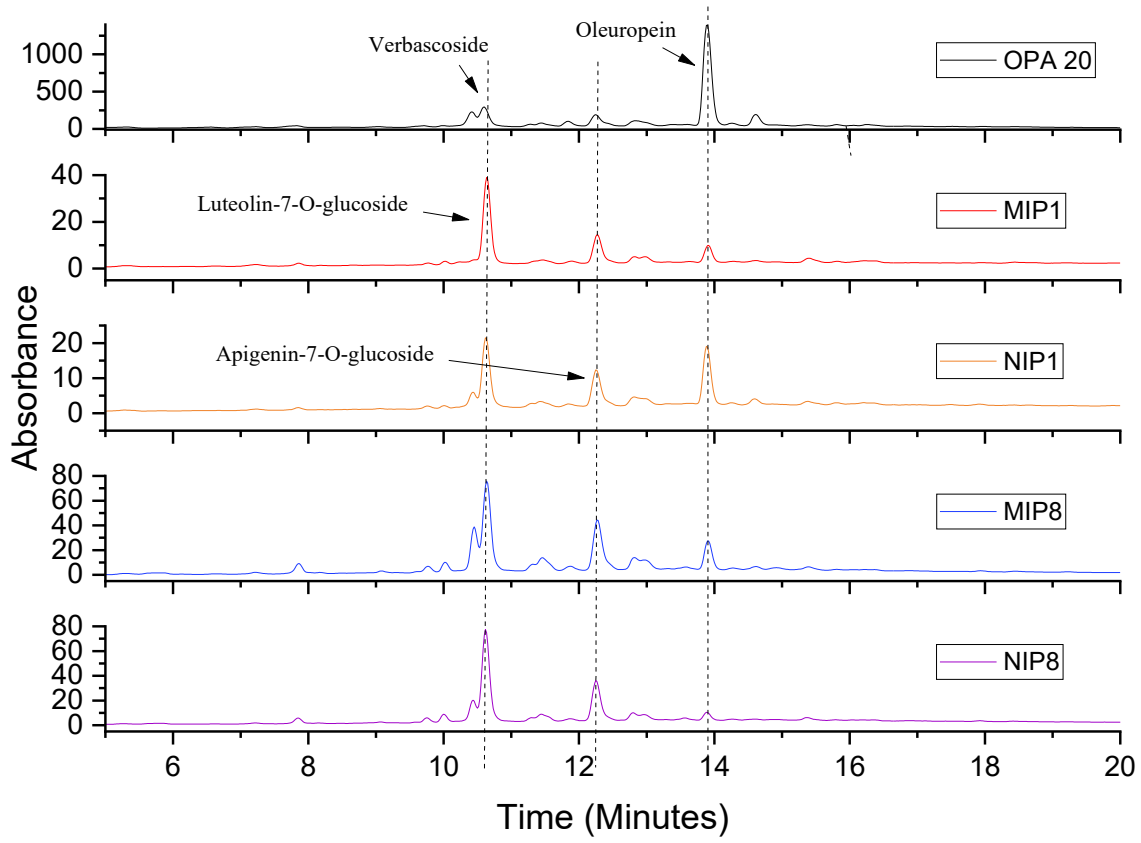

Figure 24: HPLC-DAD chromatograms at 280 nm for the extract OPA 20 and for the ethanol/water (50:50 v/v) (elution 4) fractions eluted from MIP/NIP1 and MIP/NIP8.

The results summarized in **Table 8** represent the mean enrichment factor (E) from three replicates (n=3), calculated based on the area ratio between the elution fraction 4, and the original extract.

Table 8: Average enrichment factors (E) for oleuropein and luteolin-7-O-glucoside in the elution fraction 4 (ethanol/water 50:50 v/v) based on HPLC-DAD measurements at λ= 280 nm (n=3).

Compound	MIP1	NIP1	MIP8	NIP8
Oleuropein	0.32	0.37	0.34	0.29
Luteolin-7-O-glucoside	2.85	2.62	2.59	3.17

Oleuropein showed low enrichment across all materials, with values ranging from 0.29 to 0.37. These results indicate lower retention of this secoiridoid compound, which is consistent with its lower

hydrogen bonding capacity. On the other hand, luteolin-7-O-glucoside showed substantially higher enrichment in all systems. MIP1 exhibited the highest enrichment among the imprinted materials (E = 2.85), which may reflect the influence of molecular imprinting in enhancing selective retention. However, the highest overall enrichment was found in NIP8 (E = 3.17), likely due to stronger non-specific interactions from the highly functionalized surface [30].

The materials were further tested using the industrial olive leaf extract VR2 SS1, characterized by a complex matrix rich in triterpenoids, mainly maslinic acid and oleanolic acid, and phenolic compounds, including luteolin-7-O-glucoside and its aglycone, luteolin. The coexistence of structurally distinct classes of molecules within the same extract presents an ideal scenario for evaluating the selective sorption performance of the materials.

To evaluate the retention profile of polyphenolic compounds in the VR2 SS1 extract, HPLC-DAD measurements at λ = 280 nm were used, which correspond to the typical absorbance range of flavonoids and related phenolics. **Figure 25** shows that the absorbance values increased rapidly with extract loading for all materials, with only minor variations observed beyond 20 mL. This indicates a fast saturation behavior, likely due to the high concentration of polyphenols in the extract. While differences were observed in the progression of the curves, these results provide an initial overview of retention behavior. Full saturation profiles are available in **Appendix 6**.

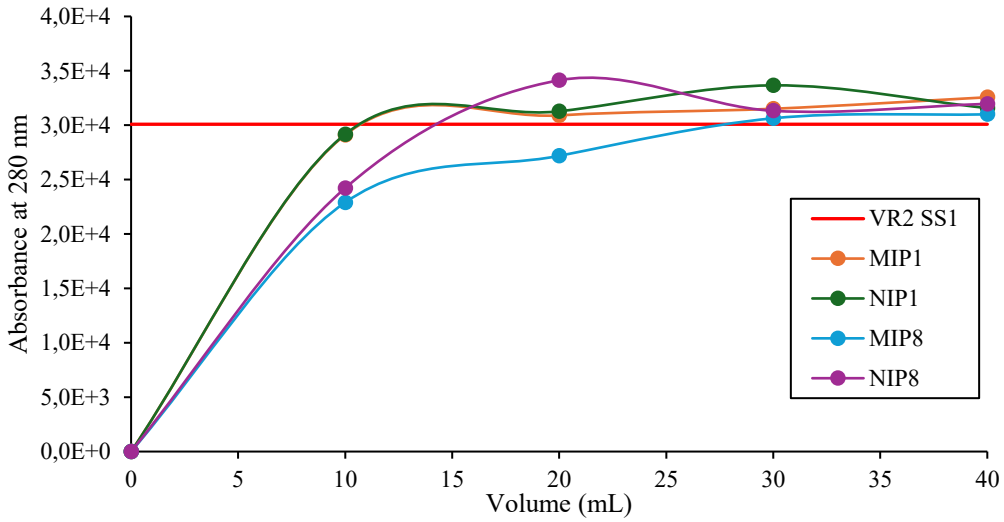

Figure 25: HPLC-DAD analysis of eluates collected after increasing loading volumes (10-40 mL) of the VR2 SS1 extract for polyphenols (λ = 280 nm).

MIP1 and NIP1, both synthesized with thinner polymer shells, demonstrated a faster saturation profile and higher maximum absorbance values compared to MIP8 and NIP8. This suggests more accessible interaction sites and effective retention of polyphenolic species. The similar performance between MIP1 and its non-imprinted counterpart points to a considerable role of non-specific

interactions, though the cleaner profiles observed later in elution suggest that MIP1 offers improved selectivity.

MIP8 and NIP8, prepared with higher monomer content and denser polymer networks, exhibited more gradual retention of polyphenols, which may be attributed to limited diffusion of binding sites. Although all materials reached similar final absorbance values, the difference in saturation profiles suggests that polymer structure plays a key role in retention dynamics.

In the elution step two (**Figure 26**), carried out using ethanol/water (75:25, v/v), MIP8 showed significantly sharper and more intense peaks in the regions corresponding to luteolin-7-O-glucoside (~10-11 min), apigenin-7-O-glucoside (~12 min) and luteolin (~15.5-16.5 min) when compared to its NIP counterpart (all elution graphics are attached in **Appendix 7**). This suggests a higher affinity for these polyphenols and supports a certain degree of selective retention enabled by the imprinting process, despite the thicker polymer shell.

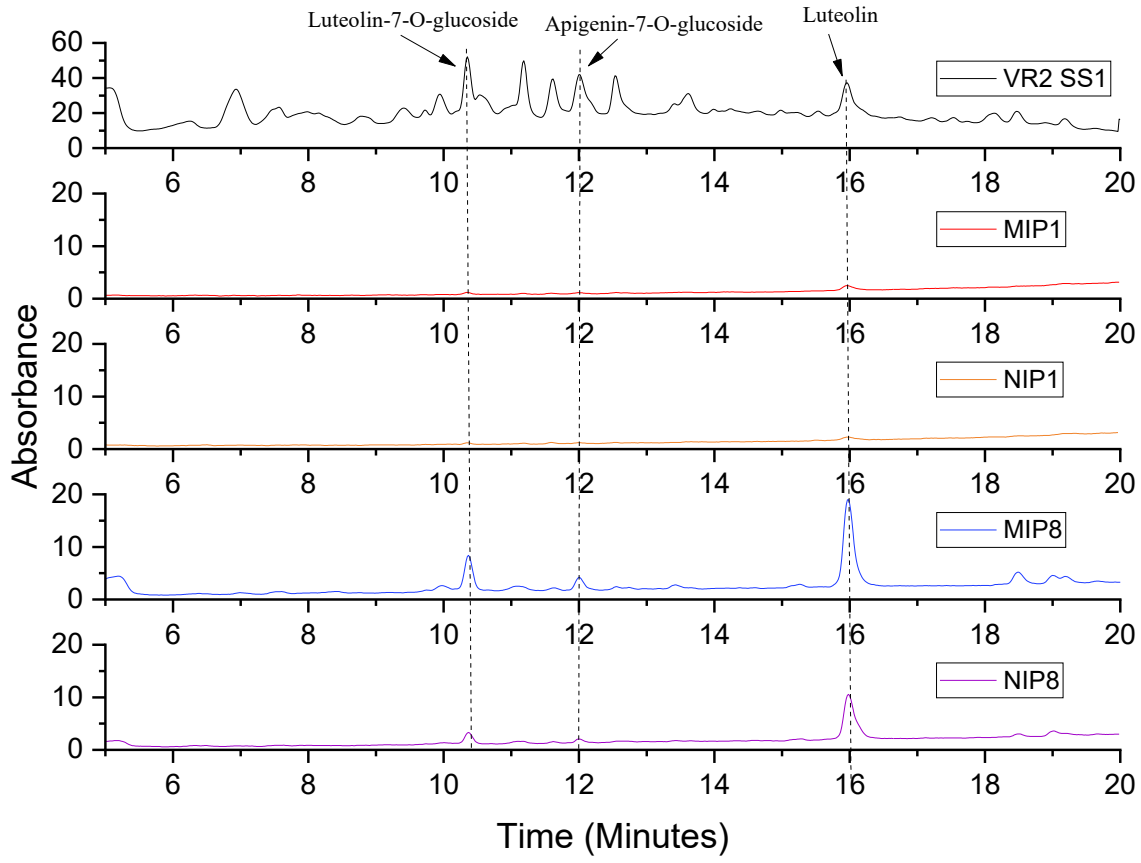

Figure 26: Elution chromatograms (λ = 280 nm) for polyphenol-rich fractions from VR2 SS1 extract and from materials MIP1/NIP1 and MIP8/NIP8, desorbed with ethanol/water (75:25, v/v) (elution 2).

In contrast, MIP1 did not display noticeable enrichment of specific flavonoids relative to NIP1, with both materials showing minimal signals in the eluted fraction. This lack of selectivity may

indicate that most polyphenols were either not retained during loading or were lost during the washing step, particularly in thinner-shell systems under these conditions.

These results indicate that although both MIPs retained a considerable amount of polyphenols, their ability to selectively release these compounds during elution seems to depend on how accessible the binding sites are and how strong the interactions are within those sites. In this case, MIP8 performed better than MIP1, suggesting that adjusting factors like shell thickness and functional group density can improve the selective recovery of polyphenols.

To investigate the behavior of triterpenoid compounds in the VR2 SS1 extract, which contains oleanolic and maslinic acids as major constituents, both saturation and elution experiments were carried out using MIP and NIP materials. Quantification was performed by HPLC-DAD at λ = 210 nm, the most representative absorption wavelength for triterpenoids.

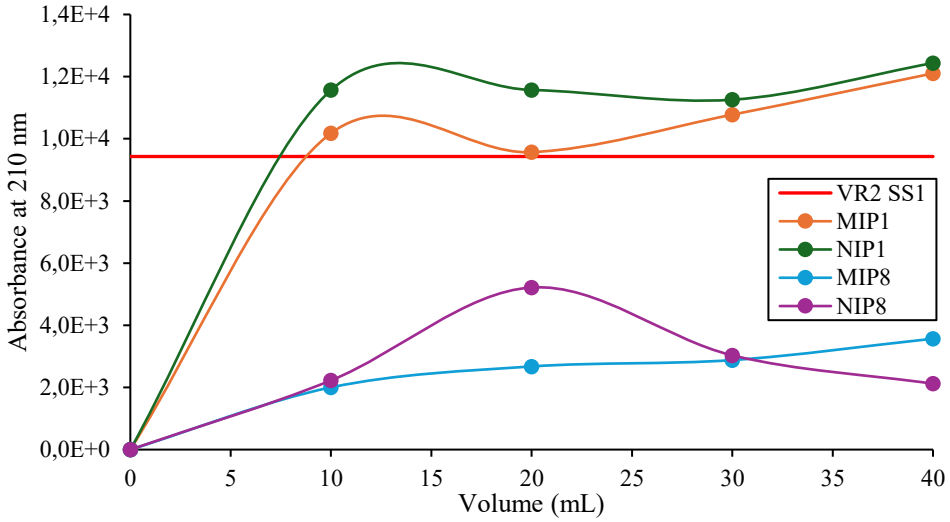

Figure 27: HPLC-DAD analysis of eluates collected after increasing loading volumes (10-40 mL) of the VR2 SS1 extract for triterpenoids (λ = 210 nm).

As illustrated in **Figure 27**, MIP1 and NIP1 showed rapid saturation, reaching saturation levels already at 10 mL (all the saturation profiles can be found attached in **Appendix 6**). However, this reflets the lower capacity of these materials to retain triterpenoids, as confirmed by the elution results in **Figure 28 (**all the elution steps are attached in **Appendix 7)**. The corresponding desorption profiles of MIP1 and NIP1 show virtually no detectable peaks associated with triterpenoids. This suggests that these materials, designed for polyphenol recognition, do not retain triterpenoids effectively. The signal observed in the saturation curves indicates that these materials, synthesized to target polyphenols, have low affinity with the triterpenoids present in the VRSS1 extract.

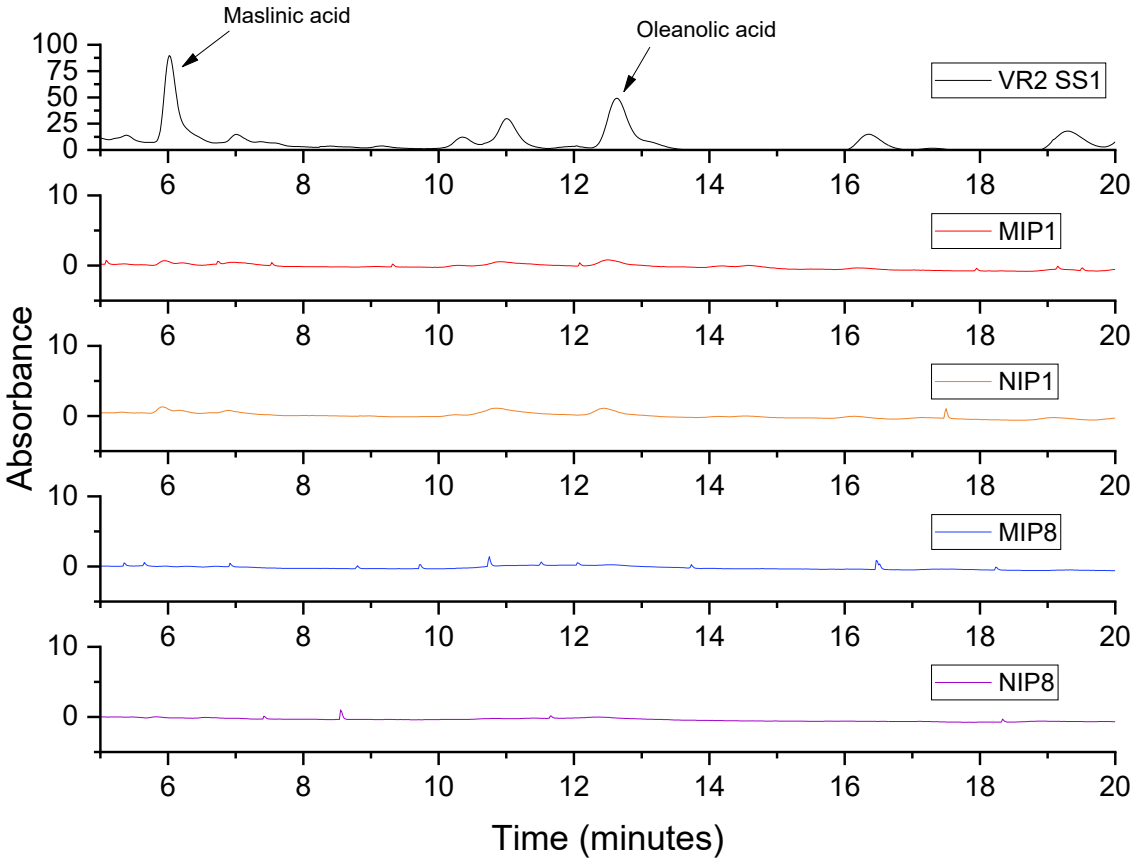

Figure 28: Elution chromatograms (λ = 210 nm) for triterpenoids-rich fractions from VR2 SS1 extract and from materials MIP1/NIP1 and MIP8/NIP8, desorbed with ethanol/water (75:25, v/v) (elution 2).

In contrast, MIP8 and NIP8 showed consistently lower absorbance values than the extract across all volumes, which indicates that some retention did occur. However, this interaction does not appear to be stable: in the elution chromatograms, the characteristic peaks of triterpenoids are again nearly absent, even in the earliest fractions. This implies that the adsorbed compounds were not strongly held and were likely washed out during the initial steps of the desorption sequence.

Overall, these results confirm that none of the materials tested were effectively suited for the specific retention of triterpenoids under the current synthesis and testing conditions. While some interaction may occur in the denser polymer matrices (e.g., MIP8), it does not translate into stable binding, and no significant enrichment or targeted separation of triterpenoids was achieved.

To assess the selective recovery of key compounds from the VR2 SS1 extract, enrichment factors were calculated for four representative analytes in the eluted fractions. These values, summarized in **Table 9**, reflect the ratio between the peak area in the eluate and the crude extract, providing a comparative measure of retention and release efficiency across the tested materials.

Table 9: Enrichment factors (E) calculated for selected compounds in the VR2 SS1 extract after desorption with ethanol/water (75:25, v/v). The values represent the ratio of peak area in the eluted fraction to the crude extract (mean of n = 2).

Compound	MIP1	NIP1	MIP8	NIP8
Luteolin-7-O-glucoside	0.8	1.8	1.0	0.6
Apigenin-7-O-glucoside	0.0	0.4	0.7	0.4
Luteolin	4.1	1.6	5.1	5.8
Oleanolic acid	0.9	0.9	0.5	2.7

The enrichment values confirm distinct retention behaviors among the materials tested. For luteolin, both MIP8 (E = 5.1) and NIP8 (E = 5.8) exhibited high enrichment, indicating strong overall retention. However, the minimal difference between imprinted and non-imprinted materials suggests that these interactions were largely non-specific, likely driven by surface functionalities and polymer density rather than imprinting [30].

In contrast, luteolin-7-O-glucoside was more enriched in MIP8 (E=1.0) than in NIP8 (E=0.6), suggesting that imprinting may have contributed to a more controlled and selective uptake of this glycosylated flavonoid. A similar pattern was observed with apigenin-7-O-glucoside, where MIP8 again outperformed its NIP counterpart (E=0.7 vs. 0.4), while MIP1 retained none of this compound. These results point to the role of polymer thickness and functionality density in enabling interaction with lower-abundance polyphenols, especially in the case of MIP8 [30].

For luteolin, MIP1 also demonstrated significant enrichment (E=4.1), outperforming NIP1 (E=1.6) and confirming that even thinner-shell materials can exhibit selective binding. This reinforces the effectiveness of the quercetin-based imprinting strategy in capturing structurally related flavonoids.

Regarding oleanolic acid, a non-target compound in these materials, most sorbents exhibited low enrichment (E=0.5-0.9), with the exception of NIP8, which showed a notably higher value (E=2.7). This unexpected result reflects the non-specific retention mechanisms enhanced by the high surface functionality and denser matrix of NIP8, though it does not imply selective binding in the absence of imprinting [30].

Maslinic acid was not included in the enrichment table, as its signals in the eluted fractions were either absent or negligible under the tested conditions, indicating no meaningful retention by any of the materials.

Altogether, these results highlight the multifactorial nature of selectivity in real matrices. While MIP8 demonstrates moderate imprinting effects for certain flavonoids, particularly glycosylated ones, non-specific interactions still play a dominant role in some cases. The data further illustrates that imprinting performance is not only determined by the presence of recognition cavities, but also by

factors such as polymer morphology, analyte solubility, and elution strength. These insights are crucial for guiding the next stages of material design and validating sorbents under industrially relevant extraction conditions.

9.4. Tests using a packed column

9.4.1. Effect of solvent composition on quercetin sorption isotherms

MIP3 was selected for packed column experiments due to its combination of effective sorption capacity and favorable physical properties. Among the various materials tested, those synthesized using DMF exhibited limited flow compatibility and were considered unsuitable for use under continuous flow conditions due to excessive backpressure. In contrast, MIP3, prepared with ethanol as solvent, presented adequate permeability and stable packing behavior, making it a viable candidate continuous flow systems. This enabled further investigation of its adsorption performance under dynamic conditions, specifically the comparison of its isotherms with those of two different solvent systems.

Quercetin adsorption isotherms were constructed in recirculating column mode at constant room temperature, using two different solvents, ethanol/water ratios: 80:20 and 50:50 (v/v). In each case, six increasing concentrations of quercetin (0.05 to 0.8 mg/mL) were tested. After each concentration step, the quercetin content in the solution was quantified by UV-Vis spectroscopy at 360 nm. These values were used to calculate two main parameters: the equilibrium concentration in the liquid phase (C, mM) and the amount of quercetin adsorbed per gram of MIP3 (concentration in the solid phase) (q, µmol/g). The calculations were performed in duplicate (n=2), and the mean values and standard deviations were used to build the isotherms.

The average values of q and C, along with their respective standard deviations, will subsequently be fitted to two classical isotherm models, Langmuir and Freundlich, to provide insights into the adsorption mechanism. The Langmuir model assumes monolayer adsorption on a homogeneous surface, while the Freundlich model describes multilayer adsorption on heterogeneous surfaces [33].

The mathematical expressions of both models were applied to fit the experimental data and assess their suitability under each solvent condition. The corresponding equations are presented below, followed by the isotherm plots and curve fitting results.

The equation representing Langmuir parameters is:

$$q = \frac{q_{max} k_L C}{1 + k_L C} \quad (1)$$

where q is the amount of solute adsorbed at equilibrium (μmol/g), C is the equilibrium concentration in solution (mM), q_{max} is the maximum sorption capacity (μmol/g), and k_L is the Langmuir constant, which reflects the affinity between the adsorbate and the binding sites [33].

The Freundlich model is described by the following equation:

$$q = K_F C^{1/n} \quad (2)$$

where K_F is the Freundlich constant related to sorption capacity, and n is an empirical parameter associated with the heterogeneity of the sorbent surface [33].

The calculated parameters from both models for each solvent system are summarized in **Table 10**, providing a comprehensive evaluation of the sorption behavior of quercetin onto MIP3 under different ethanol/water compositions. The resulting Freundlich isotherm fits were performed using the lsqcurvefit function in MATLAB and are shown in **Figure 29**.

Table 10: Fitting parameters of Langmuir and Freundlich isotherm models for quercetin sorption onto MIP3 in ethanol/water mixtures (50:50 and 80:20, v/v). The Langmuir model comprises the affinity constant (k_L), maximum sorption capacity (q_m), and the product ($q_m \times k_L$), along with the coefficient of determination (R^2). The Freundlich model includes the sorption capacity constant (K_F), heterogeneity index (n), and R^2.

		Parameter	**Quercetin**
Langmuir isotherm model	Ethanol/water 50/50 (v/v)	k_L	119.7
		q_{max}	9.9
		$q_{max} \times k_L$	1187.2
		R^2	0.96
	Ethanol/water 80/20 (v/v)	k_L	2.7
		q_{max}	4.2
		$q_{max} \times k_L$	11.2
		R^2	0.75
Freundlich isotherm model	Ethanol/water 50/50 (v/v)	K_F	20.7
		n	2.8
		R^2	0.95
	Ethanol/water 80/20 (v/v)	K_F	2.8
		n	3.4
		R^2	0.82

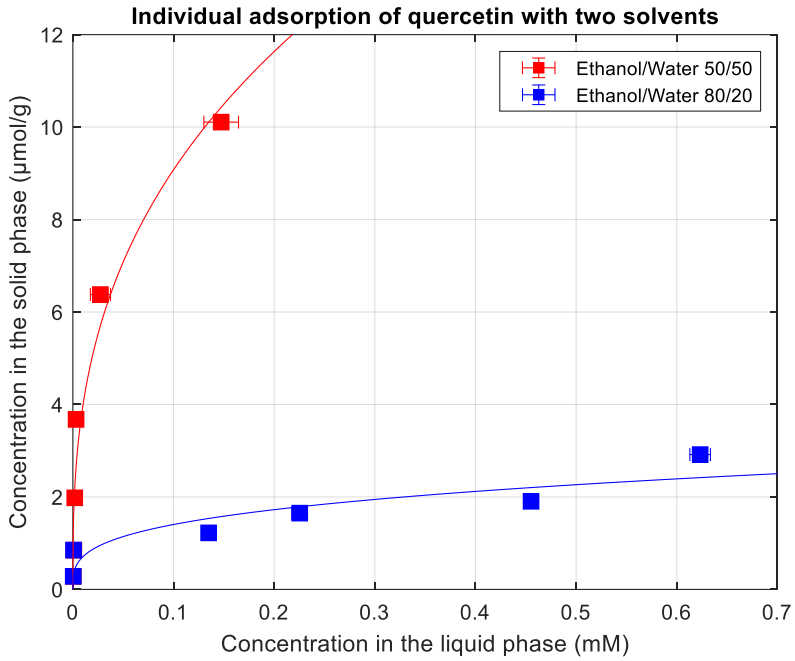

Figure 29: Sorption isotherms of quercetin on MIP3 in dynamic recirculating mode using ethanol/water (50:50 and 80:20, v/v) as solvent systems. Symbols represent experimental data (mean ± standard deviation, n = 2), and solid lines correspond to nonlinear fits using the Freundlich model [30].

The isotherm data demonstrates that quercetin sorption onto MIP3 is strongly influenced by solvent composition. In the ethanol/water 50:50 system, both isotherm models indicate superior sorption performance compared to the 80:20 mixture. For the Freundlich model, the sorption capacity constant (K_F = 20.7) and the heterogeneity index (n = 2.8), together with a high coefficient of determination (R^2 = 0.95), reflect stronger and more diverse binding interactions. These results suggest a heterogeneous surface with significant affinity toward quercetin under more aqueous conditions [30].

Similarly, the Langmuir model reveals a notable difference between the two solvent systems. In the 50:50 mixture, the maximum adsorption capacity (q_{max}) reached 9.9 µmol/g, with an affinity constant (k_L) of 119.7 mL/mg, resulting in a $q_{max} \times k_L$ product of 1187.2, and a high R^2 value (0.96), confirming an efficient monolayer sorption process. In contrast, the 80:20 solvent system showed a much lower sorption capacity, a reduced affinity, and a weaker correlation, indicating less favorable and less specific interactions [30].

These findings confirm that the ethanol/water 50:50 (v/v) mixture provides more favorable conditions for the selective capture of quercetin by MIP3. This enhanced performance can be attributed to the higher polarity of the 50:50 system, which promotes stronger hydrogen bonding between the hydroxyl groups of quercetin and the polar functional groups within the polymer matrix. Additionally, the increased water content may improve the solvation of quercetin, facilitating its diffusion into the imprinted cavities and increasing the probability of specific binding [30]. These solvent-dependent

effects are consistent with previous reports showing that aqueous-rich environments enhance the selectivity and affinity of MIPs toward polyphenolic compounds [6], [8], [14]. Such behavior supports the strategic use of 50:50 hydroalcoholic systems in gradient-based sorption-desorption processes aimed at targeted flavonoid recovery from complex plant extracts.

9.4.2. Sorption isotherms under competitive multi-analyte conditions

To further assess the performance of MIP3, a sorption experiment was carried out using a mixture of quercetin, vanillic acid, and oleuropein to mimic a more complex medium at a constant room temperature. Each compound was selected as a key representative of the flavonoids, secoiridoids, and phenolic acids present in the olive leaves extract. An equimolar concentration of these compounds was used, and sorption was performed in a packed column operating under continuous recirculation with ethanol/water (50:50, v/v) as solvent. This setup aimed to simulate competitive binding scenarios relevant to the selective separation of polyphenols from complex plant matrices.

The fitting results of the individual Langmuir and Freundlich models to the competitive sorption data are summarized in **Table 11**, which provides a comparative view of the sorption performance of MIP3 for each compound. Nonlinear regressions were performed using the lsqcurvefit function in MATLAB, yielding distinct model parameters for each polyphenol. These results are graphically represented in **Figure 30**, which displays the isotherms and highlights the markedly different affinities of MIP3 toward the analytes.

Table 11: Parameters for Langmuir and Freundlich isotherm models fitted to individual sorption data of quercetin, vanillic acid, and oleuropein from ternary mixtures using MIP3 and ethanol/water (50:50, v/v) as solvent.

	Parameter	Quercetin	Vanillic Acid	Oleuropein
Langmuir isotherm model	k_L	41.6	9.3	33.5
	q_m	10.4	5.7	0.48
	$q_m \times k_L$	432.9	53.2	15.9
	R^2	0.59	0.98	0.77
Freundlich isotherm model	K_F	48.0	11.1	0.6
	n	1.7	1.6	3.7
	R^2	0.63	0.97	0.60

The fitting results of the Langmuir and Freundlich models reveal distinct sorption behaviors for quercetin, vanillic acid, and oleuropein. Among the three, quercetin displayed the highest sorption capacity and affinity, with a Langmuir q_{max} of 10.4 µmol/g and k_L of 41.6 mL/mg, resulting in a $q_{max} \times k_L$ product of 432.9, which reflects both strong binding and a large number of available sites. This is further supported by the high Freundlich K_F value (48.0) and a heterogeneity index (n = 1.7), consistent with a moderately heterogeneous binding environment favorable to quercetin [30].

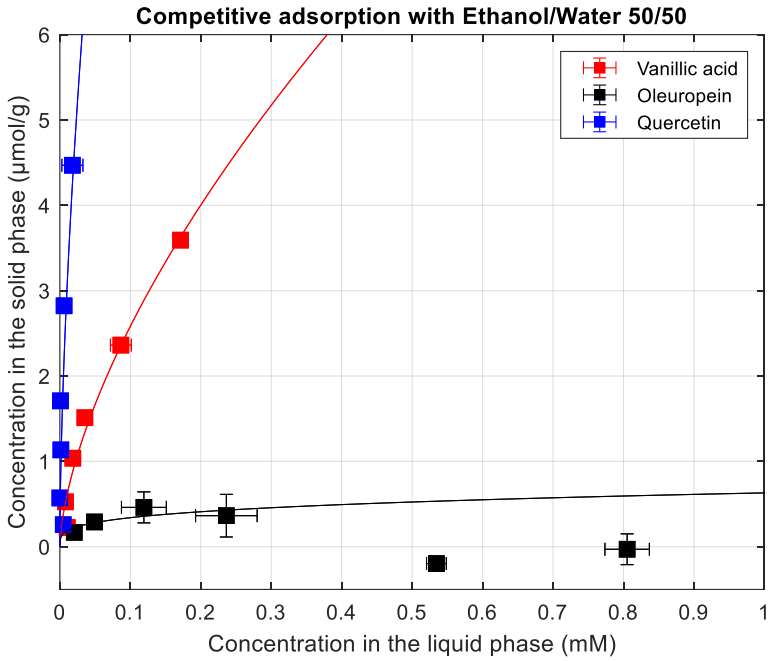

Figure 30: Individual sorption isotherms of quercetin, vanillic acid, and oleuropein from ternary mixtures in ethanol/water (50:50, v/v) on MIP3. Symbols represent experimental data (mean ± standard deviation, n = 2solid lines correspond to nonlinear fits using the Freundlich model [30].

Vanillic acid, while not the original template, also showed good sorption, particularly reflected by its high R^2 values in both models (0.98 Langmuir; 0.97 Freundlich). Its q_{max} (5.7 µmol/g) and K_F (11.1) indicate moderate retention, likely driven by hydrogen bonding between its hydroxyl/carboxylic acid groups and the pyridyl functionalities of MIP3. These interactions may be enhanced by the smaller size and planar structure of vanillic acid, which favors diffusion and accessibility to surface cavities [5], [8], [30].

In contrast, oleuropein showed very low sorption across both models. The Langmuir q_{max} was only 0.48 µmol/g, and K_F was 0.6, with lower model fit values (R^2 = 0.77 Langmuir, 0.60 Freundlich), suggesting weak and nonspecific interactions. This is likely due to the bulky and complex structure of oleuropein, a glycosylated secoiridoid, which may hinder access to the imprinted sites. Additionally, its lower π-character and reduced hydrogen-bonding complementarity with the pyridyl groups further explain its limited retention [5], [8], [30].

The clear differences in sorption behavior among the three compounds demonstrate that the combination of MIP3 and the ethanol/water (50:50, v/v) system is effective for the selective separation of distinct classes of polyphenols based on their structural features and interaction profiles. The notably lower retention of oleuropein compared to the other two compounds supports the idea of using a hydroalcoholic gradient or competitive elution strategy for effective separation. As previously discussed, while empirical isotherm models such as Langmuir and Freundlich provide valuable insight

and process guidance, they may fall short in fully capturing the complexity of multicomponent sorption in systems involving diverse molecular structures and affinities [5], [6], [8], [9], [14], [26], [29], [30]. Nonetheless, the high R^2 values observed for vanillic acid and acceptable fits for quercetin support the validity of the approach for initial process design and optimization.

9.5. Selective retention of triterpenoids using oleanolic acid-based MIPs in SPE

Following the evaluation of MIP3 and related materials imprinted with quercetin, additional experiments were conducted using MIPs prepared with oleanolic acid as template. These assays aimed to extend the imprinting approach to other structurally distinct bioactive compounds present in olive leaf extracts. The selected materials were tested under comparable conditions, using ethanol/water (80:20, v/v) as solvent and operating in loading/washing/elution mode, and applied to a range of analytes, namely, maslinic acid, oleanolic acid, and quercetin.

9.5.1. Retention efficiency of maslinic acid and oleanolic acid in oleanolic acid-imprinted sorbents

To evaluate the selectivity of the oleanolic acid-imprinted materials toward structurally related triterpenoids, an sorption experiment was performed using maslinic acid and oleanolic acid as analytes. The test was carried out on the oleanolic acid tailored materials (MIP/NIP9 and 10), MIP3, and CF using ethanol/water (80:20, v/v) as solvent, in which each compound was tested at a concentration of 0.15 mM. The procedure was performed in duplicate (n=2), and the resulting retention profiles allowed assessment of the material's affinity and potential for selective enrichment of triterpenoid compounds.

The average retention values obtained for each material were plotted to allow direct comparison of performance across the different sorbents. **Figure 31** shows the retention of maslinic acid, while **Figure 32** presents the results for oleanolic acid. In both cases, the bars represent the mean retention values from duplicate experiments (n=2), with error bars indicating the respective standard deviations.

The retention values obtained for both maslinic and oleanolic acids were generally low and showed minimal variation across all tested materials (MIP/NIPs, and CF). No clear retention advantage was observed for the oleanolic acid-imprinted materials (MIP9 and MIP10) compared to their non-imprinted counterparts or to the cellulose. These results suggest that, under the tested conditions, the materials did not exhibit selective binding toward the target triterpenoids. This outcome is likely related to the limited interaction of these compounds with the polymer surfaces in the neutral ethanol/water medium, where acidic groups on the analytes remain largely uncharged and unable to engage effectively in ionic or hydrogen-bonding interactions.

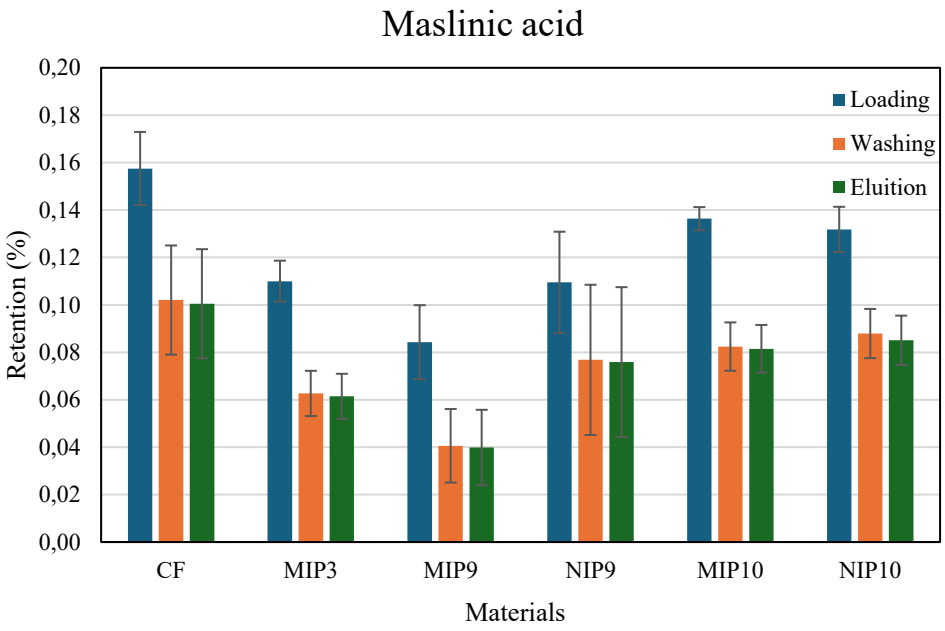

Figure 31: Average retention (%) of maslinic acid after the loading/washing/elution. Results are shown as mean ± standard deviation (n = 2).

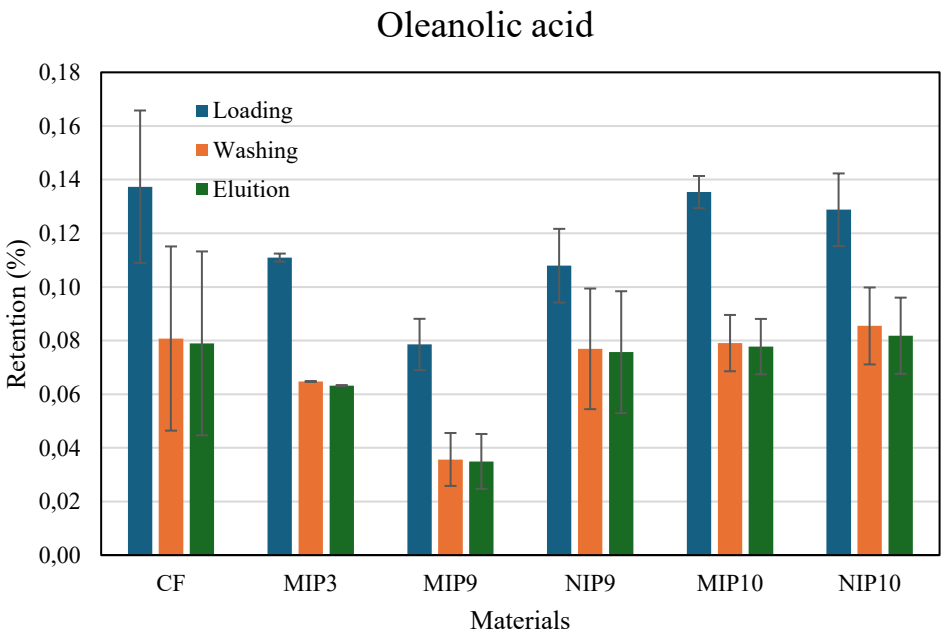

Figure 32: Mean retention (%) of oleanolic acid after the loading/washing/elution. Results are shown as mean ± standard deviation (n = 2).

Although prior characterization confirmed successful functionalization and polymer growth, these results highlight that performance cannot be inferred solely from structural features. The low and uniform retention values across different formulations suggest that neither imprinting nor functional monomer choice (DMAEMA) was sufficient to enhance sorption under the tested conditions. This

emphasizes the importance of testing MIPs in chemically suitable environments, where the interaction mechanisms intended during synthesis are more likely to be activated.

In the case of DMAEMA-based polymers, stronger interaction with acidic analytes such as oleanolic and maslinic acids may depend on protonation of the amine groups, thus requiring a lower pH to promote electrostatic interactions. Adjusting the pH of the sorption medium could therefore improve affinity and help reveal differences in performance among the materials. This has been observed in other MIP systems, where analyte ionization and functional group charged state play a critical role in retention performance [6], [8], [29]. Furthermore, additional tests using mixtures of compounds with varied physicochemical properties, such as quercetin and other polyphenols, may offer broader insight into the sorbent's behavior in competitive and application-relevant scenarios.

9.5.2. Retention of quercetin in ethanol/water (80:20, v/v) using different sorbent materials

To investigate the retention behavior of quercetin under low-polarity conditions, a new sorption experiment was carried out using ethanol/water (80:20, v/v) as the solvent system. The sorbents tested included molecularly imprinted polymers (MIP9 and 10), their corresponding non-imprinted references (NIP9 and 10), cellulose (CF), and quercetin imprinted polymer (MIP3). The experimental procedure followed a typical loading, washing, and elution sequence, and absorbance measurements were taken at 375 nm. Each test was performed in duplicate (n=2), and the results are expressed as average values with standard deviation.

The results, presented in **Figure 33,** reinforce the critical role of template-analyte complementarity in determining the success of molecular imprinting. MIP3, specifically imprinted for quercetin, stood out in retaining this flavonoid with high efficiency under the tested conditions, confirming the creation of high-affinity binding sites tailored to its structure. In contrast, materials imprinted with oleanolic acid, showed minimal interaction with quercetin.

Although the template molecule used in MIPs 9 and 10 (oleanolic acid) differs structurally from quercetin, some retention was still observed in the loading step, particularly for MIP10. This may be attributed to non-specific interactions and partial functional group complementarity, such as hydrogen bonding and π-π stacking between aromatic systems. Comparable retention with the corresponding NIPs further supports this interpretation, indicating that retention in these cases is not due to the imprinting effects. Despite this, the performance of MIP10 compared to CF suggests that functionalization alone already improves retention.

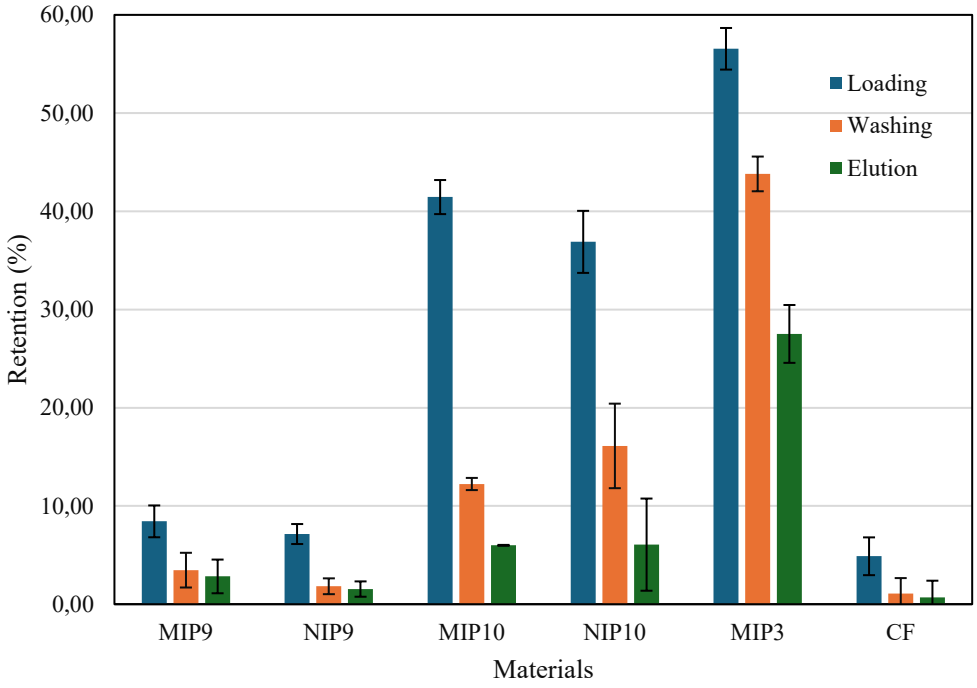

Figure 33: Average retention of quercetin (%) during the loading, washing, and elution steps for each tested sorbent material using ethanol/water (80:20, v/v) as solvent. Materials include MIPs imprinted with oleanolic acid (M9 and M10), their corresponding NIPs (N9 and N10), cellulose fiber (CF), and MIP3, imprinted with quercetin. Results are shown as mean ± standard deviation (n = 2).

This highlights that, even when imprinting is not fully effective, polymer modification contributes to better interaction with the analyte and may offer practical advantages such as increasing retention capacity, improving flow properties and reducing backpressure. Overall, both imprinting and surface functionalization play an important role in designing efficient sorbents for complex plant matrices.

Conclusion and future research

This work was driven by the goal of transforming olive leaf, an abundant agricultural by-product, into a valuable source of bioactives through selective and sustainable extraction technologies. By integrating material science, polymer chemistry, and analytical method development, the study focused on creating sorbents capable of isolating specific compound families from complex plant matrices. The outcome was not only the synthesis of hybrid functional materials, but also the establishment of a systematic strategy for tailored separation based on sorption/desorption using molecular imprinted polymers.

Building from this vision, the first phase of the work focused on the functionalization of cellulose, chosen for its abundance, renewability, chemical versatility, and compatibility with ATRP-based surface polymerization. Modified cellulose particles were synthesized and used as a platform for developing eight different quercetin-imprinted MIPs, systematically varying the type of cellulose, solvent, and monomer-template ratios. Among these, MIP3 emerged as a leading candidate, exhibiting high retention capacity, outstanding selectivity, and mechanical stability suitable for continuous sorption/desorption operations in chromatography columns.

Comprehensive characterization by FTIR, SEM and BET confirmed successful surface functionalization and polymer growth. Sorption experiments under dynamic flow demonstrated that solvent polarity plays a decisive role in modulating binding behavior: ethanol/water 50:50 (v/v) yielded significantly higher retention compared to 80:20 (v/v), a result supported by Langmuir and Freundlich isotherm fitting and statistical validation through ANOVA, particularly for MIP3 and MIP8.

Performance was further validated under competitive binding conditions, where the MIPs selectively retained quercetin over other phenolics like oleuropein and vanillic acid, reinforcing the importance of molecular recognition. These differences became even more relevant when the materials were tested with industrial extracts such as NATAC OPA 20 and VR2 SS1, confirming that the optimized MIPs could selectively enrich flavonoid glycosides such as luteolin-7-O-glucoside from complex mixtures using only hydroalcoholic solvents. Enrichment factors of up to 5 were obtained in simple desorption steps, revealing the potential of these materials for green extraction processes. As expected, none of the materials demonstrated strong or stable retention of triterpenoids under flavonoid-optimized conditions. These results confirmed that targeted extraction of each compound family requires dedicated imprinting strategies, and that sorbent architecture must be fine-tuned not only for selectivity, but for kinetic and elution behavior.

To enable use in continuous flow systems, MIP3 was synthesized at gram scale, packed into a chromatography column, and tested under dynamic recirculation. Isotherms confirmed high affinity and binding site heterogeneity, with stable performance under mild conditions, showing no degradation over multiple cycles and no excessive backpressure. This represents not only a proof of concept but a tangible step toward industrial implementation.

Recognizing the chemical diversity of olive leaf extracts, a second imprinting strategy was developed using oleanolic acid as the template and DMAEMA as the functional monomer. Although the DMAEMA-based MIPs (MIP9 and MIP10) did not show selective retention of triterpenoids under the tested hydroalcoholic conditions, the experiment still highlighted the advantages of performing cellulose modification. This indicates that surface modification alone contributes positively to retention. Moreover, the results suggest that stronger interactions with acidic analytes like oleanolic and maslinic acids may require specific pH conditions to activate electrostatic mechanisms. Future work should explore pH optimization and competitive assays with other compound families to unlock the full potential of these materials.

Overall, the findings highlight that both molecular imprinting and surface modification contribute to sorbent efficiency. Imprinting ensures selectivity when the template and target are structurally aligned, while polymer functionalization can enhance retention and improve material properties relevant to column operation, such as packing behavior and flow resistance.

Looking ahead, the same systematic approach used for flavonoids can be applied to other compound classes. The long-term goal is to assemble a modular purification system composed of MIP-based columns, each tailored to a specific family (flavonoids, triterpenes, and secoiridoids) operating sequentially and efficiently. Such a system would represent a new generation of bio-based separation technology: scalable, reusable, solvent-efficient, and precise. It would also serve as a model for the sustainable valorization of other agricultural subproducts and contribute to the broader goals of green chemistry and the circular bioeconomy.

Importantly, the relevance of this work has already been recognized through the publication of a reviewed scientific article in the *Functional Polymers* journal (Elsevier, impact factor = 4.5, Q1), entitled *"Pyridyl-functionalized and surface molecularly imprinted cellulose particles to target bioactive compounds in olive leaf"*. This publication summarizes the relevance of the developed methodology and its contribution to the field of selective extraction. Additional details from this study are available in **Appendix 8**.

Overall, this thesis offers more than a collection of materials, it provides a blueprint for the intelligent design of sorbents for the sustainable recovery of bioactive compounds, and the future of biorefinery processes based on molecular recognition. It provides a foundation for technologies that are not only effective and sustainable, but also adaptable and aligned with future demands in bioresource utilization.

References

[1] H. Sales, J. Nunes, and M. C. Vaz Patto, 'Achievements and challenges towards a sustainable conservation and use of "galega vulgar" olea europaea Variety', Oct. 01, 2020, *MDPI AG*. doi: 10.3390/agronomy10101467.

[2] M. de la L. Cádiz-Gurrea, D. Pinto, C. Delerue-Matos, and F. Rodrigues, 'Olive fruit and leaf wastes as bioactive ingredients for cosmetics—a preliminary study', *Antioxidants*, vol. 10, no. 2, pp. 1–18, Feb. 2021, doi: 10.3390/antiox10020245.

[3] 'World Market of Olive Oil and Table Olives - Data From December 2024 - International Olive Council'. [Online]. Available: https://www.internationaloliveoil.org/world-market-of-olive-oil-and-table-olives-data-from-december-2024/

[4] M. de la L. Cádiz-Gurrea, D. Pinto, C. Delerue-Matos, and F. Rodrigues, 'Olive fruit and leaf wastes as bioactive ingredients for cosmetics—a preliminary study', *Antioxidants*, vol. 10, no. 2, pp. 1–18, Feb. 2021, doi: 10.3390/antiox10020245.

[5] C. P. Gomes, R. C. S. Dias, and M. R. P. F. N. Costa, 'Surface Molecularly Imprinted Cellulose-Synthetic Hybrid Particles Prepared via ATRP for Enrichment of Flavonoids in Olive Leaf', *Macromol React Eng*, vol. 17, no. 3, Jun. 2023, doi: 10.1002/mren.202300011.

[6] C. Gomes, G. Sadoyan, R. C. S. Dias, and M. R. P. F. N. Costa, 'Development of molecularly imprinted polymers to target polyphenols present in plant extracts', *Processes*, vol. 5, no. 4, Dec. 2017, doi: 10.3390/pr5040072.

[7] P. Pérez-Larrán, B. Díaz-Reinoso, A. Moure, J. L. Alonso, and H. Domínguez, 'Adsorption technologies to recover and concentrate food polyphenols', Oct. 01, 2018, *Elsevier Ltd*. doi: 10.1016/j.cofs.2017.10.005.

[8] A. Almeida, C. Martins, R. C. S. Dias, and M. R. P. F. N. Costa, 'Competitive Adsorption of Phenolic Acids, Secoiridoids, and Flavonoids in Quercetin Molecularly Imprinted Polymers and Application for Fractionation of Olive Leaf Extracts', *J Chem Eng Data*, Oct. 2023, doi: 10.1021/acs.jced.3c00543.

[9] C. P. Gomes, R. C. S. Dias, and M. R. P. F. N. Costa, 'Hybrid cellulose-poly(4-vinylpyridine) adsorbents produced via ATRP and their application to target polyphenols in winemaking, olive oil production and almond processing residues', *React Funct Polym*, vol. 164, Jul. 2021, doi: 10.1016/j.reactfunctpolym.2021.104930.

[10] T. Aziz *et al.*, 'A Review on the Modification of Cellulose and Its Applications', Aug. 01, 2022, *MDPI*. doi: 10.3390/polym14153206.

[11] M. Flejszar and P. Chmielarz, 'Surface-initiated atom transfer radical polymerization for the preparation ofwell-defined organic-inorganic hybrid nanomaterials', Sep. 01, 2019, *MDPI AG*. doi: 10.3390/ma12183030.

[12] K. Matyjaszewski, ‘Atom Transfer Radical Polymerization (ATRP): Current status and future perspectives’, *Macromolecules*, vol. 45, no. 10, pp. 4015–4039, May 2012, doi: 10.1021/ma3001719.

[13] H. Mondal Editor, ‘Polymers and Polymeric Composites: A Reference Series Cellulose-Based Superabsorbent Hydrogels’. [Online]. Available: http://www.springer.com/series/15068

[14] C. P. Gomes, R. C. S. Dias, and M. R. P. F. N. Costa, ‘Fractionation of flavonols and anthocyanins in winemaking residues using molecularly imprinted cellulose-synthetic hybrid particles with pyridyl active surface’, *Nano Select*, vol. 5, no. 5, May 2024, doi: 10.1002/nano.202300153.

[15] C. Dong, H. Shi, Y. Han, Y. Yang, R. Wang, and J. Men, ‘Molecularly imprinted polymers by the surface imprinting technique’, Feb. 15, 2021, *Elsevier Ltd*. doi: 10.1016/j.eurpolymj.2020.110231.

[16] C. Didaskalou, S. Buyuktiryaki, R. Kecili, C. P. Fonte, and G. Szekely, ‘Valorisation of agricultural waste with an adsorption/nanofiltration hybrid process: From materials to sustainable process design’, *Green Chemistry*, vol. 19, no. 13, pp. 3116–3125, 2017, doi: 10.1039/c7gc00912g.

[17] J. Berbel and A. Posadillo, ‘Review and analysis of alternatives for the valorisation of agro-industrial olive oil by-products’, Jan. 17, 2018, *MDPI*. doi: 10.3390/su10010237.

[18] R. Abbattista, G. Ventura, C. D. Calvano, T. R. I. Cataldi, and I. Losito, ‘Bioactive compounds in waste by-products from olive oil production: Applications and structural characterization by mass spectrometry techniques’, Jun. 01, 2021, *MDPI AG*. doi: 10.3390/foods10061236.

[19] R. Palmeri *et al.*, ‘Olive Leaves, a Promising Byproduct of Olive Oil Industry: Assessment of Metabolic Profiles and Antioxidant Capacity as a Function of Cultivar and Seasonal Change’, *Agronomy*, vol. 12, no. 9, Sep. 2022, doi: 10.3390/agronomy12092007.

[20] ‘OLEAF4VALUE Home - OLEAF4VALUE’. [Online]. Available: https://oleaf4value.eu/

[21] L. Abaza, A. Taamalli, H. Nsir, and M. Zarrouk, ‘Olive tree (Olea europeae L.) leaves: Importance and advances in the analysis of phenolic compounds’, Dec. 01, 2015, *MDPI*. doi: 10.3390/antiox4040682.

[22] D. Ryan, P. D. Prenzler, S. Lavee, M. Antolovich, and K. Robards, ‘Quantitative changes in phenolic content during physiological development of the olive (Olea europaea) cultivar Hardy’s Mammoth’, *J Agric Food Chem*, vol. 51, no. 9, pp. 2532–2538, Apr. 2003, doi: 10.1021/jf0261351.

[23] M. Antónia Nunes, S. Pawlowski, A. S. G. Costa, R. C. Alves, M. B. P. P. Oliveira, and S. Velizarov, ‘Valorization of olive pomace by a green integrated approach applying sustainable extraction and membrane-assisted concentration’, *Science of the Total Environment*, vol. 652, pp. 40–47, Feb. 2019, doi: 10.1016/j.scitotenv.2018.10.204.

[24] E. Roselló-Soto *et al.*, ‘Emerging opportunities for the effective valorization of wastes and by-products generated during olive oil production process: Non-conventional methods for the

recovery of high-added value compounds', Oct. 01, 2015, *Elsevier Ltd*. doi: 10.1016/j.tifs.2015.07.003.

[25] P. Gullón *et al.*, 'Valorization of by-products from olive oil industry and added-value applications for innovative functional foods', Nov. 01, 2020, *Elsevier Ltd*. doi: 10.1016/j.foodres.2020.109683.

[26] A. Bzainia, R. C. S. Dias, and M. R. P. F. N. Costa, 'Enrichment of Quercetin from Winemaking Residual Diatomaceous Earth via a Tailor-Made Imprinted Adsorbent', *Molecules*, vol. 27, no. 19, Oct. 2022, doi: 10.3390/molecules27196406.

[27] A. A. Özcan and Ş. Demirli, 'Molecular Imprinted Solid-Phase Extraction System for the Selective Separation of Oleuropein from Olive Leaf', *Separation Science and Technology (Philadelphia)*, vol. 49, no. 1, pp. 74–80, 2014, doi: 10.1080/01496395.2013.814678.

[28] F. Lorandi, M. Fantin, and K. Matyjaszewski, 'Atom Transfer Radical Polymerization: A Mechanistic Perspective', Aug. 31, 2022, *American Chemical Society*. doi: 10.1021/jacs.2c05364.

[29] C. P. Gomes, R. C. S. Dias, and M. R. P. F. N. Costa, 'Preparation of Molecularly Imprinted Adsorbents with Improved Retention Capability of Polyphenols and Their Application in Continuous Separation Processes', *Chromatographia*, vol. 82, no. 6, pp. 893–916, Jun. 2019, doi: 10.1007/s10337-019-03728-7.

[30] A. Almeida, R. M. Gaspar, S. Ferreira-Dias, M. R. P. F. N. Costa, and R. C. S. Dias, 'Pyridyl-functionalized and surface molecularly imprinted cellulose particles to target bioactive compounds in olive leaf', *React Funct Polym*, vol. 214, Sep. 2025, doi: 10.1016/j.reactfunctpolym.2025.106338.

[31] A. Altwala and R. Mokaya, 'Modulating the porosity of activated carbons via pre-mixed precursors for simultaneously enhanced gravimetric and volumetric methane uptake', *J Mater Chem A Mater*, vol. 10, no. 26, pp. 13744–13757, May 2022, doi: 10.1039/d2ta00421f.

[32] J. G. Pribyl, K. M. L. Taylor-Pashow, T. C. Shehee, and B. C. Benicewicz, 'High-Capacity Poly(4-vinylpyridine) Grafted PolyHIPE Foams for Efficient Plutonium Separation and Purification', *ACS Omega*, vol. 3, no. 7, pp. 8181–8189, Jul. 2018, doi: 10.1021/acsomega.8b01057.

[33] Y. A. B. Neolaka *et al.*, 'A Cr(VI)-imprinted-poly(4-VP-co-EGDMA) sorbent prepared using precipitation polymerization and its application for selective adsorptive removal and solid phase extraction of Cr(VI) ions from electroplating industrial wastewater', *React Funct Polym*, vol. 147, Feb. 2020, doi: 10.1016/j.reactfunctpolym.2019.104451.

Appendix

***Appendix 1*:** FTIR-ATR spectra of cellulose (CF and MCC), modified cellulose (CF-Br and MCC-Br), functional monomer (4VP), and cellulose-based MIPs and their respective NIPs.

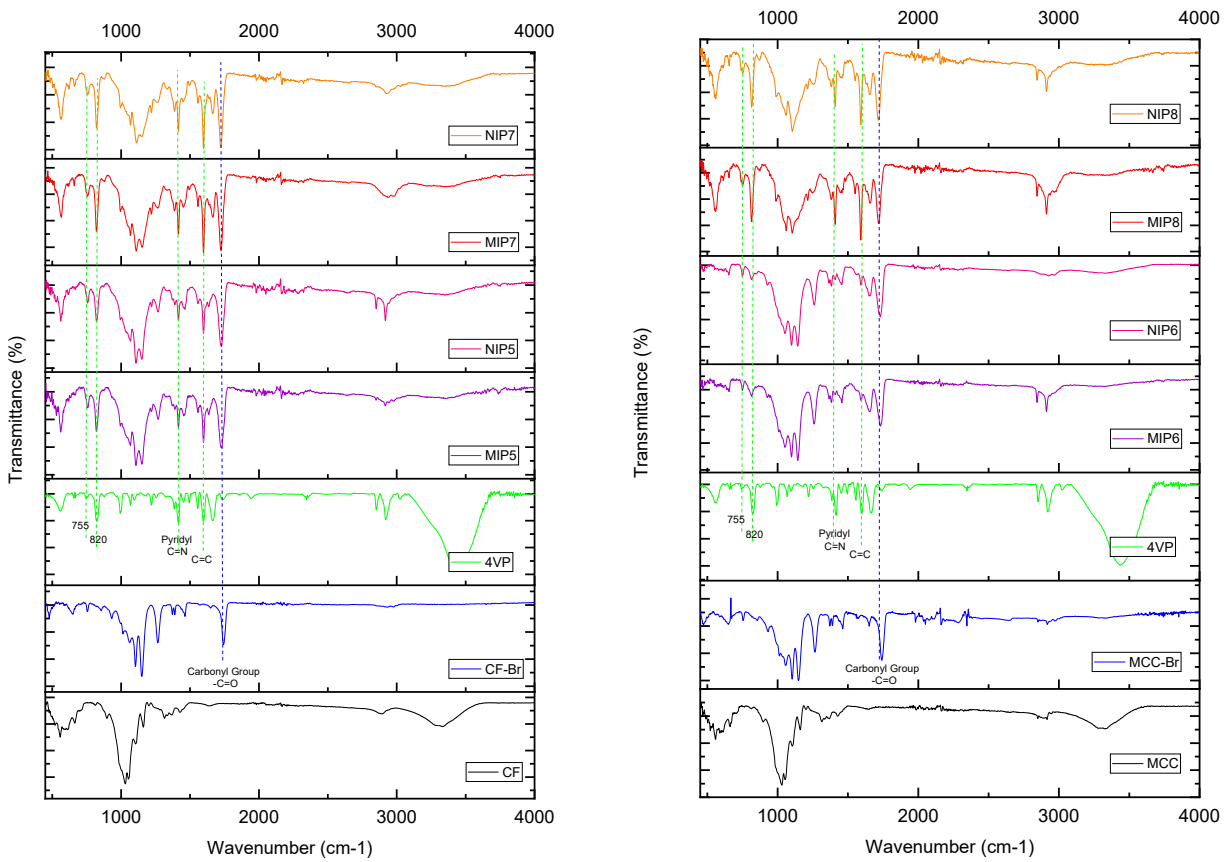

Figure 34: Comparative FTIR-ATR spectra confirming ATRP initiator immobilization and pyridyl-functionalized polymer grafting on cellulose-based supports: **(a)** Spectra of CF, CF-Br, 4VP, and MIP/NIP5 and MIP/NIP7; **(b)** Spectra of MCC, MCC-Br, 4VP, and MIP/NIP6 and MIP/NIP8. The appearance of new absorption bands in both cases indicates successful functionalization and polymerization processes.

b

Appendix 2: Statistical comparison of quercetin retention in MIP/NIP pairs using acetonitrile.

Statistical analysis was conducted to evaluate the retention of quercetin in material pairs MIP/NIP1 to MIP/NIP8 using acetonitrile as the solvent. Each condition was tested in three independent experimental replicates (n = 3), assessing the amount of quercetin retained after the loading, washing, and elution steps.

Table 12: Summary of one-way ANOVA results (single-factor) applied to each MIP/NIP pair to assess differences in quercetin retention after SPE in acetonitrile. The p-values highlight which pairs exhibit statistically significant differences in retention efficiency.

	Average	**Variance**	**Test_Statis**	**p value**
MIP/NIP1	0.031902	0.002895	1.778847784	0.056575
MIP/NIP2	0.029566	0.003298	1.544470841	0.080527
MIP/NIP3	0.038924	0.034052	0.632810502	0.272258
MIP/NIP4	0.005718	0.04773	0.078521498	0.469671
MIP/NIP5	-0.19811	0.021212	-4.080816157	0.998235
MIP/NIP6	-0.32617	0.017718	-7.351098666	0.99996
MIP/NIP7	-0.02245	0.006366	-0.84395579	0.788395
MIP/NIP8	0.117659	0.036042	1.859263825	0.050022

Table 13: Global ANOVA analysis across all MIP/NIP pairs indicating statistically significant variation among the groups ($p < 0.001$), suggesting that at least one pair differs significantly from the others.

Source of Variation	*SS*	*df*	*MS*	*F*	*P-value*	*F crit*
Between Groups	1.353454	7	0.193351	9.135804	8.94E-08	2.156424
Within Groups	1.354498	64	0.021164			
Total	2.707952	71				

Appendix 3: Peak area ratios during SPE under Competitive Conditions (ethanol/water 80:20 v/v).

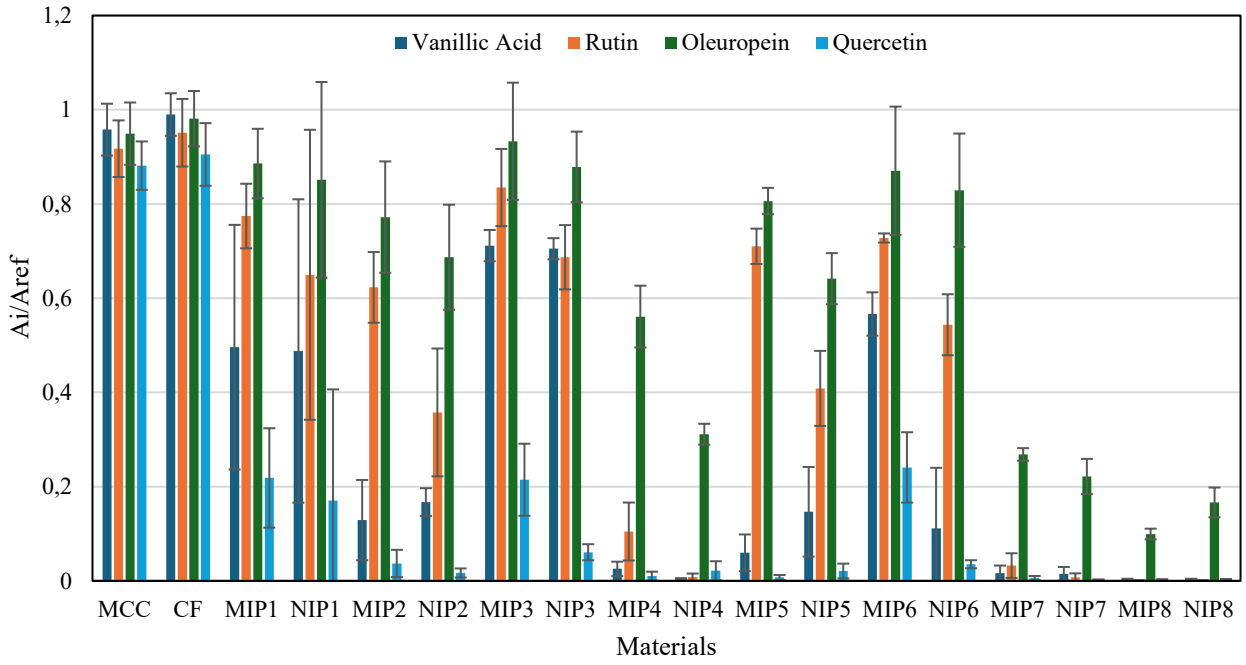

Figure 35: Peak area ratios of each analyte (quercetin, vanillic acid, rutin, and oleuropein) in the loading fraction across the different MIP/NIP and reference materials. Values represent the area of each compound relative to its initial concentration in the mixture.

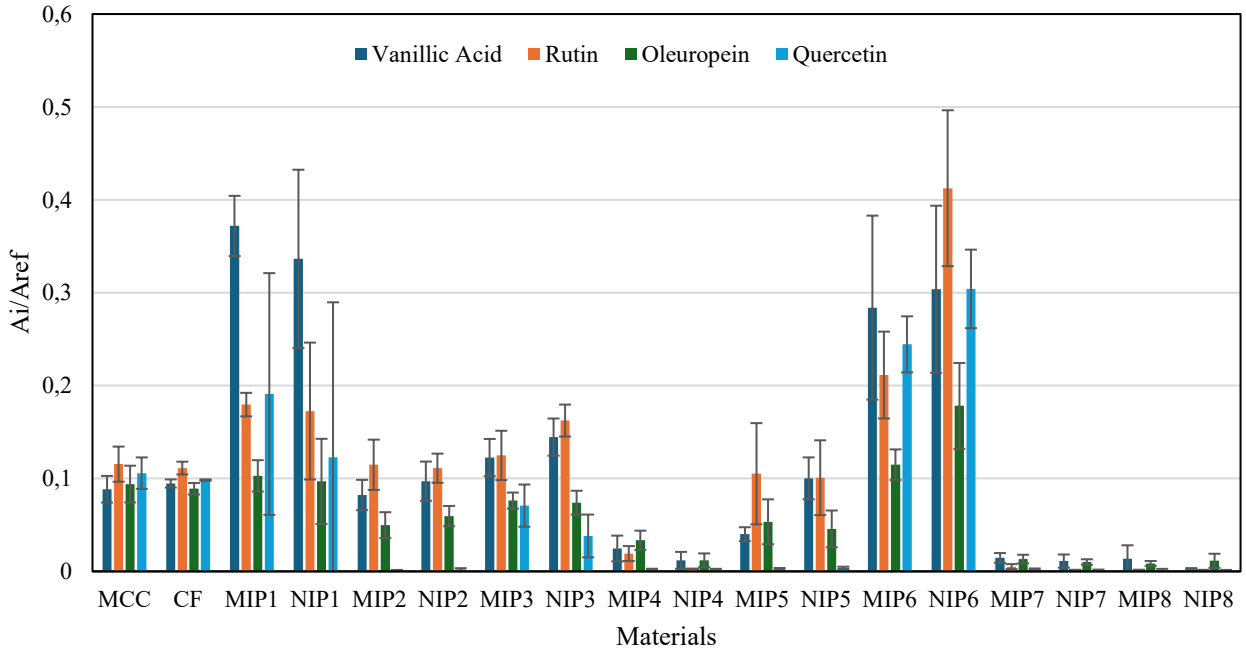

Figure 36: Peak area ratios of each analyte in the washing fraction, showing the extent of non-retained or weakly retained compounds following initial sorption.

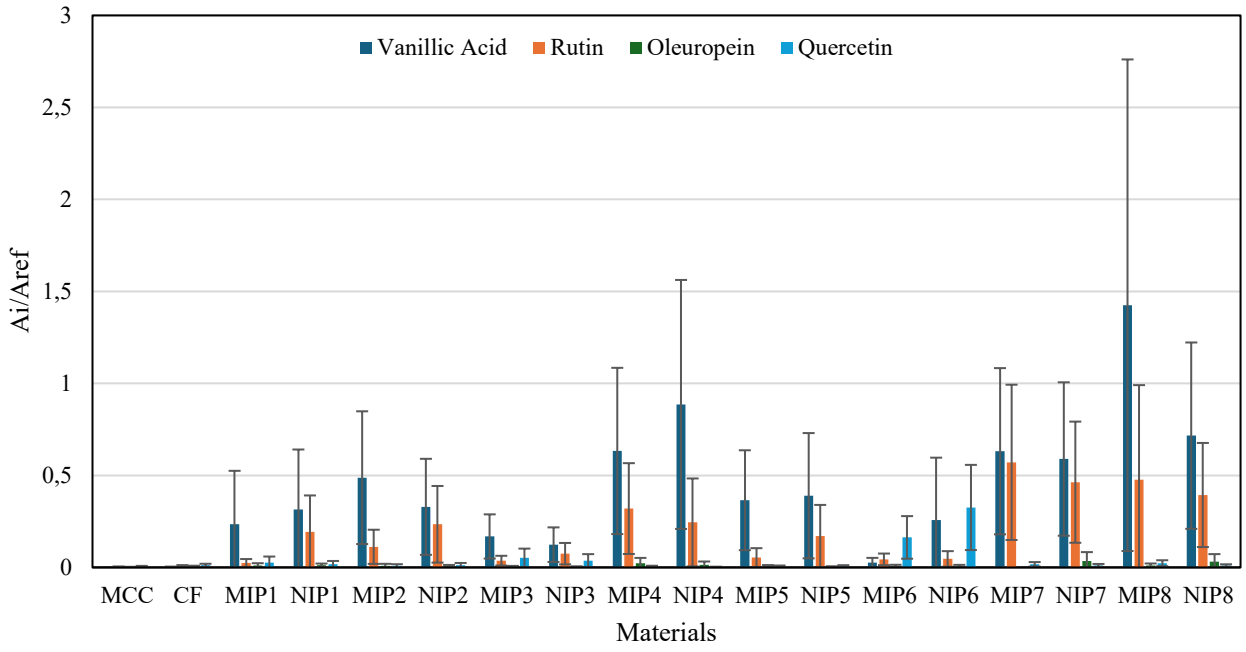

Figure 37: Peak area ratios of each analyte in the elution fraction, indicating the efficiency of desorption and selectivity of each sorbent toward individual polyphenols.

Appendix 4: Statistical evaluation of competitive sorption in MIP/NIP and native cellulose materials using ethanol/water (80:20, v/v).

Statistical analysis for the competitive retention of quercetin, vanillic acid, rutin, and oleuropein in the material pairs MIP/NIP1 to MIP/NIP8, MCC, and CF, using ethanol/water (80:20, v/v) as solvent. Three independent experimental replicates were performed (n = 3), measuring the amount of each compound retained in the 18 tested materials.

Table 14: Summary of the two-factor ANOVA with replication applied to the competitive retention data. The analysis confirms statistically significant differences between materials, between compounds, and for their interaction, highlighting the distinct sorption behavior of each compound-material combination.

ANOVA						
Source of Variation	SS	df	MS	F	P-value	F crit
Sample	173151.7	17	10185.39223	79.95519564	2.00061E-64	1.694149
Columns	71846	3	23948.66593	187.9967139	1.36425E-49	2.667443
Interaction	37327.36	51	731.9090929	5.745476794	6.65025E-17	1.435924
Within	18343.98	144	127.3887476			
Total	300669	215				

Appendix 5: HPLC-DAD chromatograms at 280 nm for the extract OPA 20 and for the various ethanol/water fractions eluted from MIP/NIP1 and MIP/NIP8.

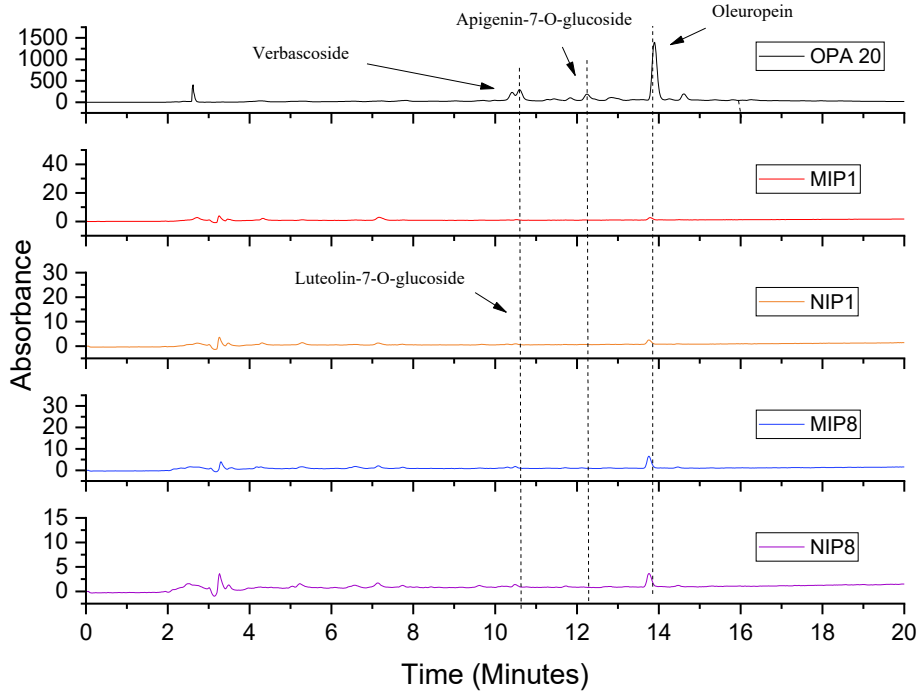

Figure 38: HPLC-DAD chromatograms at 280 nm for the extract OPA 20 and for the water fractions eluted (elution 1) from MIP/NIP1 and MIP/NIP8.

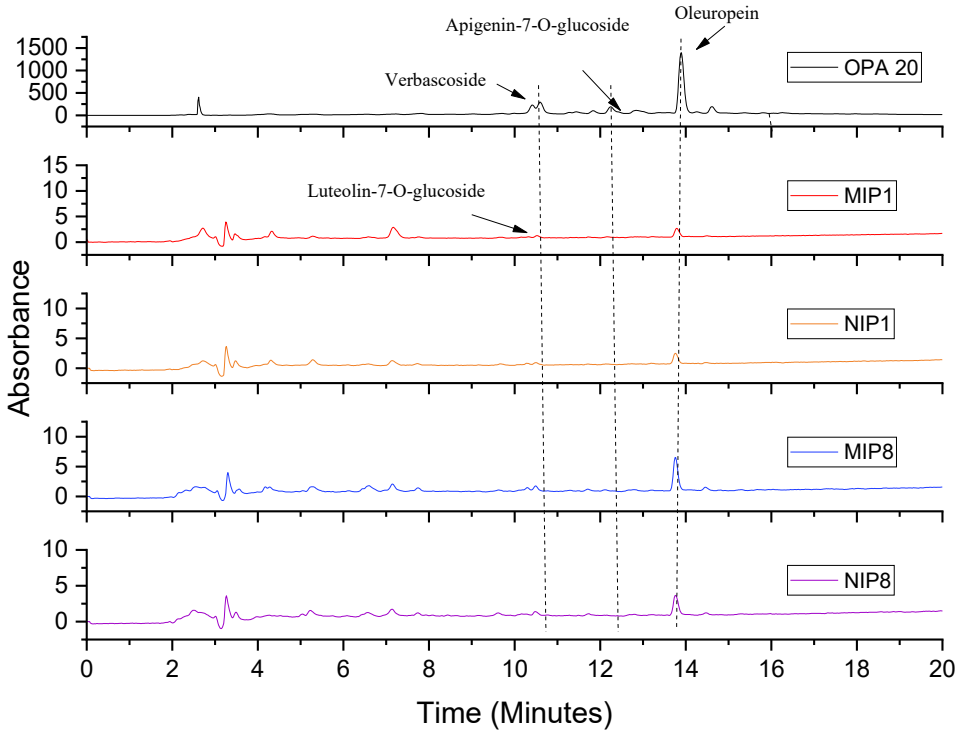

Figure 39*:* HPLC-DAD chromatograms at 280 nm for the extract OPA 20 and for the pH3 water fractions eluted (elution 2) from MIP/NIP1 and MIP/NIP8.

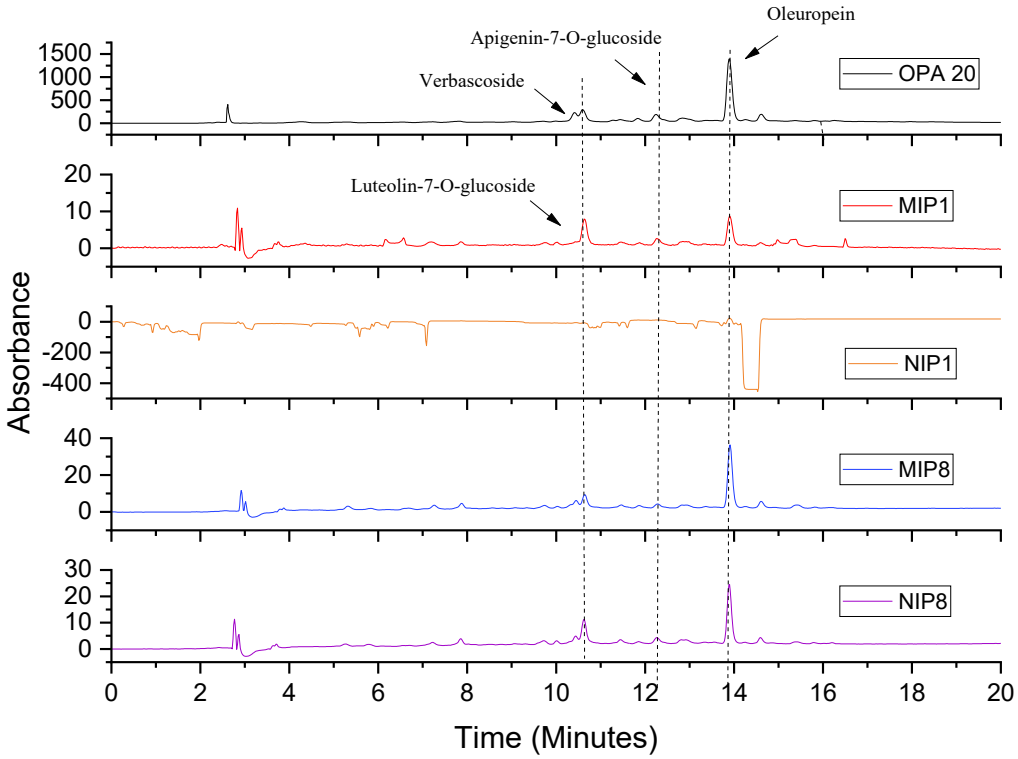

Figure 40: HPLC-DAD chromatograms at 280 nm for the extract OPA 20 and for the ethanol/water (25:75, v/v) (elution 3) fractions eluted from MIP/NIP1 and MIP/NIP8.

Appendix 6: HPLC-DAD analysis of eluates collected after increasing loading volumes (10-40 mL) of the VR2 SS1 extract for polyphenols and triterpenoids.

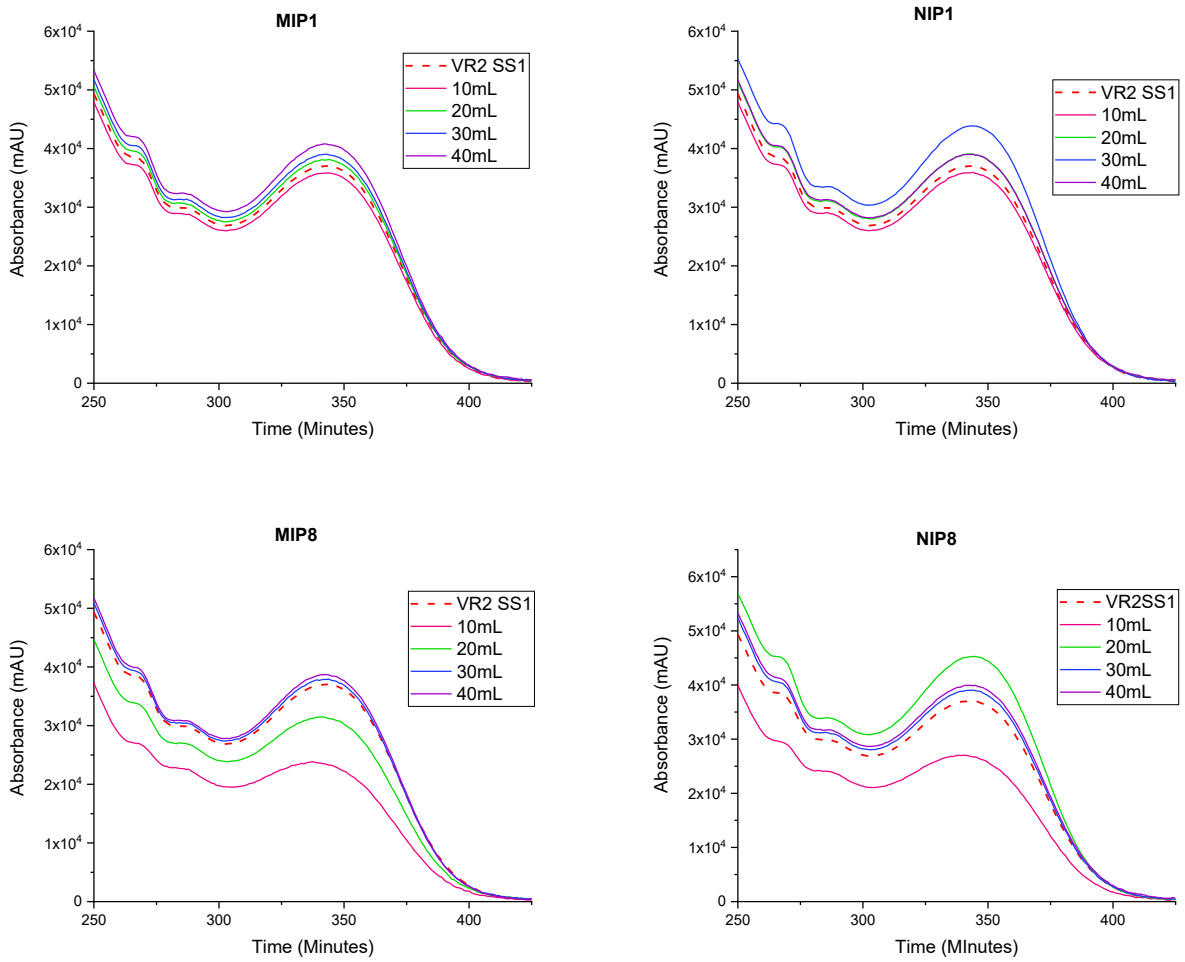

Figure 41: HPLC-DAD chromatograms using the polyphenols method after loading 10-40 mL of the OPA 20 extract. The profiles correspond to the saturation behavior of MIP/NIP 1 and 8, showing the evolution of retained compounds with increasing extract volume.

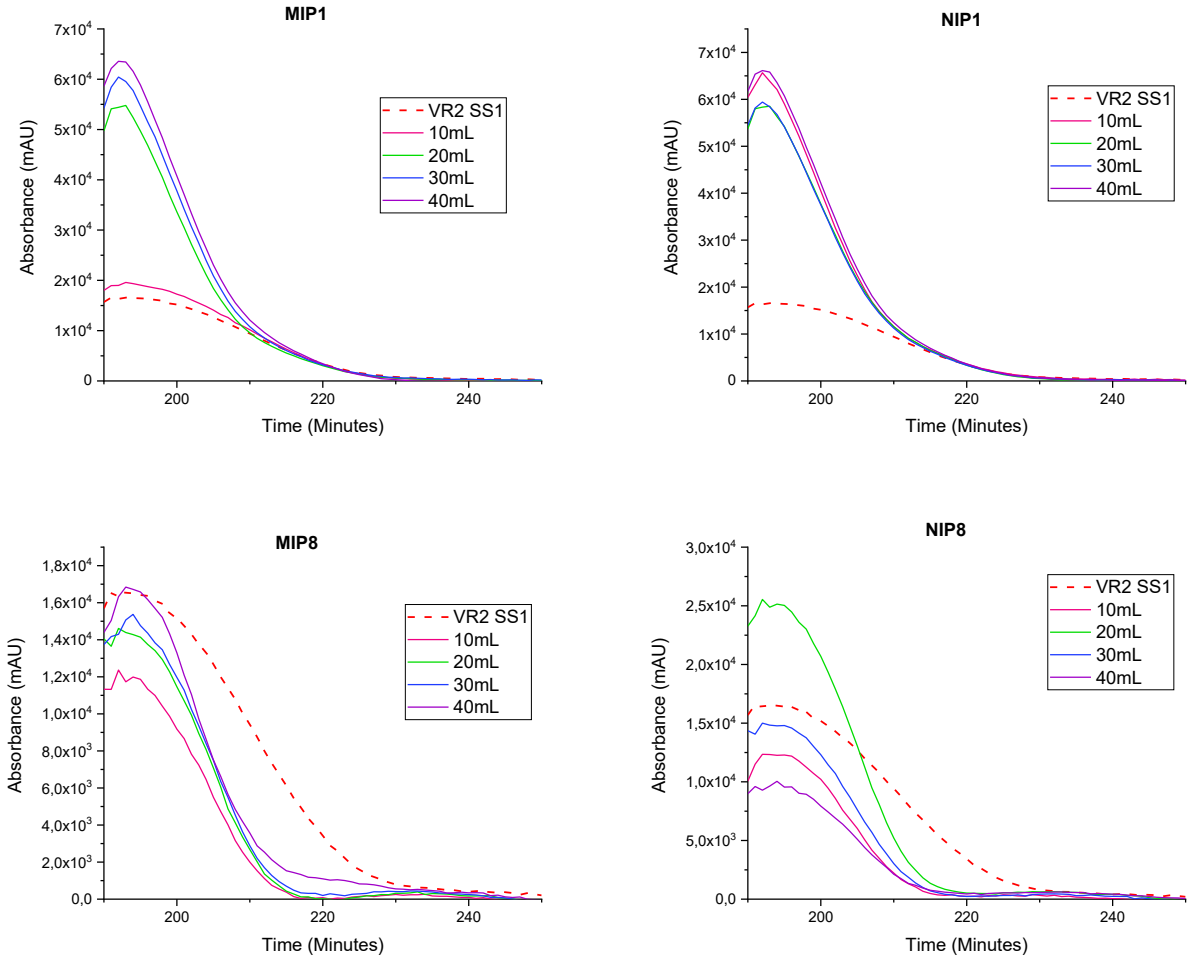

Figure 42: HPLC-DAD chromatograms using the triterpenoids method after loading 10-40 mL of the OPA 20 extract. The profiles correspond to the saturation behavior of MIP/NIP 1 and 8, showing the evolution of retained compounds with increasing extract volume.

Appendix 7: HPLC-DAD chromatograms at 210 nm for triterpenoids and 280 nm for polyphenols, of the extract VR2 SS1 and for the various ethanol/water fractions eluted from MIP/NIP1 and MIP/NIP8.

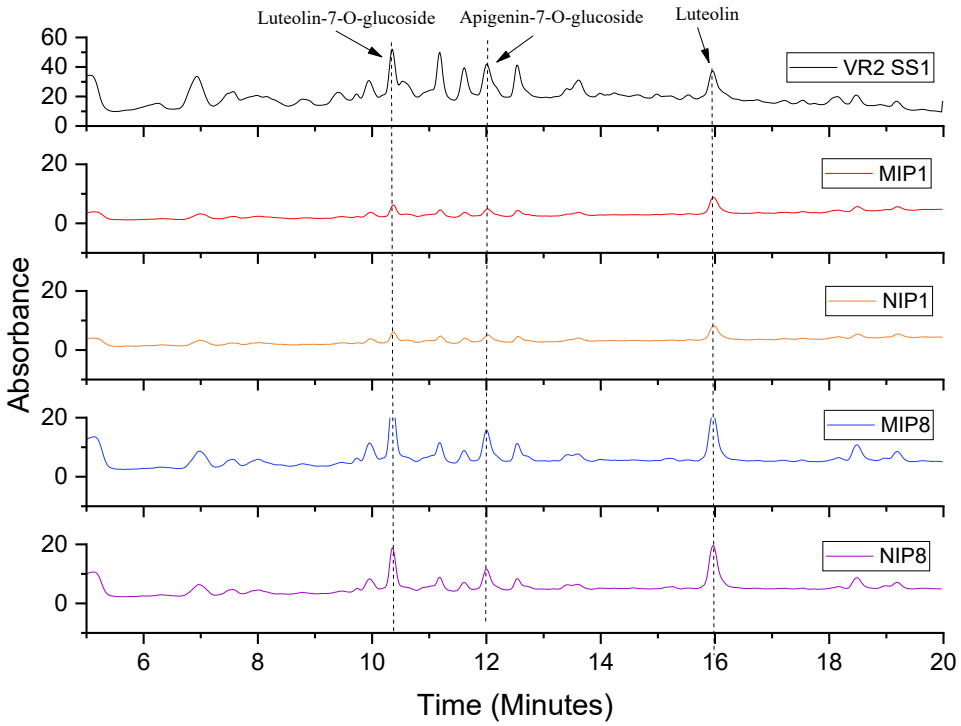

Figure 43: Elution chromatograms (λ = 280 nm) for polyphenols-rich fractions from VR2 SS1 extract and from materials MIP1/NIP1 and MIP8/NIP8, desorbed with ethanol/water (65:35, v/v) (elution 1).

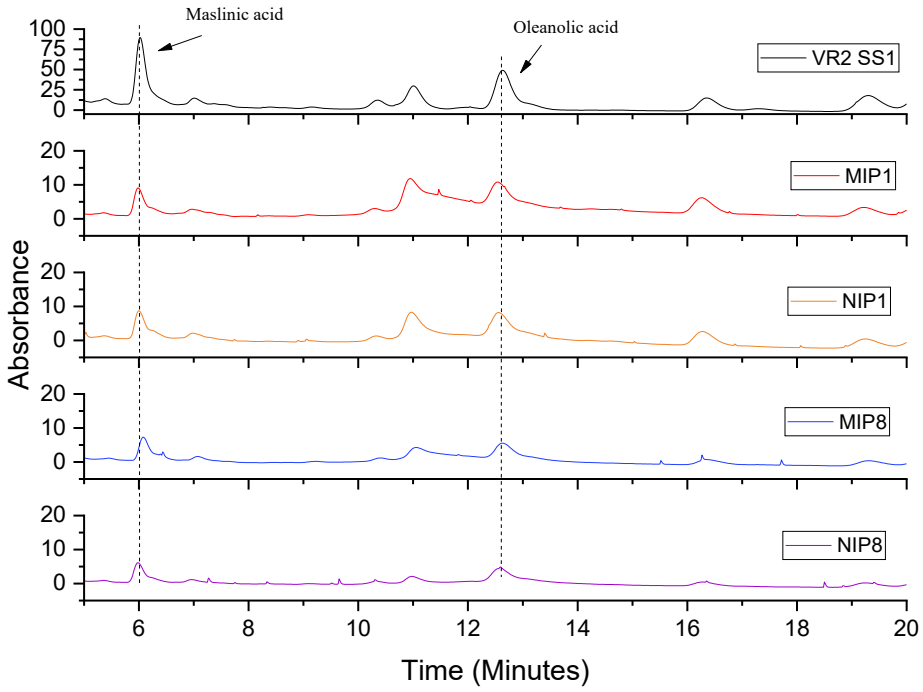

Figure 44*:* Elution chromatograms (λ = 210 nm) for triterpenoids-rich fractions from VR2 SS1 extract and from materials MIP1/NIP1 and MIP8/NIP8, desorbed with ethanol/water (65:35, v/v) (elution 1).

Appendix 8: Published article.

Almeida, A., Gaspar, R. M., Ferreira-Dias, S., Costa, M. R. P. F. N., & Dias, R. C. S. (2025). *Pyridyl-functionalized and surface molecularly imprinted cellulose particles to target bioactive compounds in olive leaf*. Reactive and Functional Polymers, 214, 106338. https://doi.org/10.1016/j.reactfunctpolym.2025.106338